

# Book of Abstracts

## Actinides revisited 2022

Dresden, 21<sup>st</sup> to 23<sup>rd</sup> September 2022

**HZDR**

HELMHOLTZ ZENTRUM  
DRESDEN ROSSENDORF

## Preface

Dear colleagues,

welcome to the "Actinides Revisited" conference in Dresden! The CoViD-19 pandemic has affected the scientific community in many ways in the last years. Notably, a large number of international meetings, also in our field of actinide chemistry, have been held online, postponed or outright cancelled, significantly hindering scientific exchange. Particularly young scientists have been hurt by this absence of conferences, which they could normally have used to begin to build their own scientific networks.

In this light, Lisa Vondung, Karsten Meyer, Florian Kraus and myself agreed to organize an one-off international meeting with a focus on actinide science, to give especially our young colleagues the opportunity to present and discuss their scientific results. Therefore, we are thrilled to see the "Actinides revisited" take shape and particularly to see so many PhD students participating and sharing their results in the exciting field of actinide chemistry!

We are grateful to the German Federal Ministry of Education and Research for supporting "Actinides Revisited" via funding for the project "f-Char". We are all looking forward to interesting contributions, intensive discussions, and an intriguing and most importantly enjoyable event!

Let's enjoy the days in Dresden together, on behalf of the entire team,



Thorsten Stumpf



© HZDR / André Wirsig

## Plenary Speaker

The organizers of “Actinides revisited” are most grateful for the support of the five distinguished experts in the various fields of actinide research who agreed to give plenary lectures at this conference.

**Steve Liddle** is Head of Inorganic Chemistry and Co-Director of the Centre for Radiochemistry Research at The University of Manchester. His research interests include metal-ligand multiple bonding, metal-metal bonding, small molecule activation and catalysis, and single-molecule magnetism, with a particular focus on actinide chemistry. He has published over 230 papers, reviews, book chapters, books, and articles to date.



**Thomas Albrecht-Schönzart** is a Distinguished Professor and Director of the Nuclear Science and Engineering Center at the Colorado School of Mines. He is a Fellow of the Royal Society of Chemistry and the AAAS and winner of several American Chemical Society awards including the Glenn T. Seaborg Award for Nuclear Chemistry. His research interests center on the chemistry, physics, and materials science of radioactive elements, especially heavy elements like berkelium and californium.

**Hans-Conrad zur Loye** is a Distinguished Professor at the University of South Carolina. His research interests include the crystal growth of new materials, including new scintillating and luminescing oxides and fluorides, and new uranium and thorium containing structures aiming to synthesize new hierarchical wasteform materials for the effective immobilization of nuclear waste in persistent architectures.



**Suzanne Bart** is an Associate Professor at Purdue University in West Lafayette, IN, USA. Her research interests include organometallic transformations and small molecule activation mediated by organoactinide species, with an emphasis on alkyl and redox-active ligands. Suzanne has been the recipient of an NSF CAREER award, and has been named a 2012 Cottrell Scholar, a 2014 Organometallics Young Investigator Fellow, and a 2015 Rising Star from the Women’s Chemist Committee of the American Chemical Society.

**David Clark** is a Fellow of the Los Alamos National Laboratory. He is the Director of the National Security Education Center at LANL. His research interests include the molecular and electronic structure of actinide materials, the behaviour of such materials in the environment and the application of synchrotron radiation to nuclear security. He is the author of over 175 papers, reviews, encyclopedia and book chapters.



## Conference at a glance

	Wednesday	Thursday	Friday
<i>Start</i>			
9:00	Welcome		
9:15	Liddle	zur Loye	Clark
9:30			
9:45	Daronnat	Barluzzi	Mamat
10:00	Popa	Kraus	Vallet
10:15	Straka	Komorovsky	Svitlyk
10:30	Kretzschmar	Poulin-Ponnelle	Patzschke
10:45	Coffee	Coffee	Coffee
11:00			
11:15	Mills	Wilden	Wenzel
11:30	Chilton	Fischer	Chen
11:45	Cho	Modder	Graubner
12:00	Minasian	Amidani	Closing remarks
12:15	Lunch	Lunch	Lunch
13:15			
13:30	Albrecht-Schönzart	Bart	
13:45			
14:00	März	Gilson	
14:15	Swift	Kersting	
14:30	Bolvin	Schreckenbach	
14:45	Düllmann	Berndt	
15:00	Coffee	Coffee	
15:15			
15:30	Walter	La Pierre	
15:45	Kohlmann	Kestel	
16:00	Kvashnina	Gericke	
16:15	Coffee	Announcements	
16:30		Coffee	
16:45	Poster Session		
18:30			
19:00		Poster Prize Ceremony	

## Detailed schedule

### Wednesday

09:00 Welcome address of Prof. Dr. S. Schmidt, Scientific Director, HZDR, Dresden

09:05 Welcome address of the scientific committee

#### Session 1 (Chair: D. Clark)

- 09:15 Recent Advances in Actinide-Ligand Multiple Bonding S. Liddle
- 09:45 Influence of the complexing site amino acids of calmodulin on its interaction with plutonium L. Daronnat
- 10:00 Radiation effects in americium ceramic compounds K. Popa
- 10:15 Actinide-Actinide Bonding: A challenge for theory M. Straka
- 10:30 NMR spectroscopy of selected aqueous systems investigated at HZDR-IRE J. Kretzschmar
- 10:45 Coffee

#### Session 2 (Chair: P. Kaden)

- 11:15 Recent Adventures in Lanthanide and Actinide Silicon Chemistry D. Mills
- 11:30 Relativistic calculations of hyperfine coupling in molecules N. Chilton
- 11:45 Fluorine-19 NMR Study of Electronic Structure in Actinide Tetrafluorides H. Cho
- 12:00 Covalency in Actinide Organometallics from Carbon K-edge XAS and Electronic Structure Calculations S. Minasian
- 12:15 Lunch

#### Session 3 (Chair: S. Liddle)

- 13:30 Enhancing Frontier Orbital Interactions in the f-Block Through Applications of Pressure and Electric Fields T. Albrecht-Schönzart
- 14:00 Early An(IV) complexes with N-donor ligands J. März
- 14:15 Small Scale Pyrochemistry with In-situ Material Doping A. Swift
- 14:30 Paramagnetic NMR in actinide complexes: experiment and modeling. H. Bolvin
- 14:45 Actinide samples from Mainz University for applications in chemistry and physics research C. Düllmann
- 15:00 Coffee

#### Session 4 (Chair: M. Schmidt)

- 15:30 The molecular approach for actinide materials O. Walter
- 15:45 Metal-semiconductor transitions in  $U_3S_5$  H. Kohlmann
- 16:00 High energy Resolution X-ray Spectroscopy for Actinide Science K. Kvashnina
- 16:15 Coffee

#### 16:45 Poster Session

## Thursday

### Session 1 (Chair: S. Bart)

- 09:15 From Mild Hydrothermal to High Temperature Solutions: Crystal Growth of New Uranium and Transuranium Phases H.-C. zur Loye
- 09:45 Exploring the chemistry of super-reduced uranium organometallics L. Barluzzi
- 10:00 Some Recent Results of our Solid-State Uranium Chemistry and Reactions of Uranium Halides in pure HCN and NH<sub>3</sub> F. Kraus
- 10:15 Relativistic theory of pNMR and EPR S. Komorovsky
- 10:30 Speciation of An<sup>VI</sup> complexes in solution by combining pNMR and classical Molecular Dynamics simulations C. Poulin-Ponnelle
- 10:45 Coffee

### Session 2 (Chair: F. Kraus)

- 11:15 Process development studies for the separation of trivalent actinides from used nuclear fuel solutions A. Wilden
- 11:30 Variability of crystal surface reactivity controls the migration and sorption of radionuclides C. Fischer
- 11:45 Masked Uranium(II) Delivery by a Diuranium(III) complex for Multi-Electron Transfer D. Modder
- 12:00 The M<sub>4,5</sub> edges HERFD XANES: approaches to calculations L. Amidani
- 12:15 Lunch

### Session 3 (Chair: T. Albrecht-Schönzart)

- 13:30 Harnessing Multi-Electron Redox Chemistry to Access Unprecedented Actinide Moieties S. Bart
- 14:00 Unusual Building Units and Properties of Actinide Metal-Organic Frameworks S. Gilson
- 14:15 Calix[4]arenes with phosphoryl and salicylamide functional groups: synthesis, complexation and selective extraction of f-element cations B. Kersting
- 14:30 Actinium Chemistry in Silico G. Schreckenbach
- 14:45 Resonance ionization spectroscopy on <sup>254,255</sup>Es and <sup>255</sup>Fm with a “boostered” sample S. Berndt
- 15:00 Coffee

### Session 4 (Chair: L. Vondung)

- 15:30 High-Valent U, Np, and Pu Imidophosphorane Mono-Oxo Complexes H. La Pierre
- 15:45 Uranium Going the Soft Way: Studies of the Electronic Structure of U(III)-Complexes with a Series of new S-based Chelating Ligands B. Kestel
- 16:00 [An(acac)<sub>4</sub>] complexes revisited R. Gericke
- 16:15 Announcements
- 16:30 Coffee

### 19:00 Poster Prize Ceremony

at MARCOLINIS WELT, Bautzner Straße 96, Dresden

## Friday

### Session 1 (*Chair: C. zur Loye*)

- 09:15 Applications of  $^{238}\text{Pu}$  are Out of this World D. Clark
- 09:45 PSMA-Macropa-Conjugates for Radiolabeling with Actinium-225 and Iodine-123 C. Mamat
- 10:00 Exploring excited state potential energy profile and luminescence properties of uranyl-based complexes by TRLFS and ab initio method V. Vallet
- 10:15 Solubility limits and structural properties in the thorite-zircon pseudo-binary system for nuclear waste storage V. Svitlyk
- 10:30 Actinide bonding trends through the eye of the theoretician M. Patzschke
- 10:45 Coffee

### Session 2 (*Chair: T. Stumpf*)

- 11:15 Insights at the molecular level into the formation of oxo-bridged trinuclear uranyl complexes M. Wenzel
- 11:30 DFT + U study of  $\text{UO}_2$  and  $\text{PuO}_2$  with Occupation Matrix Control J. Chen
- 11:45 Chemistry of Uranium Halides in liquid Ammonia T. Graubner
- 12:00 Closing remarks
- 12:15 Lunch

**End of conference**

## Table of contents

<b>Preface</b> .....	<b>1</b>
<b>Plenary Speaker</b> .....	<b>2</b>
<b>Conference at a glance</b> .....	<b>3</b>
<b>Detailed schedule</b> .....	<b>4</b>
<b>Table of contents</b> .....	<b>7</b>
<b>Abstracts – oral presentation</b> .....	<b>13</b>
<b>Recent Advances in Actinide-Ligand Multiple Bonding</b> Stephen T. Liddle*	14
<b>Influence of the complexing site amino acids of calmodulin on its interaction with plutonium</b> L. Daronnat <sup>a,*</sup> , L. Berthon <sup>a</sup> , N. Boubals <sup>a</sup> , T. Dumas <sup>a</sup> , P. Moisy <sup>a</sup> , S. Sauge-Merle <sup>b</sup> , D. Lemaire <sup>b</sup> , C. Berthomieu <sup>b</sup>	15
<b>Radiation effects in americium ceramic compounds</b> Karin Popa <sup>a,*</sup> , Jean-François Vigier <sup>a</sup> , Laura Martel <sup>a</sup> , Oliver Dieste Blanco <sup>a</sup> , Eric Colineau <sup>a</sup> , Jean-Christophe Griveau <sup>a</sup> , Daniel Freis <sup>a</sup> , Rudy J.M. Konings <sup>a</sup>	16
<b>Actinide–Actinide Bonding: A challenge for theory</b> Adam Jaroš, Cina Foroutan-Nejad, Michal Straka*	17
<b>NMR spectroscopy of selected aqueous systems investigated at HZDR-IRE</b> Jérôme Kretzschmar*, Thorsten Stumpf	18
<b>Recent Adventures in Lanthanide and Actinide Silicon Chemistry</b> David P. Mills*, Benjamin L. L. Réant, Victoria E. J. Berryman, Annabel R. Basford, Lydia E. Nodaraki, Ashley J. Wooles, Floriana Tuna, John A. Seed, Alasdair Formanuk, Nikolas Kaltsoyannis*, and Stephen T. Liddle*	19
<b>Relativistic calculations of hyperfine coupling in molecules</b> Nicholas F. Chilton <sup>a,*</sup> , Letitia Birnoschi <sup>a</sup> , Eric J. L. McInnes <sup>a</sup>	20
<b>Fluorine-19 NMR Study of Electronic Structure in Actinide Tetrafluorides</b> Herman Cho <sup>a,*</sup> , Eric Walter <sup>a</sup> , Cigdem Capan <sup>b</sup> , Gian Surbella <sup>a</sup> , Sejun Park <sup>a</sup> , Amanda Casella <sup>a</sup> , Jennifer Carter <sup>a</sup> , Bruce McNamara <sup>a</sup> , Chuck Soderquist <sup>a</sup> , Sergey Sinkov <sup>a</sup> , Richard Clark <sup>a</sup> , Forrest Heller <sup>a</sup> , Lucas Sweet <sup>a</sup> , Jordan Corbey <sup>a</sup>	21
<b>Covalency in Actinide Organometallics from Carbon K-edge XAS and Electronic Structure Calculations</b> Stefan Minasian <sup>a,*</sup> , Jochen Autschbach <sup>b</sup> , Enrique Batista <sup>c</sup> , Jacob Branson <sup>a</sup> , David Clark <sup>c</sup> , Alexander Ditter <sup>a</sup> , Gaurab Ganguly <sup>b</sup> , Olivia Gunther <sup>a</sup> , Jason Keith <sup>c</sup> , Stosh Kozimor <sup>c</sup> , Richard Martin <sup>c</sup> , Danil Smiles <sup>a</sup> , Yusen Qiao <sup>a</sup> , Dumitru-Claudiu Sergentu <sup>b</sup> , David Shuh <sup>a</sup> , Chantal Stieber <sup>d</sup> , Taoxiang Sun <sup>e</sup> , Tolek Tylliszczak <sup>a</sup>	22

<b>Enhancing Frontier Orbital Interactions in the f-Block Through Applications of Pressure and Electric Fields</b>	
Thomas Albrecht-Schönzart <sup>a</sup>	23
<b>Early An(IV) complexes with N-donor ligands</b>	
Juliane März <sup>a,*</sup> , Sebastian Fichter <sup>a,b</sup> , Michael Patzschke <sup>a</sup> , Peter Kaden <sup>a</sup> , Luisa Köhler <sup>a</sup> , Moritz Schmidt <sup>a</sup> , Thorsten Stumpf <sup>a</sup>	24
<b>Small Scale Pyrochemistry with In-situ Material Doping</b>	
S.A. Simpson <sup>a</sup> , D.J. Roberts <sup>a</sup> , A.M. Parkes <sup>b</sup> , A.J. Swift <sup>a,*</sup> , C. Zhang <sup>a</sup> , K. R. Holliday <sup>a</sup>	25
<b>Paramagnetic NMR in actinide complexes: experiment and modeling.</b>	
Hélène Bolvin <sup>a,*</sup> , Md. Ashraful Islam <sup>a</sup> , Matthieu Autillo <sup>b</sup> , Claude Berthon <sup>b</sup>	26
<b>Actinide samples from Mainz University for applications in chemistry and physics research</b>	
Ch.E. Düllmann <sup>a,b,c,*</sup> , E. Artes <sup>a,b,c</sup> , S. Berndt <sup>a</sup> , A. Dragoun <sup>a,c</sup> , K. Eberhardt <sup>a</sup> , R. Haas <sup>a,b,c</sup> , C.-C. Meyer <sup>a,c</sup> , L. Reed <sup>a,c</sup> , D. Renisch <sup>a,c</sup> , M. Rapps <sup>a(†)</sup> , J. Runke <sup>a,c</sup> , C. Mokry <sup>a,c</sup> , P. Thörle-Pospiech <sup>a,c</sup> , N. Trautmann <sup>a</sup>	27
<b>The molecular approach for actinide materials</b>	
Olaf Walter <sup>*</sup> , Karin Popa	28
<b>Metal-semiconductor transitions in U<sub>3</sub>S<sub>5</sub></b>	
Holger Kohlmann <sup>a,*</sup> , Heribert Wilhelm <sup>b</sup> , Marcel Voest <sup>c</sup> , Wolfgang Scherer <sup>c</sup> , Badal Mondal <sup>d</sup> , Ralf Tonner-Zech <sup>d</sup>	29
<b>High energy Resolution X-ray Spectroscopy for Actinide Science</b>	
Kristina Kvashnina <sup>a,b,*</sup>	30
<b>From Mild Hydrothermal to High Temperature Solutions: Crystal Growth of New Uranium and Transuranium Phases</b>	
Hans-Conrad zur Loye <sup>a,b,*</sup> , Kristen A. Pace <sup>a,b</sup> , Travis K. Deason <sup>a,b,c</sup> , Adrian Hines <sup>a,b</sup> , Gregory Morrison <sup>a,b</sup> , Hunter Tisdale <sup>a,b</sup> , Theodore Besmann <sup>a,b</sup> , Jake Amoroso <sup>b,c</sup> , David DiPrete <sup>b,c</sup>	31
<b>Exploring the chemistry of super-reduced uranium organometallics</b>	
Luciano Barluzzi <sup>a,*</sup> , Richard A. Layfield <sup>a</sup>	32
<b>Some Recent Results of our Solid-State Uranium Chemistry and Reactions of Uranium Halides in pure HCN and NH<sub>3</sub></b>	
Florian Kraus <sup>a,*</sup> , S. S. Rudel <sup>a</sup> , H. L. Deubner <sup>a</sup> , B. Scheibe <sup>a</sup> , M. Conrad <sup>a</sup> , M. Sachs <sup>a</sup>	33
<b>Relativistic theory of pNMR and EPR</b>	
Stanislav Komarovskiy <sup>a,*</sup>	34
<b>Speciation of An<sup>VI</sup> complexes in solution by combining pNMR and classical Molecular Dynamics simulations</b>	
Clovis Poulin-Ponnelle <sup>a,*</sup> , Thomas Dumas <sup>a</sup> , Magali Duvail <sup>b</sup> , Claude Berthon <sup>a</sup>	35
<b>Process development studies for the separation of trivalent actinides from used nuclear fuel solutions</b>	
Andreas Wilden <sup>a,*</sup> , Andreas Geist <sup>b</sup> , Giuseppe Modolo <sup>a</sup>	36

<b>Variability of crystal surface reactivity controls the migration and sorption of radionuclides</b>	
Tao Yuan <sup>a</sup> , Stefan Schymura <sup>a</sup> , Till Bollermann <sup>a</sup> , Konrad Molodtsov <sup>a</sup> , Paul Chekhonin <sup>a</sup> , Moritz Schmidt <sup>a</sup> , Thorsten Stumpf <sup>a</sup> & Cornelius Fischer <sup>a,*</sup>	37
<b>Masked Uranium(II) Delivery by a Diuranium(III) complex for Multi-Electron Transfer</b>	
Dieuwertje K. Modder <sup>1</sup> , Chad T. Palumbo <sup>1</sup> , Iskander Douair <sup>2</sup> , Rosario Scopelliti <sup>1</sup> , Farzaneh Fadaei-Tirani <sup>1</sup> , Laurent Maron <sup>2</sup> , Marinella Mazzanti <sup>*1</sup>	38
<b>Unusual Building Units and Properties of Actinide Metal-Organic Frameworks</b>	
Sara E. Gilson <sup>a,*</sup> , Melissa Fairley <sup>a</sup> , Jennifer E.S. Szymanowsky <sup>a</sup> , Sylvia Hanna <sup>b</sup> , Patrick Julien <sup>a</sup> , Zhijie Chen <sup>b</sup> , Peng Li <sup>b</sup> , Jacob White <sup>c</sup> , Debmalya Ray <sup>c</sup> , Allen G. Oliver <sup>a</sup> , Laura Gagliardi <sup>c</sup> , Omar K. Farha <sup>b</sup> , Peter C. Burns <sup>a</sup>	39
<b>Calix[4]arenes with phosphoryl and salicylamide functional groups: synthesis, complexation and selective extraction of f-element cations</b>	
Berthold Kersting <sup>a,*</sup> , Florian Gasneck <sup>a</sup> , Quirina I. Roode-Gutzmer <sup>b</sup> , Thorsten Stumpf <sup>b</sup>	40
<b>Actinium Chemistry in Silico</b>	
Georg Schreckenbach <sup>a,*</sup> , Yang Gao <sup>a,b</sup> , Cen Li <sup>a</sup> , Josef Tomeček <sup>a,c</sup> , Payal Grover <sup>a</sup>	41
<b>Resonance ionization spectroscopy on <sup>254,255</sup>Es and <sup>255</sup>Fm with a “boosted” sample</b>	
S. Berndt <sup>a,*</sup> , Th.E. Albrecht-Schönzart <sup>b</sup> , M. Block <sup>a,c,d</sup> , H. Dorrer <sup>a</sup> , Ch.E. Düllmann <sup>a,c,d</sup> , J.G. Ezold <sup>c</sup> , M. Kaja <sup>a</sup> , T. Kieck <sup>c,d</sup> , N. Kneip <sup>a</sup> , U. Köster <sup>f</sup> , J. Lantis <sup>a</sup> , C. Mokry <sup>a,c</sup> , D. Münzberg <sup>a,c,d</sup> , S. Nothhelfer <sup>a,c,d</sup> , S. Raeder <sup>c,d</sup> , D. Renisch <sup>a,c</sup> , J. Runke <sup>a,d</sup> , M. Stemmler <sup>a</sup> , D. Studer <sup>a</sup> , P. Thörle-Pospiech <sup>a,c</sup> , N. Trautmann <sup>a</sup> , J. Warbinek <sup>d</sup> , F. Weber <sup>a</sup> , K. Wendt <sup>a</sup>	42
<b>High-Valent U, Np, and Pu Imidophosphorane Mono-Oxo Complexes</b>	
Henry S. La Pierre <sup>a,b,*</sup> , and Julie E. Niklas <sup>a</sup>	43
<b>Uranium Going the Soft Way: Studies of the Electronic Structure of U(III)-Complexes with a Series of new S-based Chelating Ligands</b>	
Benedikt Kestel <sup>a</sup> , Daniel Pividori <sup>a</sup> , Matthias E. Mieli <sup>a</sup> , Frank W. Heinemann <sup>a</sup> , Andreas Scheurer <sup>a</sup> , Michael Patzschke <sup>b</sup> , Karsten Meyer <sup>a,*</sup>	44
<b>[An(acac)<sub>4</sub>] complexes revisited</b>	
Robert Gericke <sup>*</sup> , Peter Kaden	45
<b>Applications of <sup>238</sup>Pu are Out of this World</b>	
David L Clark <sup>a,*</sup>	46
<b>PSMA-Macropa-Conjugates for Radiolabeling with Actinium-225 and Iodine-123</b>	
Ritchie Kranzen <sup>a</sup> , Falco Reissig <sup>a</sup> , Hans-Jürgen Pietzsch <sup>a</sup> , Klaus Kopka <sup>a</sup> , Constantin Mamat <sup>a,*</sup>	47
<b>Exploring excited state potential energy profile and luminescence properties of uranyl-based complexes by TRLFS and ab initio method</b>	
Valérie Vallet <sup>a,*</sup> , Hanna Oher <sup>a,b</sup> , Florent Réal <sup>a</sup> , Thomas Vercouter <sup>b</sup> , André Severo Pereira Gomes <sup>a</sup> , Richard E. Wilson <sup>c</sup>	48
<b>Solubility limits and structural properties in the thorite-zircon pseudo-binary system for nuclear waste storage</b>	
Volodymyr Svitlyk <sup>a,b,*</sup> , Stephan Weiss <sup>a</sup> , Salim Shams <sup>a</sup> , Christoph Hennig <sup>a,b</sup>	49

### **Actinide bonding trends through the eye of the theoretician**

Michael Patzschke<sup>a,\*</sup>, Benjamin Scheibe<sup>b</sup>, Roger Kloditz<sup>a</sup>, Thomas Radoske<sup>a</sup>, Juliane März<sup>a</sup>, Peter Kaden<sup>a</sup>, Luisa Köhler<sup>a</sup>, Moritz Schmidt<sup>a</sup>, Thorsten Stumpf<sup>a</sup>

50

### **Insights at the molecular level into the formation of oxo-bridged trinuclear uranyl complexes**

Gerrit Schaper<sup>a</sup>, Marco Wenzel<sup>a</sup>, Uwe Schwarzenbolz<sup>b</sup>, Johannes Steup<sup>a</sup>, Felix Hennersdorf<sup>a</sup>, Thomas Henle<sup>b</sup>, Jan J. Weigand<sup>a,\*</sup>

51

### **DFT + *U* study of UO<sub>2</sub> and PuO<sub>2</sub> with Occupation Matrix Control**

Jiali Chen<sup>a,\*</sup>, Nikolas Kaltsoyannis<sup>a</sup>

52

### **Chemistry of Uranium Halides in liquid Ammonia**

T. Graubner<sup>a,\*</sup>, A. Barba<sup>a</sup>, F. Kraus

54

## **Abstracts – Poster .....55**

### **Insights into the solution structure of hydrated uranium and thorium ions from neutron scattering experiments**

Samuel J. Edwards<sup>a</sup>, Daniel T. Bowron<sup>b</sup>, Robert J. Baker<sup>a\*</sup>

56

### **In situ HERFD-XAS experiments on uranium state under high temperature**

Elena Bazarkina<sup>a,b,\*</sup>, Stephen Bauters<sup>a,b</sup>, Jean-Louis Hazemann<sup>c</sup>, Denis Testemale<sup>c</sup>, Kristina Kvashnina<sup>a,b</sup>

57

### **Quantification of the impact of defect density on Eu<sup>3+</sup> sorption efficiency on alpha particle irradiated biotite crystals**

M.A. Cardenas Rivera<sup>a,\*</sup>, S. Akhmadaliev<sup>b</sup>, C. Fischer<sup>a</sup>

58

### **Synthetic Organometallic Pathways to Produce Uranium Cermet Materials via Laser Decomposition**

Bradley C. Childs<sup>a,\*</sup>, Michelle M. Greenough<sup>a</sup>, Maryline G. Ferrier<sup>a</sup>, Aiden A. Martin<sup>a</sup>, Kiel S. Holliday<sup>a</sup>, Jason R. Jeffries

59

### **Computational Studies of Iron-Actinide Chemistry of Importance to UK Nuclear Waste Clean-up**

Ryan Dempsey<sup>a,\*</sup>, Samuel Shaw<sup>b</sup>, Katherine Morris<sup>b</sup>, Nikolas Kaltsoyannis<sup>a</sup>

60

### **Influence of organic complexing agents on the sorption of Eu(III) to C-S-H phases: a TRLFS study**

Sophie Dettmann<sup>a</sup>, Michael U. Kumke<sup>a,\*</sup>

61

### **Solvent extraction studies of different diastereomers of modified diglycolamide ligands for An(III) and Ln(III) extraction**

Laura Diaz Gomez<sup>a,\*</sup>, Andreas Wilden<sup>a</sup>, Giuseppe Modolo<sup>a</sup>, Wim Verboom<sup>b</sup>

62

### **Synthesis and Coordination Chemistry of N-Donor Ligands with early Actinides**

T. Duckworth<sup>a,\*</sup>, J. März<sup>a</sup>, P. Kaden<sup>a</sup>, M. Patzschke<sup>a</sup>, N. Schwarz<sup>b</sup>, G. Greif<sup>b</sup>, T. Stumpf<sup>a</sup>

63

### **Complexation of Eu(III) and Cm(III) by aminopolycarboxylic acids related to EGTA**

Sebastian Friedrich<sup>a,\*</sup>, Linus Holtmann<sup>b</sup>, Jérôme Kretzschmar<sup>a</sup>, Björn Drobot<sup>a</sup>, Thorsten Stumpf<sup>a</sup>, Astrid Barkleit<sup>a</sup>

64

## **Electron Paramagnetic Resonance Spectroscopy of Early d- and f-Block Metal(III)-Silanides**

Gemma K. Gransbury<sup>a</sup>, Benjamin L. L. Réant<sup>a</sup>, Ashley J. Wooles<sup>a</sup>, Jack Emerson-King<sup>a</sup>, Nicholas F. Chilton<sup>a</sup>, Stephen T. Liddle<sup>a,\*</sup>, David P. Mills<sup>a,\*</sup> 65

## **U value revisit of PuO<sub>2</sub> and its surface reactions with H<sub>2</sub>O and NO**

Xiaoyu Han<sup>a,\*</sup>, Nikolas Kaltsoyannis<sup>a</sup> 66

## **Two new Diffractometers for Actinide Research at the Rossendorf Beamline / ESRF**

Christoph Hennig<sup>a,b,\*</sup>, Volodymyr Svitlyk<sup>a,b</sup> 67

## **Coordination Chemistry of Tri- and Tetravalent Actinides with Benzamidinate Ligands**

Boseok Hong<sup>a,\*</sup>, Sebastian Fichter<sup>a</sup>, Adrian Näder<sup>a</sup>, Juliane März<sup>a</sup>, Peter Kaden<sup>a</sup>, Michael Patzschke<sup>a</sup>, Moritz Schmidt<sup>a</sup>, Thorsten Stumpf<sup>a</sup> 68

## **Spin Orbit Coupling Parameters for Semi-Empirical Methods: DFTB & GFN-xTB**

Gautam Jha<sup>a,b,\*</sup>, Thomas Heine<sup>a,b,c</sup> 69

## ***Ab initio* modelling of magnetite surfaces for radionuclide retention**

Anita Katheras<sup>a,\*</sup>, Konstantinos Karalis<sup>a</sup>, Matthias Krack<sup>b</sup>, Andreas C. Scheinost<sup>c,d</sup>, Sergey V. Churakov<sup>a,c</sup> 70

## **Discrete and Cationic Thorium-Incorporated Palladium(II)-Oxo Clusters**

Saurav Bhattacharya and Ulrich Kortz<sup>\*</sup> 71

## **A density functional investigation of dinuclear hydrolysis complexes [(AnO<sub>2</sub>)<sub>2</sub>(OH)]<sup>q</sup> for An = U and Np**

I. Chiorescu<sup>a</sup>, S. Krüger<sup>a,\*</sup> 72

## **Crystal-chemical investigation of MU<sub>8</sub>S<sub>17</sub> and Ln<sub>6</sub>U<sub>12</sub>S<sub>31</sub>I compounds (M = 3d metal; Ln = lanthanide metal)**

Marvin Michak<sup>a</sup>, Paula Huth<sup>b</sup>, Reinhard Denecke<sup>b</sup>, Holger Kohlmann<sup>a,\*</sup> 73

## **Magnetic Relaxation of Actinide-based Single Molecule Magnets**

Meagan S. Oakley<sup>a,\*</sup>, Nicholas Chilton<sup>a</sup> 74

## **Characterization of f-element complexes with *soft-donor* ligands for selective Americium separation**

Fynn Sören Sauerwein<sup>a,\*</sup>, Andreas Wilden<sup>a</sup>, Giuseppe Modolo<sup>a</sup> 75

## **Investigation of the ligand configuration in Th(IV) N-donor ligand complexes**

Thomas Sittel<sup>a,b,\*</sup>, Michael Trumm<sup>a</sup>, Christian Adam<sup>a</sup>, Andreas Geist<sup>a</sup>, Petra Panak<sup>a,b</sup> 76

## **Brewer's spent grain: A promising starting material for efficient uranyl ion adsorbents?**

Yi Su<sup>a</sup>, Marco Wenzel<sup>a</sup>, Wendelin Böhm<sup>b</sup>, Silvia Paasch<sup>c</sup>, Markus Seifert<sup>a</sup>, Margret Acker<sup>d</sup>, Thomas Doert<sup>e</sup>, Eike Brunner<sup>c</sup>, Thomas Henle<sup>b</sup>, Jan J. Weigand<sup>a,\*</sup> 77

## **Improving computational methods for active elements: structures of mixed d- and f-elements oxides (MUO<sub>4</sub>) from experiment and first principles simulations**

Rebekka Tesch<sup>a,b,c,\*</sup>, Gabriel L. Murphy<sup>d</sup>, Zhaoming Zhang<sup>e</sup>, Brendan J. Kennedy<sup>f</sup>, Piotr M. Kowalski<sup>a,b</sup> 78

**Insight into the Separation of An(III) from Ln(III) Using Bis(2,4,4-trimethylpentyl)dithiophosphinic Acid**

Guoxin Tian,<sup>a,b\*</sup> Qiling Guo<sup>a</sup>, Tuo Fang<sup>a</sup>, Tiantian Xia<sup>a</sup>, Qiaorui Sui<sup>a</sup>, Qing Deng<sup>a</sup>, Qian Liu<sup>a</sup>, Liyang Zhu<sup>a</sup>, Suliang Yang<sup>a</sup>

79

**Homoleptic Acetylacetonate (acac) and  $\beta$ -Ketoimnate (acnac) Complexes of Uranium**

Pablo Waldschmidt, Judith Riedhammer, Douglas Hartline, Frank W. Heinemann and Karsten Meyer\*

80

**Incorporation and diffusion of krypton and xenon in uranium mononitride; a density functional theory study**

Lin Yang<sup>\*</sup>, Nikolas Kaltsoyannis

81

**An innovative approach of studying uranium dioxide corrosion at the microscale**

Jennifer Yao<sup>a</sup>, Nabajit Lahiri<sup>b</sup>, Shalini Tripathi<sup>a</sup>, Shawn L. Riechers<sup>a</sup>, Eugene S. Ilton<sup>b</sup>, Sayandev Chatterjee<sup>c</sup>, Edgar C Buck<sup>a,\*</sup>

82

**Venue – Poster Prize Ceremony.....83**

Abstracts – oral presentation

# Recent Advances in Actinide-Ligand Multiple Bonding

Stephen T. Liddle\*

*The University of Manchester, Department of Chemistry and Centre for Radiochemistry Research, Oxford Road, Manchester, M13 9PL, UK.*

---

## Abstract

Over the past fifteen years the Liddle group has contributed to the development of the synthesis, reactivity, spectroscopy, magnetism, and quantum chemical characterisation of early actinide (uranium and thorium) -ligand multiple bonding,<sup>1-10</sup> with the occasional foray into actinide-actinide bonding.<sup>11</sup> Our motivation for undertaking this endeavour is simple – we wish to address a central aim of actinide science to quantify, and hence understand, the extent and nature of covalency in the chemical bonding of actinide ions.<sup>12</sup> When considering the ways in which to achieve this aim, studying the aforementioned types of linkage is an attractive place to start since they tend, by definition, to exhibit appreciable amounts of covalency, or unusual bonding motifs, which are amenable to interrogation by the wide range of available modern-day experimental and computational characterisation techniques. The study of early actinide systems is also an attractive area to research because the resulting body of work becomes the baseline from which to develop comparisons to transuranium and lanthanide analogues; this will in turn develop a well-rounded understanding of the f-elements more generally and help to contextualise their bonding with respect to the much more extensively investigated transition metals.

Here, we will provide an update on our research to date, including the evolution of our work to include transuranium derivatives.<sup>13,14</sup> These complexes are now enabling quantification of actinide bonding and also actinide-actinide and actinide-lanthanide comparisons to be made. Certain comparisons have previously proven elusive for studies centred around thorium and uranium alone, so this work will demonstrate the value of studying transuranium chemistry, sometimes delivering novel actinide-ligand linkages before thorium and uranium analogues, despite the significant challenges associated with working with transuranium radioisotopes.

We thank the Engineering and Physical Sciences Research Council, European Research Council, Royal Society, ActUsLab, Euroatom ENEN+, Cost Association, US DOE-BES, The University of Manchester, European Union Joint Research Centre Karlsruhe, Los Alamos National Laboratory, and the National Nuclear Laboratory for generous funding and support of our work.

## References

1. Du J. *et al.*, Nat. Commun. 2021, 12, 5649.
2. Chatelain, L. *et al.*, Nat. Commun. 2020, 11, 337.
3. Du J. *et al.*, Nat. Commun. 2019, 10, 4203.
4. Wooles, A. J. *et al.*, Nat. Commun. 2018, 9, 2097.
5. Wildman, E. P. *et al.*, Nat. Commun. 2017, 8, 14769.
6. King, D. M. *et al.*, Nat. Commun. 2016, 7, 13773.
7. Gardner, B. M. *et al.*, Nat. Chem. 2015, 7, 582.
8. Cleaves, P. A. *et al.*, Angew. Chem. Int. Ed. 2014, 53, 10412.
9. King, D. M. *et al.*, Nat. Chem. 2013, 5, 482.
10. King, D. M. *et al.*, Science, 2012, 337, 717.
11. Boronski J. T. *et al.*, Nature 2021, 598, 72.
12. Liddle, S. T. Angew. Chem. Int. Ed. 2015, 54, 8604.
13. Dutkiewicz M. S. *et al.*, Nat. Chem. 2022, 14, 342.
14. Goodwin C. A. P. *et al.*, J. Am. Chem. Soc. 2022, 144, 9764.

---

\* Corresponding author. Tel.: +44-161-275-4612.  
E-mail address: steve.liddle@manchester.ac.uk

# Influence of the complexing site amino acids of calmodulin on its interaction with plutonium

L. Daronnat<sup>a\*</sup>, L. Berthon<sup>a</sup>, N. Boubals<sup>a</sup>, T. Dumas<sup>a</sup>, P. Moisy<sup>a</sup>, S. Sauge-Merle<sup>b</sup>, D. Lemaire<sup>b</sup>, C. Berthomieu<sup>b</sup>

<sup>a</sup>CEA, DES, ISEC, DMRC, Univ Montpellier, Marcoule, France

<sup>b</sup>CEA, DRF, BIAM, IPM, Univ Aix-Marseille, Cadarache, France

## Abstract

Pu is an actinide of major societal relevance due to its large stock worldwide and its key role in the cleanup challenges of legacy nuclear sites. Although its physiological impact has been widely investigated, understanding its interactions with biological molecules remains limited. The knowledge relative to actinide transportation mechanism, and in particular, the direct interaction of Pu at the molecular scale with proteins is still unclear. Recent publications have pointed that Pu interaction with transferrin or ferritin<sup>1</sup>, an iron carrier of blood, could be at the origin of its internalization in cells<sup>2</sup> and that calcium-binding proteins are possible Pu targets ( because as Pu, Ca is hard cation – strong Lewis acid)<sup>3</sup>.

This work aims at investigating the interaction between actinide elements, and more specifically plutonium, and biological molecules.<sup>4-6</sup> Calcium-binding EF-hand protein motifs of the calmodulin N-terminal domain, which contains seven coordination sites were chosen for this study. Calmodulin is an important protein expressed in all eukaryotic cells and is involved in a large number of signal transduction pathways.

In vivo, plutonium is mainly present at oxidation state +IV, and at this oxidation state, plutonium is a very high hydrolyses propensity. In this work, we will focus on the interaction of the plutonium (IV) with two variants of the calmodulin. CaM-WT, which is the wild type calmodulin, and CaME variant in which one threonine is replaced by one glutamate, thus increasing the number of hard donor carboxylate ligands in the binding site. Different routes taking into account the constraints due to the hydrolysis of plutonium (IV) at physiological pH have been used and will be discussed.

The interactions between Pu and calmodulin ligand were then characterized using visible and X-ray absorption spectroscopies and ESI-MS and showed the formation of different type of complexes for CaM-E and CaM-WT.

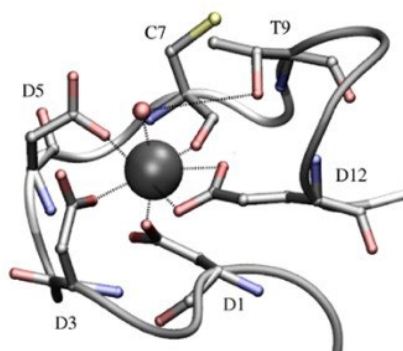


Figure 1. Complex calmodulin-plutonium

## References

1. Zurita et al., Chemistry- A European Journal, **2020**, 27,2393-2401
2. Jensen et al., Nature Chem. Biol., **2011**, 7, 560
3. Aryal et al., J. Proteomics, **2012**, 75, 1505
4. Sauge-Merle et al. Dalton Trans **2017**, 46, 1389-1396
5. Vidaud et al. Scientific Reports **2019**, 9, 17584
6. Sauge-Merle et al. Chemistry, A European Journal, **2017**, 23, 15505-15517

\* Corresponding author. Tel.: +33-624-05-2487;  
E-mail address: loic.daronnat@cea.fr.

## Radiation effects in americium ceramic compounds

Karin Popa<sup>a,\*</sup>, Jean-François Vigier<sup>a</sup>, Laura Martel<sup>a</sup>, Oliver Dieste Blanco<sup>a</sup>, Eric Colineau<sup>a</sup>, Jean-Christophe Griveau<sup>a</sup>, Daniel Freis<sup>a</sup>, Rudy J.M. Konings<sup>a</sup>

<sup>a</sup> European Commission, Joint Research Centre, Karlsruhe, Germany

---

### Abstract

The potential use of the decay heat of  $^{241}\text{Am}$  as a heat source in Radioisotope Power Systems for space exploration is under consideration by the European Space Agency. In this context, several ceramic compounds with substantial Am-contents (> 70 wt.%) were synthesized and investigated as potential space power source components in our laboratories.

These materials include oxides such as  $\text{Am}_x\text{U}_{1-x}\text{O}_2$  [1],  $\text{AmAlO}_3$  [2],  $\text{AmPO}_4$  [3],  $\text{AmVO}_3$  and  $\text{AmVO}_4$  [*unpublished results*]. Their aging was studied over several years by techniques such as PXRD, DTA-TG, Raman, MAS-NMR, SEM, and TEM. The effects of self-irradiation due to alpha-decay was different in these materials: (i) moderate swelling of the cell volume due to accumulation of defects with preservation of crystallinity in the fluorite structure [1]; (ii) important swelling of the cell volume followed by amorphization occurred in the perovskite structure [2]; (iii) shrinking of the cell volume followed by amorphization in the zircon structure; and (iv) a complex restructuring manifesting differently at micro- / microscale in the monazite structure [3].

We have also studied in detail the effects of the self-irradiation in fluorite by low-temperature heat-capacity measurements of  $\text{U}_{1-x}\text{Am}_x\text{O}_2$  ( $x=0.01$  and  $0.05$ ) solid solutions [*unpublished results*]. Two  $C_p$  anomalies were detected at low temperature in the freshly annealed materials, showing the effect of disorder induced in the crystal lattice by Am-substitution and the concomitant charge compensation. Their shape and magnitude are strongly affected by aging time due to the increasing disorder in the crystal lattice resulting from defect creation by the alpha decay of Am.

### References

1. Vigier, J.-F.; Freis, D.; Pöml, P.; Prieur, D.; Lajarge, P.; Gradeur, S.; Guiot, A.; Bouëxière, D.; Konings, R.J.M. *Inorganic Chemistry*, 2018, 57(8) 4317-4327.
2. Vigier, J.-F.; Popa, K.; Martel, L.; Manara, D.; Dieste Blanco, O.; Freis, D.; Konings, R.J.M. *Inorganic Chemistry*, 2019, 58(14) 9118-9126.
3. Popa, K.; Vigier, J.-F.; Martel, L.; Manara, D.; Colle, J.-Y.; Dieste Blanco, O.; Wiss, T.; Freis, D.; Konings, R.J.M. *Inorganic Chemistry*, 2020, 59(9) 6595-6620.

---

\* Corresponding author. Tel.: +49-7247-951148.  
E-mail address: karin.popa@ec.europa.eu

## Actinide–Actinide Bonding: A challenge for theory

Adam Jaroš, Cina Foroutan-Nejad, Michal Straka\**<sup>a</sup>Institute of Organic Chemistry and Biochemistry of the Czech Academy of Sciences, Flemingovo nám. 2, CZ-16610, Prague, Czech Republic***Abstract**

Actinide–actinide bonds are rare. Only a few experimental systems with An–An bonds have been observed so far, in particular the multiple bonds in U<sub>2</sub> and Th<sub>2</sub>, single Th–Th bond in Th<sub>2</sub>@C<sub>80</sub> and multiple one-electron two-center bonds in U<sub>2</sub>@C<sub>80</sub> and possibly in U<sub>2</sub>@C<sub>78</sub>. [1–2] We have investigated theoretically (DFT BP86) An–An bonds inside various fullerene cages (C<sub>70</sub>, C<sub>80</sub>, C<sub>90</sub>) across the Ac–Cm actinide series and showed that systems form cage-dependent An–An bonds, mostly OETC ones. [3–4] The bonding interactions were predicted even between two Pu atoms separated by 5.9 Å. Our most fresh investigations, however, unravel a strong dependence of the An–An bond orders, expressed, e.g. via the delocalization index from QTAIM analysis, or Mayers bond orders, on the method used. Pure DFT functionals predict stronger bonding interaction, i.e. more electron density between the actinide atoms, while hybrid and range-separated functionals predict weaker interactions, ca 3x smaller. A calibration study using CASPT2 and MC-pDFT calculations on the DFT optimized structures show that pure functionals predict better molecular structures, while the range-separated DFT functionals provide the most reliable description of An–An bonding. Thus, combination of different functionals for optimization and bonding analysis should be considered in the future studies of An–An bonding. [5]

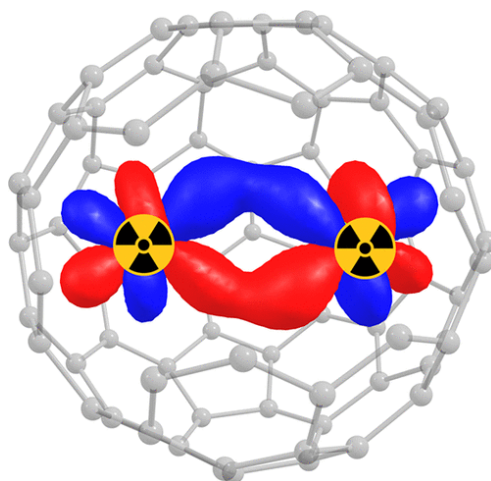


Figure 2 Example of a Pu–Pu OETC bond.

**Acknowledgments:** Czech Science Foundation, grant 21-17806S.

**References**

- [1] Acc. Chem. Res. 2019, **52**, 182.
- [2] Nat. Com. | 2021, **12**, 2372.
- [3] Jaroš et al: *From  $\pi$  bonds without  $\sigma$  bonds to the longest metal–metal bond ever: a survey on actinide–actinide bonding in fullerenes*. Inorg. Chem. 2020, **59**, 12608.
- [4] Foroutan-Nejad, et al *Unwilling U–U bonding in U<sub>2</sub>@C<sub>80</sub>: cage-driven metal–metal bonds in di-uranium fullerenes*. Phys. Chem. Chem. Phys. 2015, **17**, 24182.
- [5] Manuscript in preparation.

\* Corresponding author.

E-mail address: straka@uochb.cas.cz

# NMR spectroscopy of selected aqueous systems investigated at HZDR-IRE

Jérôme Kretzschmar\*, Thorsten Stumpf

*Helmholtz-Zentrum Dresden-Rossendorf, Institute of Resource Ecology, Bautzner Landstraße 400, 01328 Dresden, Germany*

---

## Abstract

Nuclear magnetic resonance (NMR) spectroscopy is a powerful method for both structure elucidation of molecules and their metal complexes, and also for studying their behavior in terms of thermodynamics and kinetics, as well as reactions occurring *in situ* in dependence on a variety of physico-chemical parameters. In this context, NMR spectroscopy of aqueous (D<sub>2</sub>O) solutions features some peculiarities. That is, first and foremost, the pH (pD) of the solution affects the speciation of both the molecule (ligand) and the metal ion (actinide or lanthanide) under study. Furthermore, the ligand can be subject to deuteration, and either component can undergo redox reactions.

The intracellularly occurring tripeptide glutathione (GSH) constitutes a redox equilibrium with its oxidized (dimeric) form glutathione disulfide (GSSG). Hexavalent uranium, U(VI), forms complexes with the latter over a wide pH range, while GSH reduces U(VI) to U(IV). However, the redox reaction occurs only between pH 6 and 10, *i.e.* close to the thiol group's pK<sub>a</sub>, presumably due to homolytic cleavage of the S–H group in GSH's cysteine residue. The redox reaction appears to take place intermolecularly without the need for U(VI) complexation by the reductant [1, 2].

Uranyl(VI) citrate dimeric and trimeric complexes exhibit interesting structural and (<sup>17</sup>O) NMR spectroscopic features such as superstructure formation upon varying pH or concentration, and polarization of uranyl units acting as Lewis base in metal ion coordination (O=U=O→M<sup>n+</sup>) [3, 4]. Irradiation of uranyl(VI) citrate by visible light yields complexes of lower valent uranium. The reaction again occurs intermolecularly, whereby *in situ* oxidation of excessive ligand through several intermediates can be comprehended by NMR spectroscopy.

In case of U(VI) and the flavonoid quercetin, complex formation and light-induced redox reaction were studied by NMR and EPR spectroscopy, respectively. The latter revealed a single-electron transfer upon formation of a quercetin radical and U(V) [5].

In studies investigating the interaction of radionuclides (RNs) with a solid phase in equilibrium with an aqueous phase, the influence of organics on RN retention can be complemented by qualitative and quantitative solution NMR methods by determining their speciation (free, metal ion-bound, oxidized) and concentration in the supernatant.

NMR spectroscopy can also be utilized as a robust and elegant method for determining ligand's pK<sub>a</sub> along with the originating site of the abstracted proton as shown for GSH/GSSG, 2-phosphonobutane-1,2,4-tricarboxylic acid (PBTC), as well as nitrilotriacetate (NTA) and ethylene glycol-bis(aminoethyl ether)-*N,N,N',N'*-tetraacetic acid (EGTA) [6]. The latter two, being representatives of the so-called complexones, show Lewis acid-catalyzed *in situ* deuteration of the *N*-acetyl methylene groups in NaOD media, which is applied for speciation analyses in artificial body fluids by means of <sup>2</sup>H NMR spectroscopy as the only deuterated component.

## Acknowledgement

This research received funding by the German Federal Ministry for Economic Affairs and Energy (BMWi) within the GRaZ II projects, nos. 02E11860B and 02E11860G, the German Federal Ministry of Education and Research (BMBF) within the RADEKOR project, no. 02NUK057A, as well as by the European Union's Horizon 2020 research and innovation programme's CORI project, no. 847593.

## References

- [1] Kretzschmar, J.; Haubitz, T.; et al. *Chem. Commun.*, 2018, 54, 8697–8700.
- [2] Kretzschmar, J.; Strobel, A.; et al. *Inorg. Chem.*, 2020, 59, 4244–4254.
- [3] Kretzschmar, J.; Tsushima, S.; et al. *Chem. Commun.*, 2020, 56, 13133–13136.
- [4] Kretzschmar, J.; Tsushima, S.; et al. *Inorg. Chem.*, 2021, 60, 7998–8010.
- [5] Kretzschmar, J.; Gericke, R.; et al. *J. Hazard Mater.*, *manuscript submitted*.
- [6] Kretzschmar, J.; Wollenberg, A.; et al. *Molecules*, *manuscript submitted*.

---

\* Corresponding author. Tel.: +49-351-260-3136; fax: +49-351-260-3553.  
E-mail address: j.kretzschmar@hzdr.de.

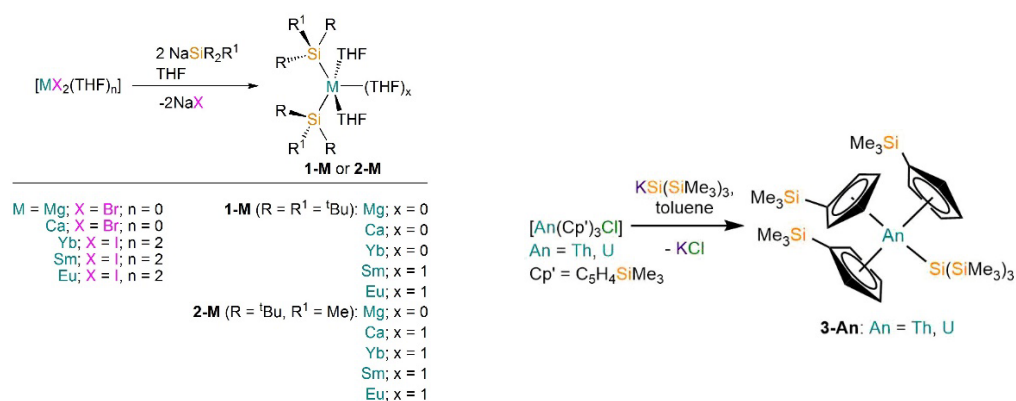
## Recent Adventures in Lanthanide and Actinide Silicon Chemistry

David P. Mills\*, Benjamin L. L. Réant, Victoria E. J. Berryman, Annabel R. Basford, Lydia E. Nodaraki, Ashley J. Wooles, Floriana Tuna, John A. Seed, Alasdair Formanuk, Nikolas Kaltsoyannis\*, and Stephen T. Liddle\*

\*The University of Manchester, Department of Chemistry, Oxford Road, Manchester, M13 9PL, U.K.

## Abstract

Compared to the extensive array of f-block compounds supported by carbon, nitrogen, and oxygen ligands there are comparatively few silicon congeners.<sup>1</sup> In recent years there have been an increasing number of f-block metal-silicon bonds being prepared and studies in order to better understand the physicochemical properties of these linkages. One method that has been extensively used to experimentally probe the nature of metal-ligand linkages is Nuclear Magnetic Resonance (NMR) spectroscopy, which provides chemical shift data; this can be a direct probe of the electronic environment, and when combined with Density Functional Theory (DFT) it becomes a powerful reporter of the amount of covalency.<sup>2</sup> Here we present some of our recent results in lanthanide (Ln) and actinide (An) silicon chemistry.



Scheme 1. Left: Synthesis of **1-M** and **2-M**. Right: Synthesis of **3-An**.

The M(II) complexes  $[M(Si^iBu_3)_2(THF)_2(THF)_x]$  (**1-M**) and  $[M(Si^iBu_2Me)_2(THF)_2(THF)_x]$  (**2-M**) have been synthesised and characterised (Scheme 1, M = Mg, Ca, Yb, No; No *in silico* due to experimental unavailability). DFT calculations and <sup>29</sup>Si NMR spectroscopy of **1-M** and **2-M** together with {Si(SiMe<sub>3</sub>)<sub>3</sub>}, {Si(SiMe<sub>2</sub>H)<sub>3</sub>}, and {SiPh<sub>3</sub>}-substituted known analogues provides twenty representative examples spanning five silanide ligands and four metals. Having this family of molecules has permitted us to elucidate trends as a function of varying the metal or silanide substituents. Calculations indicate that the covalency of these M(II)–Si linkages is ordered as No(II) > Yb(II) > Ca(II) ~ Mg(II), challenging the traditional view of late An chemical bonding being equivalent to the late Ln.<sup>3</sup> The An(IV) complexes  $[An(Cp')_3\{Si(SiMe_3)_3\}]$  (**3-An**, An = Th, U; Cp' = C<sub>5</sub>H<sub>4</sub>SiMe<sub>3</sub>) were synthesized by salt metathesis protocols (Scheme 1),<sup>4</sup> allowing us to directly compare Th–Si and U–Si chemical bonds. <sup>29</sup>Si NMR spectroscopy was used to detect the metal-bound silicon resonances, with the signal for the U(IV) complex ( $\delta_{Si}$ : –137.09 ppm) paramagnetically shifted from that of the Th(IV) example ( $\delta_{Si}$ : –108.92 ppm). DFT calculations showed that the An%:Si% 7s-, 6d- and 5f-orbital contributions are similar in **3-Th** and **3-U**, with the latter showing marginally greater covalency.

We thank the University of Manchester (UoM) for a PhD studentship for B.L.L.R. (Nuclear Endowment), a postdoctoral fellowship to V.E.J.B., and for access to the Computational Shared Facility. We thank the Engineering and Physical Sciences Research Council (EP/R002605X/1, EP/P001386/1, EP/M027015/1, and EP/N022122/1) and European Research Council (CoG-816268 and CoG-612724) for funding, and the EPSRC UK National Electron Paramagnetic Resonance Service for access to the EPR facility and SQUID magnetometer and Mr Carlo Bawn and Dr Ralph Adams at the UoM Chemistry NMR service for assisting with <sup>171</sup>Yb NMR spectroscopic measurements

## References

1. Réant B. L. L. *et al.*, Chem. Sci., 2020, 11, 10871–10886.
2. Smiles D. E. *et al.*, J. Am. Chem. Soc., 2016, 138, 814–825, and references cited herein.
3. Réant B. L. L. *et al.*, J. Am. Chem. Soc., 2021, 143, 9813–9824.
4. Réant B. L. L. *et al.*, Chem. Commun., 2020, 56, 12620–12623.

\* Corresponding authors. David P. Mills. Tel.: +44-161-27-54606, Nikolas Kaltsoyannis, Stephen T. Liddle.

E-mail addresses: david.mills@imanchester.ac.uk, nikolas.kaltsoyannis@manchester.ac.uk, stephen.liddle@manchester.ac.uk

## Relativistic calculations of hyperfine coupling in molecules

Nicholas F. Chilton<sup>a,\*</sup>, Letitia Birnoschi<sup>a</sup>, Eric J. L. McInnes<sup>a</sup><sup>a</sup>Department of Chemistry, The University of Manchester, Oxford Road, Manchester, UK**Abstract**

Magnetic resonance techniques are able to accurately probe the interactions between electron spins, nuclear spins and external magnetic fields. This information is commonly encoded into a set of effective spin Hamiltonian parameters by a modelling procedure. Of particular interest are hyperfine coupling constants (HFCCs), which display a strong dependence on the unpaired electron (spin) density, thus providing important insight into chemical bonding.<sup>1</sup> The interpretation of isotropic HFCCs as measures of spin density at the nucleus is based on a non-relativistic Schrödinger-Pauli framework.<sup>2</sup> However, this formalism breaks down for heavy elements, as the significant relativistic effects require a 4-component Dirac treatment. However, 4-component electronic structure approaches are unfeasible for all but the simplest systems. The computational cost can be reduced by decoupling the electronic and the positronic degrees of freedom in the Dirac Hamiltonian *via* a unitary transformation. We have recently developed a new tool, called *HYPERION*, to calculate relativistic HFCCs from active space wavefunctions, with or without spin-orbit coupling using an exact 2-component framework.<sup>3</sup>

Herein, we demonstrate the use of *HYPERION* to obtain HFCCs for  $[\text{U}(\text{Cp}^{\text{t}})_3]$  and  $[\text{Th}(\text{Cp}^{\text{t}})_3]$  which have previously been studied with pulsed EPR.<sup>1,4</sup> We find that non-relativistic interpretations of HFCCs from spin Hamiltonian modelling are unreliable and substantial differences in spin-density, with implications for covalency, are obtained from the present calculations which provide accurate predictions of the experimental spectra. This work paves the way for predictive calculations of HFCC for real actinide complexes, ushering in new interpretations of magnetic resonance spectra for such materials.

We acknowledge the MoD (UK) for funding.

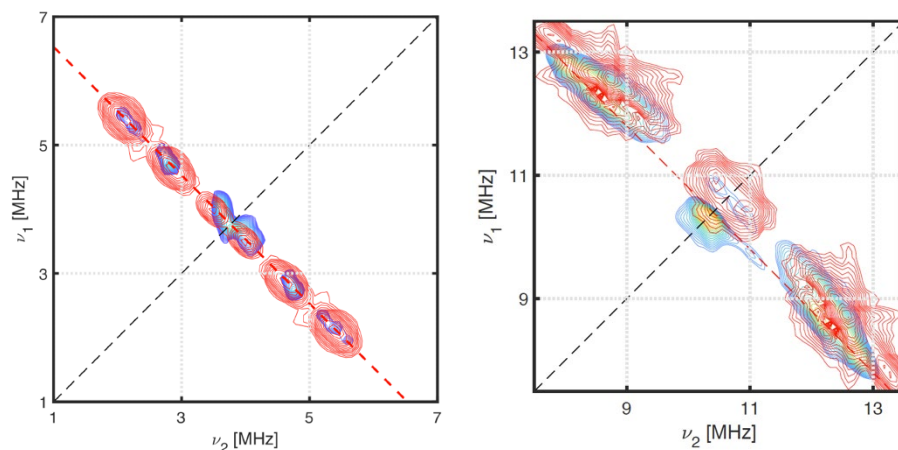


Figure 3 (left)  $^{13}\text{C}$  HYSCORE spectrum in the  $g$  parallel region for  $[\text{Th}(\text{Cp}^{\text{t}})_2]$  at 351.6 mT (blue contours) and *HYPERION* simulation based on a RAS(19,27)SCF-SO calculation (red). (right)  $^1\text{H}$  HYSCORE spectrum in the  $g_x$  region for  $[\text{U}(\text{Cp}^{\text{t}})_2]$  at 244.3 mT (blue contours) and *HYPERION* simulation based on a RAS(29,35)CI-SO calculation (red).

**References**

1. Formanuk, A. *et al. Nature Chem.* 9, 578–583 (2017).
2. Kutzelnigg, W., *Theor. Chim. Acta* 73, 173–200 (1988).
3. Birnoschi, L.; Chilton, N. F. *submitted*
4. Birnoschi, L.; McInnes, E. J. L.; Chilton, N. F. *submitted*

\* Corresponding author. Tel.: +44 161 2754 584.  
E-mail address: nicholas.chilton@manchester.ac.uk

# Fluorine-19 NMR Study of Electronic Structure in Actinide Tetrafluorides

Herman Cho<sup>a,\*</sup>, Eric Walter<sup>a</sup>, Cigdem Capan<sup>b</sup>, Gian Surbella<sup>a</sup>, Sejun Park<sup>a</sup>, Amanda Casella<sup>a</sup>, Jennifer Carter<sup>a</sup>, Bruce McNamara<sup>a</sup>, Chuck Soderquist<sup>a</sup>, Sergey Sinkov<sup>a</sup>, Richard Clark<sup>a</sup>, Forrest Heller<sup>a</sup>, Lucas Sweet<sup>a</sup>, Jordan Corbey<sup>a</sup>

<sup>a</sup>Pacific Northwest National Laboratory, P. O. Box 999, Richland, Washington 99354, USA

<sup>b</sup>Washington State University Tri-Cities, Richland, Washington 99352, USA

## Abstract

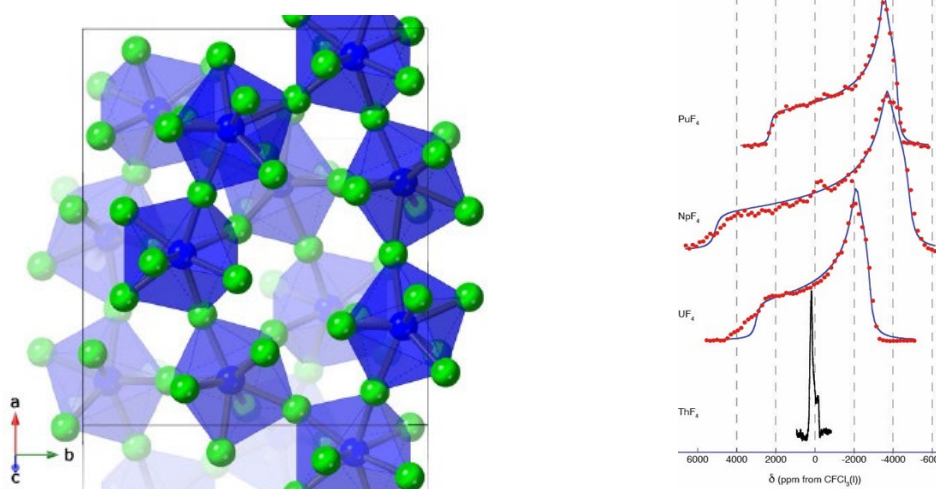
The actinide elements from thorium to californium form stable tetrafluoride solids with the same monoclinic unit cell (Fig. 1a).<sup>1</sup> The actinide tetrafluorides (AnF<sub>4</sub>) therefore present a unique platform for a systematic survey of electronic structure across the 5f row of the periodic table.

We have probed the electronic structure in a series of actinide tetrafluorides through measurements of the anisotropic local magnetic fields by solid state <sup>19</sup>F nuclear magnetic resonance (NMR) spectroscopy.<sup>2,3</sup> With the exception of ThF<sub>4</sub>, the metal centers in all of the tetrafluorides will have a partially filled valence shell, leading to large <sup>19</sup>F shifts and fast relaxation caused by the hyperfine interaction. The <sup>19</sup>F spectra reveal that the shielding anisotropy is invariant, which is evidence for a simple scaling of the magnetic shielding tensor across the series. The magnitudes of the hyperfine field display a more complicated dependence on the number of valence electrons, which has been compared with predictions derived from idealized models of the electronic structures of the An(IV) center. Pronounced deviations from the predicted behavior are seen, suggesting that the metals in AnF<sub>4</sub> cannot be described as simple f<sup>n</sup> atoms.

## References

- Haire, R. G.; Asprey, L. B. Inorg. Nucl. Chem. Lett., 1973, 9, 869-874.
- Capan, C.; Dempsey, R. J.; Sinkov, S.; McNamara, B. K.; Cho, H. Phys. Rev. B, 93, 224409.
- Walter, E. D.; Capan, C.; Casella, A. J.; Carter, J. C.; McNamara, B. K.; Soderquist, C. Z.; Sinkov, S. I.; Clark, R. A.; Heller, F. D.; Sweet, L. E.; Corbey, J. F.; Cho, H. J. Chem. Phys., 2021, 154, 211101.

Figure 4: Unit cell of AnF<sub>4</sub> viewed perpendicular to the ab plane, with An and F atoms in blue and green spheres, respectively (*left*); room temperature <sup>19</sup>F NMR spectra of AnF<sub>4</sub> powders recorded in an applied field of 7.046 T. Red dots represent amplitudes of spectra acquired at the indicated frequency (*right*).



\* Corresponding author. Tel.: +1-509-372-6046  
E-mail address: hm.cho@pnnl.gov.

# Covalency in Actinide Organometallics from Carbon K-edge XAS and Electronic Structure Calculations

Stefan Minasian<sup>a,\*</sup>, Jochen Autschbach<sup>b</sup>, Enrique Batista<sup>c</sup>, Jacob Branson<sup>a</sup>, David Clark<sup>c</sup>, Alexander Ditter<sup>a</sup>, Gaurab Ganguly<sup>b</sup>, Olivia Gunther<sup>a</sup>, Jason Keith<sup>c</sup>, Stosh Kozimor<sup>c</sup>, Richard Martin<sup>c</sup>, Danil Smiles<sup>a</sup>, Yusen Qiao<sup>a</sup>, Dumitru-Claudiu Sergentu<sup>b</sup>, David Shuh<sup>a</sup>, Chantal Stieber<sup>d</sup>, Taoxiang Sun<sup>e</sup>, Tolek Tyliszczak<sup>a</sup>

<sup>a</sup>Lawrence Berkeley National Laboratory, Chemical Sciences Division, Berkeley, CA 94720, United States

<sup>b</sup>University at Buffalo, State University of New York, Department of Chemistry, Buffalo, NY 14260, United States

<sup>c</sup>Los Alamos National Laboratory, Chemistry and Theory Divisions, Los Alamos, NM 87545, United States

<sup>d</sup>California State Polytechnic University, Pomona, California 91768, United States

<sup>e</sup>Tsinghua University, Institute of Nuclear and New Energy Technology, Beijing 100084, China

## Abstract

Researchers at Lawrence Berkeley National Laboratory and their collaborators have shown previously that measuring X-ray absorption spectra (XAS) at the K-edges for light atoms directly bound to actinide centers (collectively referred to as "Ligand K-edge XAS") is an effective approach for evaluating periodic changes in f-electron behavior. Efforts to advance computational methodology for actinides benefit greatly from ligand K-edge XAS, because the technique provides high energy resolution, feature-rich spectra while also probing interactions with both the 5f- and 6d-orbitals. Our experimental measurements of C, N, O, and F K-edge XAS have been facilitated by access to the scanning transmission X-ray microscope (STXM) on ALS beamline 11.0.2, which can mitigate the self-absorption and saturation effects that can thwart measurements on non-conducting systems. Our studies of metal–oxygen bonding in small molecules and extended solids have provided new experimental evidence of covalent 5f-orbital mixing in actinide bonds, and help unravel the complex behavior of covalent (band-like) vs ionic (atomic-like) f-electrons. Our previous studies of actinidechlorine and actinide-oxygen bonding described above prompted some new investigations of electronic structure in organometallics. New carbon K-edge XAS data were obtained for  $(C_8H_8)_2Ce$  to compare with earlier studies on  $(C_8H_8)_2Th$  and  $(C_8H_8)_2U$ .<sup>1</sup> Together with theory, the amount of f-orbital mixing in the  $\delta$ -bonding orbitals of  $e_{2u}$  symmetry was found to be nearly equivalent for  $(C_8H_8)_2Ce$  (24% C 2p, 76% Ce 4f) and  $(C_8H_8)_2U$  (28% C 2p, 71% U 5f). However, differences in the amount of orbital overlap result in a much greater increase in stability due to covalent bonding for  $(C_8H_8)_2U$ . To explore the limits of this behavior we also conducted C K-edge XAS measurements on  $[(C_7H_7)_2U]^{1-}$ , which is the only example of a pentavalent actinide metallocene.<sup>2</sup> Because  $[(C_7H_7)_2U]^{1-}$  is known to have a multiconfigurational ground state, *ab initio* calculations were necessary to accurately simulate the spectra (Figure 1). Enhanced 5f- $\delta$  mixing was also observed for  $[(C_7H_7)_2U]^{1-}$  in comparison with tetravalent  $(C_8H_8)_2U$ , as a possible consequence of lower energy 5f orbitals for the  $U^{5+}$  vs.  $U^{4+}$  metals. This presentation will discuss these measurements, as well as recent results from our ongoing efforts to synthesize transuranic organometallic complexes.

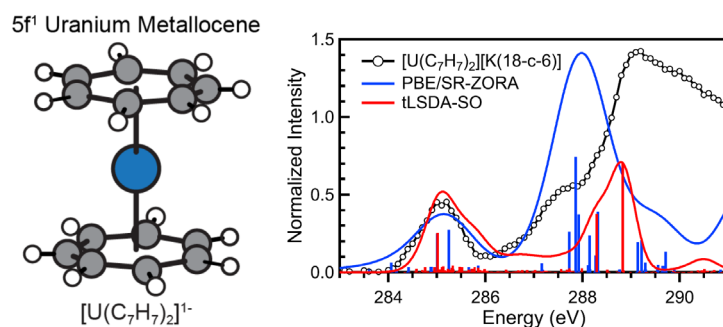


Figure 1. Carbon K-edge XAS for  $[U(C_7H_7)_2]^{1-}$ . The experimental spectrum (black) is compared with calculated spectra using scalar-relativistic TDDFT (blue) and *ab initio* calculations with spin-orbit coupling (red). Although both calculations show the similar low-energy features, higher energy transitions are best reproduced with *ab initio* methods.

## References

- Smiles, D. E.; Batista, E. R.; Booth, C. H.; Clark, D. L.; Keith, J. M.; Kozimor, S. A.; Martin, R. L.; Minasian, S. G.; Shuh, D. K.; Stieber, S. C. E.; Tyliszczak, T. *Chem. Sci.* **2020**, *11*, 2796-2809.
- Qiao, Y.; Ganguly, G.; Booth, C. H.; Branson, J. A.; Ditter, A. S.; Lussier, D. J.; Moreau, L. M.; Russo, D. R.; Sergentu, D.-C.; Shuh, D. K.; Sun, T.; Autschbach, J.; Minasian, S. G. *Chem. Commun.* **2021**, *57*, 9562-9565.

\* Corresponding author. Tel.: +1 510-229-9429  
E-mail address: sgminasian@lbl.gov.

# Enhancing Frontier Orbital Interactions in the f-Block Through Applications of Pressure and Electric Fields

Thomas Albrecht-Schönzart<sup>a</sup>

<sup>a</sup>Florida State University, Tallahassee, Florida 32306 USA

---

## Abstract

In this talk we will explore two methods for enhancing the mixing of the frontier orbitals of lanthanides and actinides with ligand orbitals with goal of gaining greater control of the electronic properties of these elements. The first approach will utilize highly polarized ligands whose dipoles will in turn polarize the electron density around *f*-block metal centers. We will show that the design of such ligands is straightforward as is calculating their hyperpolarizabilities and dipole moments. Thus, this methodology provides a broad framework for enhancing hybridization of the metal-ligand interactions. Moreover, the substituents used to achieve the large dipoles also affects the metal-ligand bond dissociation energies, and thus can also be used to achieve selectivity for specific metal ions over others. Finally, these complexes display a number of atypical properties that result from a large degree of anisotropy around the metal ions. These spectroscopic signatures will also be elaborated on.

The second approach is the application of high pressures to *f*-block molecules and materials as a method for compressing M–L bonds and forcing a greater degree of orbital overlap and mixing than occurs at ambient pressure. To achieve this, lanthanide and actinide compounds are subjected to pressures as high as 40 GPa using diamond-anvil cells. In this portion of the talk will show truly dramatic changes in the local coordination environment, spectroscopic features, and through theoretical analyses, large changes in bonding. The observation that unites both approaches is that even small changes in frontier orbital involvement cause large changes structural and spectroscopic features as well as physical properties.

---

\* Corresponding author.

Early An(IV) complexes with *N*-donor ligandsJuliane März<sup>a,\*</sup>, Sebastian Fichter<sup>a,b</sup>, Michael Patzschke<sup>a</sup>, Peter Kaden<sup>a</sup>, Luisa Köhler<sup>a</sup>, Moritz Schmidt<sup>a</sup>, Thorsten Stumpf<sup>a</sup><sup>a</sup>Institute of Resource Ecology, Helmholtz-Zentrum Dresden-Rossendorf, Bautzner Landstraße 400, 01328 Dresden, Germany<sup>b</sup>Institute of Ion Beam Physics, Helmholtz-Zentrum Dresden-Rossendorf, Bautzner Landstraße 400, 01328 Dresden, Germany**Abstract**

The *5f* electrons of particularly the early actinides are found to participate in bonding, e.g. to organic ligands, in contrast to the strongly shielded *4f* electrons of the lanthanides. Reactivity and complexation strength of such bonds are affected by donor properties of the ligand and the electronic situation of the actinide metal center. Furthermore, coinciding properties of ligand and actinide ion regarding Pearson's principle of hard and soft acids and bases (HSAB) can even drive the development of selective ligands, e.g. for extraction processes. Here, soft *N*-donor ligands were found to interact stronger with trivalent actinides in comparison to their ~~harder~~ lanthanide analogues.<sup>1</sup>

To evaluate how these electronic properties can be extended to a series of tetravalent actinides and their interactions with *N*-donor ligands, we have studied the complexation of tetravalent Th, Pa, U, Np, and Pu with the amidinate (*S,S*)-*N,N'*-bis-(1-phenylethyl)-benzamidine (PEBA), and the *Schiff* base *N,N'*-ethylene-bis((pyrrole-2-yl)methanimine (pyren)).<sup>2-4</sup>

Complex syntheses using one equivalent of AnCl<sub>4</sub>(dme)<sub>x</sub> (An = Th, U, Np, Pu; x = 0 for U, x = 2 for Th, Np, Pu) and three equivalents of PEBA, or two equivalents of pyren led to isostructural heteroleptic 3:1 complexes [AnCl(PEBA)<sub>3</sub>] or homoleptic 2:1 complexes [An(pyren)<sub>2</sub>]. Both series were analyzed in the solid state by SC-XRD and IR, as well as in solution by NMR spectroscopy. SC-XRD results and quantum chemical calculations (QCC) revealed differences in An<sup>IV</sup>-ligand bond length and strength between the different nitrogen donors (N<sub>amidinate</sub>, N<sub>imine</sub>, N<sub>pyrrolide</sub>). In addition, with the help of QCC, trends regarding the covalency of the metal-ligand bonds could be derived and assigned to the involved orbitals. Delocalization indices for N–Pa<sup>IV</sup> showed a strong preference of the highly polarizable *5f*<sup>1</sup> configuration of Pa<sup>IV</sup> to pyren in its homoleptic complex. This effect disappears in the heteroleptic amidinate complex. Calculated quadrupole moments give a first explanation, showing an isotropically distributed charge around Pa<sup>IV</sup> in [Pa(pyren)<sub>2</sub>] but a polarization in [PaCl(PEBA)<sub>3</sub>].

Halogen exchange reactions of Cl in [AnCl(PEBA)<sub>3</sub>] was successful for F, Br, and N<sub>3</sub> (see Fig. 1). NMR spectra revealed a strong effect of the halogen on the paramagnetic shift, potentially again indicating the impact of the halogen on the polarizability of charge around the tetravalent actinide.

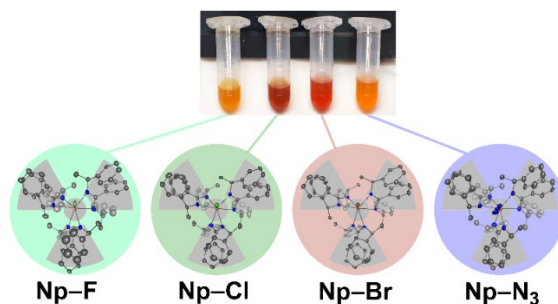


Figure 6. Complex solutions and SC-XRD molecular structures of [NpX(PEBA)<sub>3</sub>] with X = F, Cl, Br, N<sub>3</sub>

**References**

1. M. Miguirditchian, D. Guillauneux, D. Guillaumont, P. Moisy, C. Madic, M. P. Jensen, K. L. Nash, *Inorg. Chem.* **2005**, *44* (5), 1404-1412.
2. S. Fichter, S. Kaufmann, P. Kaden, T. Brunner, T. Stumpf, P. W. Roesky, J. März, *Chem. Eur. J.* **2020**, *26*, 8867-8870
3. R. Kloditz, S. Fichter, S. Kaufmann, T. S. Brunner, P. Kaden, M. Patzschke, T. Stumpf, P.W. Roesky, M. Schmidt, J. März, *Inorg. Chem.* **2020**, *59* (21), 15670-15680.
4. L. Köhler, M. Patzschke, M. Schmidt, T. Stumpf, J. März, *Chem. Eur. J.* **2021**, *27*, 18058–18065.

\* Corresponding author. Tel.: +49-351-260-3209.

E-mail address: j.maerz@hzdr.de.

## Small Scale Pyrochemistry with In-situ Material Doping

S.A. Simpson<sup>a</sup>, D.J. Roberts<sup>a</sup>, A.M. Parkes<sup>b</sup>, A.J. Swift<sup>a,\*</sup>, C. Zhang<sup>a</sup>, K. R. Holliday<sup>a</sup>

<sup>a</sup>Lawrence Livermore National Lab, 7000 East Ave, Livermore CA, United States of America

<sup>b</sup>AWE plc, Aldermaston, Reading RG7 4PR, United Kingdom

---

### Abstract

The Pu facility at Lawrence Livermore National Laboratory has demonstrated the full pyrochemical flowsheet at the 200g scale in order to meet the needs of various plutonium science programs. Interest in the aging behavior of plutonium has led to the need for producing accelerated aged alloys. Doping weapons grade Pu with various quantities of Pu-238 accelerates the long-term aging process of Pu allowing for studies at an accelerated rate. The processes needed to produce such an alloy include modified Direct Oxide Reduction (DOR), a Molten Salt Extraction (MSE), electrorefining (ER), alloying, casting, rolling and annealing. The first batch of this project processed metallic weapons-grade Pu through an MSE and ER, resulting in a 99.8% pure product. This initial batch will be used as the baseline for the aging comparisons. The second project batch started with a modified DOR comprised of 200g of weapons-grade Pu metal and 15g of Pu-238 oxide. During this process, the oxide was reduced to metal and consolidated into the metallic weapons grade Pu. In this presentation we discuss the challenges of scaling down these operations and the equipment modifications that were necessary for success.

This work was performed under the auspices of the U.S. Department of Energy by Lawrence Livermore National Laboratory under Contract DE-AC52-07NA27344.

---

\* Corresponding author. Tel.: +1 925-423-7582  
E-mail address: Swift25@llnl.gov

# Paramagnetic NMR in actinide complexes: experiment and modeling.

Hélène Bolvin<sup>a,\*</sup>, Md. Ashraful Islam<sup>a</sup>, Matthieu Autillo<sup>b</sup>, Claude Berthon<sup>b</sup>

<sup>a</sup>Laboratoire de Chimie et de Physique Quantiques, Université Toulouse 3, France

<sup>b</sup>CEA, DES, ISEC, DMRC, Univ Montpellier, Marcoule, France

---

## Abstract

Paramagnetic NMR (pNMR) measures the NMR chemical shift of paramagnetic complexes compared to their diamagnetic counterpart. This shift may be split into *dipolar* terms, arising from the magnetic dipolar interaction between the metal center and the NMR active nucleus, and the *contact* term, due to the spin delocalization leaking from the paramagnetic center towards the ligand<sup>1</sup>.

In this presentation, we will illustrate the diversity of information provided by pNMR chemical shifts measured on different nuclei of the ligands coordinated to actinide cations, the so-called Actinide Induced Shifts (AIS).

On one hand, when the dipolar term is dominant, the AIS gives access to the magnetic susceptibility tensor. Further, the temperature dependence allows to determine the energy levels and magnetic parameters of actinyls cations<sup>4</sup>. We will show that in some cases, the AIS provides structural information, as it is the case in biological molecules.

On the other hand, when the contact term is dominant, the AIS allows an experimental determination of the spin densities of the ligands, and the hyperfine contact constants of the NMR active nuclei. This allows to access to the degree of covalency in the actinide – ligand bonding<sup>5,6</sup>.

In lanthanide complexes, pNMR chemical shifts are efficiently modeled using crystal-field theory, but due to the larger covalent effects in actinide complexes, those models do not apply to actinide complexes. This will be shown by analyzing the trends of the crystal-field parameters in two series of actinide complexes<sup>2,3</sup>. We will show how *ab initio* CAS based and DFT methods are complementary tools to the experimental data in order to unravel the dipolar and contact contributions.

## References

1. M. Autillo, L. Guerin, T. Dumas, M. S. Grigoriev, A. M. Fedoseev, S. Cammelli, P. L. Solari, P. Guilbaud, P. Moisy, H. Bolvin, C. Berthon *Chem. Eur. J.* **25**, 4435 (2019).
2. J. Jung, M. A. Islam, V. L. Pecoraro, T. Mallah, C. Berthon, H. Bolvin *Chem. Eur. J.* , **25**, 15112 – 15122 (2019).
3. M. Autillo, Md. A. Islam, J. Jung, J. Pilmé, N. Galland, L. Guerin, P. Moisy, C. Berthon, C. Tamain, H. Bolvin *Phys. Chem. Chem. Phys.* **22**, 14293 (2020)
4. M. Autillo †, Md. A. Islam †, J. Héron, L. Guérin, E. Acher, C. Tamain, M. C. Illy, P. Moisy, E. Colineau, J. C. Griveau, C. Berthon, H. Bolvin *Chem. Eur. J.*, **27**, 7138 (2021).
5. L. Martel, Md. A. Islam, K. Popa, J. F. Vigier, E. Colineau, H. Bolvin, J. C. Griveau *J. Phys. Chem. C*, **125**, 22163–22174 (2021).
6. M. A. Islam, M. Autillo, L. Guerin, C. Tamain, P. Moisy, H. Bolvin, C. Berthon submitted

---

\* Corresponding author.

E-mail address: bolvin@irsamc.ups-tlse.fr

# Actinide samples from Mainz University for applications in chemistry and physics research

Ch.E. Düllmann<sup>a,b,c,\*</sup>, E. Artes<sup>a,b,c</sup>, S. Berndt<sup>a</sup>, A. Dragoun<sup>a,c</sup>, K. Eberhardt<sup>a</sup>, R. Haas<sup>a,b,c</sup>,  
C.-C. Meyer<sup>a,c</sup>, L. Reed<sup>a,c</sup>, D. Renisch<sup>a,c</sup>, M. Rapps<sup>a(†)</sup>, J. Runke<sup>a,c</sup>, C. Mokry<sup>a,c</sup>,  
P. Thörle-Pospiech<sup>a,c</sup>, N. Trautmann<sup>a</sup>

<sup>a</sup>Department of Chemistry – TRIGA Site, Johannes Gutenberg University Mainz, Fritz-Strassmann-Weg 2, 55128 Mainz, Germany

<sup>b</sup>GSI Helmholtzzentrum für Schwerionenforschung GmbH, Planckstrasse 1, 64291 Darmstadt, Germany

<sup>c</sup>Helmholtz Institute Mainz, Staudinger Weg 18, 55128 Mainz, Germany

Rare actinide isotopes are essential in many basic science research projects, yet working with them always features unique aspects, especially due to their limited availability and often high radioactivity. Collaborations from different fields therefore regularly rely on our expertise in the production and characterization of tailor-made actinide samples.

In recent years, we produced different samples of <sup>233</sup>U and of its daughter <sup>229</sup>Th, because <sup>229</sup>Th features the lowest-lying known nuclear excited state, at  $\approx 8.2$  eV excitation energy [1]; this state is populated in about 2% of the <sup>233</sup>U  $\alpha$  decays [2]. The state's low excitation energy can in principle be reached by optical laser excitation; the <sup>229m</sup>Th is therefore in the center of efforts to construct a “nuclear clock”, based on oscillations in the nucleus rather than in the electronic shell as in classical atomic clocks [3], and currently, the exact determination of the excitation energy with “laser” precision is ongoing. Many known properties of <sup>229m</sup>Th were elucidated using samples from Mainz [1,2]. Th isotopes are also in the focus of high precision spectroscopy studies of physics beyond the standard model [4], as are studies of other low-excited states like <sup>235m</sup>U situated at  $\approx 77$  eV, provided by <sup>239</sup>Pu recoil ion sources from Mainz.

Neutron-rich <sup>244</sup>Pu, <sup>243</sup>Am, <sup>248</sup>Cm, <sup>249</sup>Bk, and <sup>249</sup>Cf serve as targets for accelerator experiments on the synthesis, nuclear, and chemical properties of the heaviest elements at GSI Darmstadt [5-9]; even-Z ones were also used in nuclear reaction studies at ANU Canberra, Australia, to aid in the choice of the best reaction towards elements with  $Z > 118$  [10].

Other recently produced actinide samples include: <sup>248</sup>Cm for the muX collaboration working at PSI Switzerland for muonic spectroscopy aiming at determining the nuclear charge radius [11]; <sup>249</sup>Cf targets for the determination of the first ionization potential of the last actinide element, lawrencium at JAEA Tokai, Japan [12]; fission cross section studies on <sup>242</sup>Pu performed at CERN n\_TOF [13] and the HZDR nELBE facility [14]; actinide laser spectroscopy in Mainz including experiments with the heaviest macroscopically available elements, Es and Fm [15].

Most samples were prepared by the electrochemical “Molecular Plating” deposition technique [16]. To overcome some of the limitations of this technique, a drop-on-demand printing method was developed [17], and more recently also a spin-coating technique [18] suitable for actinide thin film production. At the workshop, an overview of actinide sample production and characterization activities in Mainz will be presented.

## References

1. v. d. Wense et al., Nature 533 (2016) 47; Seiferle et al., Nature 573 (2019) 243; Sikorsky et al., Phys. Rev. Lett. 125 (2020) 142503.
2. Thielking et al., Nature 556 (2018) 321.
3. Peik and Tamm, Europhys. Lett. 61 (2003) 181.
4. Groot-Berning et al., Phys. Rev. A 99 (2019) 023420, Flambaum, Phys. Rev. Lett. 97 (2006) 092502, Haas et al., Radiochim. Acta 108 (2020) 923.
5. Rudolph et al. Phys. Rev. Lett. 111 (2013) 112502.
6. Khuyagbaatar et al. Phys. Rev. Lett. 112 (2014) 172501; Phys. Rev. C 102 (2020) 064602.
7. Hofmann et al. Eur. Phys. J. A 48 (2012) 62; *ibid.* 52 (2016) 180.
8. Yakushev et al. Inorg. Chem. 53 (2014) 1624.
9. Samark-Roth et al., Phys. Rev. Lett. 126 (2021) 032503.
10. Albers et al., Phys. Lett. B 808 (2020) 135626.
11. Wouters, A. Knecht on behalf of the muX collaboration, SciPost Phys. Proc. 5 (2021) 022.
12. Sato et al., Nature 520 (2015) 209., T.K. Sato et al., JACS 140 (2018) 14609.
13. Lereendegui-Marco et al., EPJ Web Conf. 146 (2017) 11045
14. Kögler et al., EPJ Web Conf. 146 (2017) 11023
15. Kneip et al., Hyp. Int. 241 (2020) 45; Berndt et al., contribution to this workshop.
16. Parker and Falk, Nucl. Instrum. Meth. 16 (1962) 355., A. Vascon et al., Nucl. Instrum. Meth. A 696 (2012) 180.
17. Haas et al., Nucl. Instrum. Meth. A 874 (2017) 43.
18. Dragoun et al., in preparation for submission to Nucl. Instrum. Meth.

\* Corresponding author. Tel.: +49-6131-39-25852.

E-mail address: duellmann@uni-mainz.de

# The molecular approach for actinide materials

Olaf Walter\*, Karin Popa

<sup>a</sup> European Commission, DG Joint Research Centre, Directorate G - Nuclear Safety and Security, PO Box 2340, D-76125 Karlsruhe, GER

## Abstract

Among the existing applications engaging actinides those based on actinide materials represent the major part; still our days the actinide oxides for nuclear based energy production are the predominant but other are under development or applied on a smaller scale such as the application of radionuclides for medical tumour treatment.

For all these possible applications at the very beginning stands the synthesis and of the actinide material. This is industrially applied in the case for the reactor fuel in the nuclear fuel cycle. But for example the synthesis of target materials for the production of radionuclides for medical applications can still be improved and developed.

The starting point for all actinide chemistry and their materials is the mining from natural sources or recycling from the spent fuel. The separated actinides are normally gained in form of the oxides which are then to be re-dissolved for further transformations (Figure 1).

The presentation will briefly summarise and give an overview on what we have done to develop this kind of chemistry and showing the bridge to the materials. In more detail the main reaction pathways as depicted in Figure 1 will be explained; based on the actinide oxides as the starting point and the oxalates as one key intermediate the formation of actinide dioxide nano-materials, complexes in aqueous environment but as well organometallic complexes will be presented.

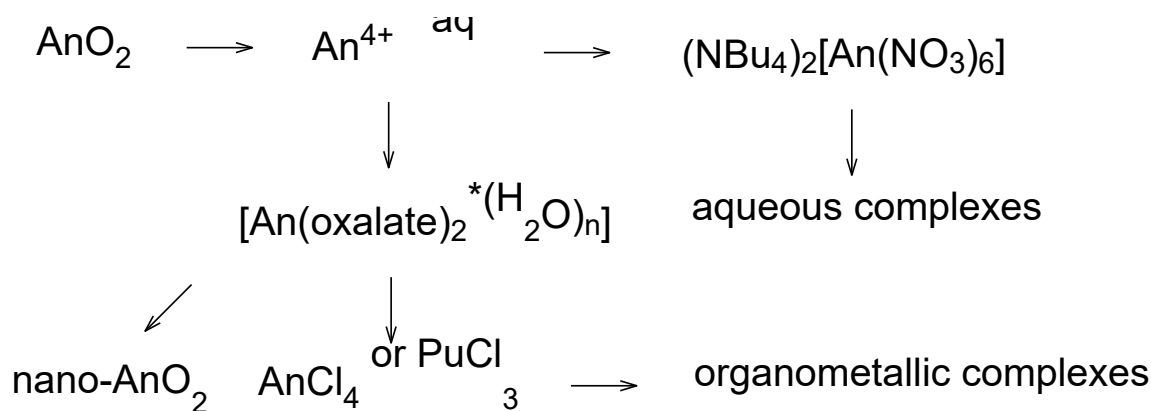


Figure 8 The actinide chemistry with some key intermediates.

## References, some recent

1. Dutkiewicz, M.S., Goodwin, C.A.P., Perfetti, M., Gaunt, A.J., Griveau, J.-C., Colineau, E., Kovács, A., Wooles, A.J., Caciuffo, R., Walter, O., Liddle, S.T., (2022) *Nature Chemistry*, 14 (3), pp. 342-349.
2. Apostolidis, C., Kovács, A., Morgenstern, A., Rebizant, J., Walter, O., (2021) *Inorganics*, 9 (6), art. no. 44, .
3. De Bona, E., Balice, L., Cognini, L., Holzhäuser, M., Popa, K., Walter, O., Cologna, M., Prieur, D., Wiss, T., Baldinozzi, G., (2021) *Journal of the European Ceramic Society*, 41 (6), pp. 3655-3663.
4. Corradetti, S., Carturan, S.M., Ballan, M., Eloirdi, R., Amador Celdran, P., Walter, O., Staicu, D., Dieste Blanco, O., Andrighetto, A., Biasetto, L., (2021) *Scientific reports*, 11 (1), p. 9058.
5. Radoske, T., März, J., Patzschke, M., Kaden, P., Walter, O., Schmidt, M., Stumpf, T., (2020) *Chemistry - A European Journal*, 26 (70), pp. 16853-16859.
6. Walter, O., (2019) *Chemistry - A European Journal*, 25 (12), pp. 2927-2934.

Metal-semiconductor transitions in  $U_3S_5$ Holger Kohlmann<sup>a,\*</sup>, Heribert Wilhelm<sup>b</sup>, Marcel Voest<sup>c</sup>, Wolfgang Scherer<sup>c</sup>, Badal Mondal<sup>d</sup>, Ralf Tonner-Zech<sup>d</sup><sup>a</sup>Leipzig University, Institute of Inorganic Chemistry, Johannisalle 29, 04103 Leipzig, Germany<sup>b</sup>Helmholtz Institute Ulm, Electrochemical Energy Storage, Helmholtzstraße 11, 89081 Ulm, Germany<sup>c</sup>Augsburg University, Section Physics and Materials Science, Universitätsstraße 1, 86159 Augsburg, Germany<sup>d</sup>Leipzig University, Wilhelm-Ostwald-Institute of Physical and Theoretical Chemistry, Linnéstr. 2, 04103 Leipzig, Germany

## Abstract

Uranium chalcogenides show a wide variety of different compositions ranging from  $UX$  to  $UX_5$  ( $X = S, Se, Te$ ). One of the key questions in view of their physical properties is the (de)localization of 5f electrons. Uranium-rich sulphides and selenides are metallic whereas the chalcogen-rich compounds are semiconductors or insulators. A convenient way to vary the subtle electronic structures in these materials is the application of pressure. Metallic  $US$ ,  $USe$  and  $UTE$  undergo a structural phase transition from NaCl to CsCl type structure around 80, 20 and 10 GPa, respectively. Several modifications of  $US_2$  are known, all of which are semiconductors. For  $\beta$ - $US_2$  a monoclinic high-pressure polymorph occurs above 10–15 GPa, but the crystal structure is not known [1].  $\alpha$ - $US_2$  (SrBr<sub>2</sub> type) transforms to  $\gamma$ - $US_2$  (anti-Fe<sub>2</sub>P type) in a belt-type apparatus at 4 GPa and 773 K.  $\gamma$ - $US_2$  also forms by a presumably topotactic reaction of  $U_3S_5$  with sulphur [2]. None of these structural transformations is accompanied by a metal–semiconductor transition.

$U_3S_5$  is the only mixed-valent uranium sulphide according to the formula  $(U^{3+})_2U^{4+}(S^{2-})_5$  as derived by XPS, IR spectroscopy, X-ray diffraction, magnetic susceptibility and electrical transport measurements. It is a semiconductor with a band gap  $\varepsilon = 78.1(4)$  meV for  $50\text{ K} < T < 298\text{ K}$  at ambient pressure [3]. Its crystal structure at ambient conditions is of the orthorhombic  $U_3Se_5$  type structure with uranium in nine-fold coordination by sulphur (Fig. 1). The electric resistivity  $\rho$  of a  $U_3S_5$  single crystal was measured as a function of temperature for several pressures. At room temperature a semiconductor–metal transition occurs between 4 and 7 GPa. At high pressure (7 and 8 GPa) another metal–semiconductor transition occurs upon cooling to about 100 K. Single-crystal diffraction data of  $U_3S_5$  in a diamond anvil cell (DAC) were collected at room temperature as a function of pressure up to 8 GPa and yielded high quality structural data for all pressures. No signs for phase transitions were found. The semiconductor–metal transition therefore seems to be of electronic nature only. At ambient conditions U1 atoms form a chain with alternating long and short U–U distances (along crystallographic  $b$ , Fig. 1). For increasing pressure this U–U distance alternation goes through a maximum at 4 GPa. This is also reflected by the changes in the slope of the  $\rho(T)$  curve and may indicate a Peierls-like distortion of the chain. Quantum-mechanical calculations and chemical-bond analysis are used to elucidate the electronic structure as a function of pressure and the nature of the observed change in transport properties.

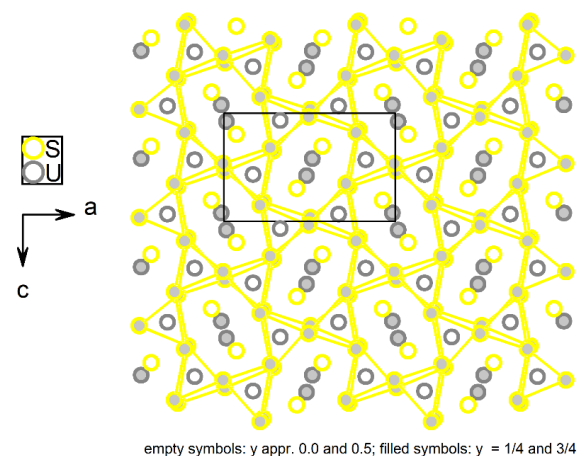


Figure 1: The crystal structure of  $U_3S_5$  ( $= (U^{3+})_2U^{4+}(S^{2-})_5$ ) as viewed along  $[100]$  highlighting the distorted Kagomé nets of sulfur atoms, which form trigonal prisms surrounding uranium atoms (U1).

## References

1. U. Benedict, C. Dufour, S. Heathman, T. Le Bihan, J. S. Olsen, L. Gerward, R. G. Haire, Y. K. Vohra, G. Gu, *High Pressure Res.* **1996**, *14*, 393–404.
2. H. Kohlmann, H. P. Beck, *Z. Anorg. Allg. Chem.* **1997**, *623*, 785–790.
3. H. Kohlmann, H. P. Beck, *J. Solid State Chem.* **2000**, *150*, 336–341.

\* Corresponding author. Tel.: +49-341-97-36201; fax: +49-341-97-36199.  
E-mail address: holger.kohlmann@uni-leipzig.de.

## High energy Resolution X-ray Spectroscopy for Actinide Science

Kristina Kvashnina<sup>a,b\*</sup><sup>a</sup>The Rossendorf Beamline at ESRF – The European Synchrotron, CS40220, 38043 Grenoble Cedex, France<sup>b</sup>Helmholtz-Zentrum Dresden-Rossendorf (HZDR), Institute of Resource Ecology, 01314 Dresden, Germany

---

**Abstract**

In recent years, scientists have progressively recognized the role of electronic structure in the characterization of chemical and physical properties for actinide containing materials. High-energy resolution X-ray spectroscopy at the actinide  $M_{4,5}$  edges emerged as a promising direction because this method can probe actinide properties at the atomic level through the possibility of reducing the experimental spectral width below the natural core-hole life time broadening.

In this lecture, I will describe the latest progress in the field of high-energy resolution X-ray spectroscopy at the actinide  $M_{4,5}$  edges<sup>1</sup>. More than 10 years passed after the first X-ray spectroscopy experiment in the high-energy resolution mode on uranium systems at the U  $M_4$  edge ( $\sim 3728$  eV) in 2009<sup>2</sup>. Quite a bit is known for the moment and X-ray absorption spectroscopy (XAS) or X-ray absorption near edge structure (XANES) in the high-energy resolution fluorescence detection (HERFD) mode together with resonant inelastic X-ray scattering (RIXS) or resonant X-ray emission spectroscopy (RXES) are now common techniques for studying the physics and chemistry of the f-block elements. I will show that the methods are able to a) provide fingerprint information on the actinide oxidation state and ground state character b) probe 5f occupancy, non-stoichiometry, defects c) investigate the local symmetry and effects of the crystal field<sup>3–12</sup>.

**References**

- 1 K. O. Kvashnina and S. M. Butorin, *Chem. Commun.*, 2022, 327–342.
- 2 K. O. Kvashnina, S. M. Butorin, P. Martin and P. Glatzel, *Phys. Rev. Lett.*, 2013, **111**, 253002.
- 3 K. O. Kvashnina, A. Y. Romanchuk, I. Pidchenko, L. Amidani, E. Gerber, A. Trigub, A. Rossberg, S. Weiss, K. Popa, O. Walter, R. Caciuffo, A. C. Scheinost, S. M. Butorin and S. N. Kalmykov, *Angew. Chemie Int. Ed.*, 2019, **58**, 17558–17562.
- 4 A. S. Kuzenkova, A. Y. Romanchuk, A. L. Trigub, K. I. Maslakov, A. V. Egorov, L. Amidani, C. Kittrell, K. O. Kvashnina, J. M. Tour, A. V. Talyzin and S. N. Kalmykov, *Carbon N. Y.*, 2020, **158**, 291–302.
- 5 Z. Pan, B. Bártoová, T. LaGrange, S. M. Butorin, N. C. Hyatt, M. C. Stennett, K. O. Kvashnina and R. Bernier-Latmani, *Nat. Commun.*, 2020, **11**, 4001.
- 6 N. Boulanger, A. S. Kuzenkova, A. Iakunkov, A. Y. Romanchuk, A. L. Trigub, A. V. Egorov, S. Bauters, L. Amidani, M. Retegan, K. O. Kvashnina, S. N. Kalmykov and A. V. Talyzin, *ACS Appl. Mater. Interfaces*, 2020, **12**, 45122–45135.
- 7 I. Pidchenko, J. März, M. O. J. Y. Hunault, S. Bauters, S. M. Butorin and K. O. Kvashnina, *Inorg. Chem.*, 2020, **59**, 11889–11893.
- 8 L. Amidani, G. B. M. Vaughan, T. V. Plakhova, A. Y. Romanchuk, E. Gerber, R. Svetogorov, S. Weiss, Y. Joly, S. N. Kalmykov and K. O. Kvashnina, *Chem. – A Eur. J.*, 2021, **27**, 252–263.
- 9 E. Gerber, A. Y. Romanchuk, I. Pidchenko, L. Amidani, A. Rossberg, C. Hennig, G. B. M. Vaughan, A. Trigub, T. Egorova, S. Bauters, T. Plakhova, M. O. J. Y. Hunault, S. Weiss, S. M. Butorin, A. C. Scheinost, S. N. Kalmykov and K. O. Kvashnina, *Nanoscale*, 2020, **12**, 18039–18048.
- 10 E. Gerber, A. Y. Romanchuk, S. Weiss, S. Bauters, B. Schacherl, T. Vitova, R. Hübner, S. Shams Aldin Azzam, D. Detollenaere, D. Banerjee, S. M. Butorin, S. N. Kalmykov and K. O. Kvashnina, *Inorg. Chem. Front.*, 2021, **8**, 1102–1110.
- 11 L. Amidani, M. Retegan, A. Volkova, K. Popa, P. M. Martin and K. O. Kvashnina, *Inorg. Chem.*, 2021, **60**, 16286–16293.
- 12 E. Gerber, A. Y. Romanchuk, S. Weiss, A. Kuzenkova, M. O. J. Y. Hunault, S. Bauters, A. Egorov, S. M. Butorin, S. N. Kalmykov and K. O. Kvashnina, *Environ. Sci. Nano*, 2022, **00**, 1–10.

---

\* Corresponding author. Tel.: +33-4-76-88-2367. <https://kristina-kvashnina.com/>  
E-mail address: [kristina.kvashnina@esrf.fr](mailto:kristina.kvashnina@esrf.fr)

# From Mild Hydrothermal to High Temperature Solutions: Crystal Growth of New Uranium and Transuranium Phases

Hans-Conrad zur Loye<sup>a,b,\*</sup> Kristen A. Pace<sup>a,b</sup>, Travis K. Deason<sup>a,b,c</sup>, Adrian Hines<sup>a,b</sup>,  
Gregory Morrison<sup>a,b</sup>, Hunter Tisdale<sup>a,b</sup>, Theodore Besmann<sup>a,b</sup>, Jake Amoroso<sup>b,c</sup>, David  
DiPrete<sup>b,c</sup>

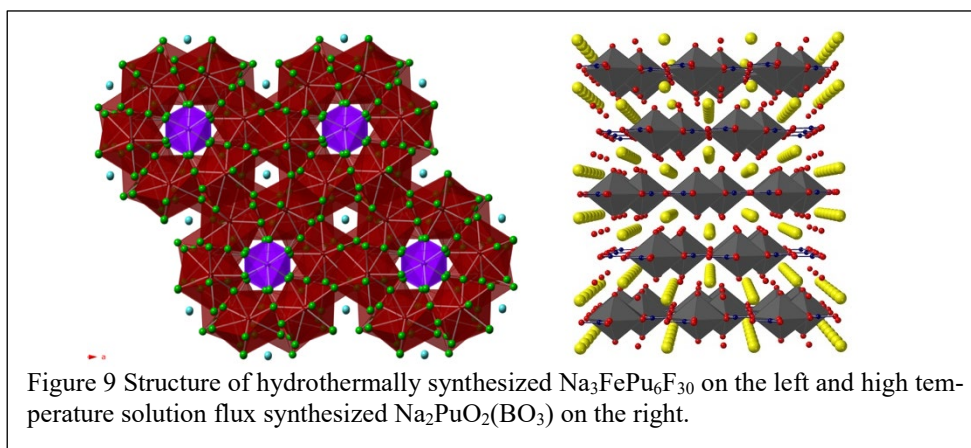
<sup>a</sup>Center for Hierarchical Waste Form Materials, Columbia, South Carolina 29208, United States

<sup>b</sup>University of South Carolina, Columbia SC, 29208, United States

<sup>c</sup>Savannah River National Laboratory, Aiken, South Carolina 29808, United States

## Abstract

The crystal growth of uranium and transuranium containing phases has been accomplished via two different crystal growth routes, mild hydrothermal and high temperature solution flux growth. In both cases we are targeting the preparation of new compositions to evaluate their potential use as nuclear waste forms. The mild hydrothermal route works extremely well for crystallizing complex fluoride phases, such as  $\text{Na}_3\text{GaU}^{\text{IV}}_6\text{F}_{30}$ ,  $\text{Na}_3\text{AlNp}^{\text{IV}}_6\text{F}_{30}$ , and  $\text{Na}_3\text{FePu}^{\text{IV}}_6\text{F}_{30}$ , while the high temperature flux route works well for crystallizing oxide phases, such as  $\text{Cs}_2\text{Pu}^{\text{IV}}\text{Si}_6\text{O}_{15}$  and  $\text{Na}_2\text{Pu}^{\text{V}}\text{O}_2(\text{BO}_3)$ . The synthesis and structures of these phases will be discussed, along with our approach of identifying potential compositions that we can pursue synthetically.



**Acknowledgements:** This work was supported as part of the Center for Hierarchical Waste Form Materials, an Energy Frontier Research Center funded by the U.S. Department of Energy, Office of Science, Basic Energy Sciences under Award No. DE-SC0016574. Work conducted at Savannah River National Laboratory was supported by the U.S. Department of Energy under contract DE-AC09-08SR22470.

## References:

1. Christian, M., Pace, K. A., Klepov, V. V., Morrison, G., zur Loye, H.-C., Besmann, T., *Cryst. Growth Design*, **2021**, *21*, 5100-5107.
2. Pace, K. A., Klepov, V. V., Berseneva, A. A., zur Loye, H.-C., *Chem. Eur. J.*, **2021**, *27*, 5835-5841.
3. Breton, L. S., Klepov, V. V., zur Loye, H.-C., *J. Am. Chem. Soc.*, **2020**, *142*, 14365-14373.
4. Pace, K. A., Klepov, V. V., Deason, T. K., Smith, M. D., DiPrete, D. P., Amoroso, J. W., zur Loye, H.-C., *Chemistry a European Journal* **2020**, *26*, 12941-12944.
5. Pace, K. A., Klepov, V. V., Christian, M. S., Morrison, G., Deason, T. K., Besmann, T. M., DiPrete, D. P., Amoroso, J. W., zur Loye, H.-C., *Chem. Commun.*, **2020**, *56*, 9501-9504.

\* Corresponding author. Tel.: +1-803-315-2571.

E-mail address: zurLoye@mailbox.sc.edu.

## Exploring the chemistry of super-reduced uranium organometallics

Luciano Barluzzi<sup>a,\*</sup>, Richard A. Layfield,<sup>a</sup><sup>a</sup>University of Sussex, Department of Chemistry, Brighton BN1 9QJ, UK**Abstract**

Oxidation state is a fundamentally important concept in chemistry. The discovery of elements in new oxidation states is, nowadays, very rare. In the context of f-element chemistry, the expansion of the available oxidation states encompasses +2 for all lanthanides <sup>[1]</sup> up to +4 for a selected few.<sup>[2],[3]</sup> Uranium coordination complexes with oxidation states ranging from +3 to +6 are well known, but only in 2013 was the first divalent uranium complex reported,<sup>[4]</sup> paving the way to the discovery of the +2 oxidation state for other actinides.

Beyond these developments, very little has been reported about the reactivity of divalent uranium. This is surprising since trivalent uranium is extremely reactive towards a range of small molecules, such as N<sub>2</sub>, H<sub>2</sub>, CO, and CO<sub>2</sub>. Our recent work has therefore focused on the reactivity of divalent uranocenes of the type [(h<sup>5</sup>-Cp<sup>R</sup>)<sub>2</sub>U].<sup>[5]</sup> The main, unexpected finding from studying the reactivity of divalent uranocenes is that they are remarkably stable. Their reactivity towards reducing agents is, however, much more unusual.

In this work, the synthesis, structure, and electronic structure of a monovalent uranium metallocene, formed via the reduction of a divalent uranocene, will be presented. Preliminary reactivity studies were also performed, showing that the complex can be oxidized to U(II) and to U(III) compounds. The stability of the monovalent uranium compound was also investigated, revealing its tendency to disproportionate to U(0) and its U(II) precursor complex.

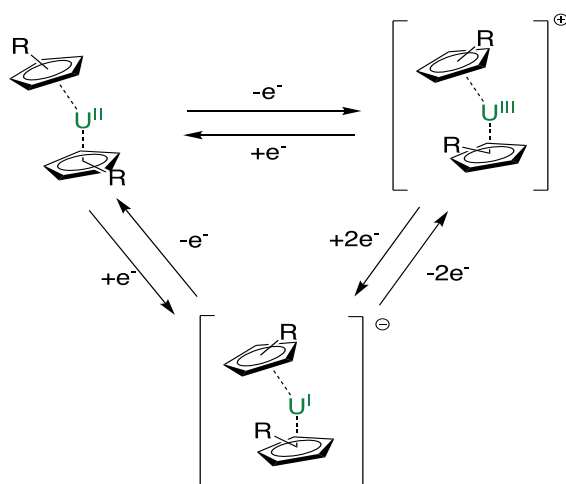


Figure 10 Redox chemistry of low valent uranocenes affording a U(I) metallocene

**References**

1. Wedal, J. C.; Evans, W. J. *J. Am. Chem. Soc.*, **2021**, *143*, 44, 18354-18367
2. Palumbo, C. T.; Mazzanti, M.; *et al. J. Am. Chem. Soc.*, **2019**, *141*, 9827-9831.
3. Willauer, A. R.; Mazzanti, M.; *et al. J. Am. Chem. Soc.*, **2020**, *142*, 5538-5542.
4. MacDonald, M. R.; Evans, W. J.; *et al. J. Am. Chem. Soc.*, **2013**, *135*, 13310-13313.
5. Guo, F.-S.; Layfield, R. A.; *et al. Angew. Chem. Int. Ed.*, **2020**, *59*, 2299-2303.

\* Corresponding author.

E-mail address: L.Barluzzi@sussex.ac.uk

# Some Recent Results of our Solid-State Uranium Chemistry and Reactions of Uranium Halides in pure HCN and NH<sub>3</sub>

Florian Kraus<sup>a,\*</sup>, S. S. Rudel<sup>a</sup>, H. L. Deubner<sup>a</sup>, B. Scheibe<sup>a</sup>, M. Conrad<sup>a</sup>, M. Sachs<sup>a</sup>

<sup>a</sup>AG Fluorchemie, Fachbereich Chemie, Philipps-Universität Marburg, Hans-Meerwein-Str. 4, 35032 Marburg, Germany

## Abstract

The facile preparation of the tetrahalides UX<sub>4</sub> and the trihalides UX<sub>3</sub> (X = F, Cl, Br, I) is presented together with a new high-pressure polymorph of UF<sub>4</sub>.<sup>[1–3]</sup>

Syntheses for UF<sub>5</sub> are shown as well as the products of the reactions of UCl<sub>4</sub> and UF<sub>5</sub> with anhydrous HCN.<sup>[4,5]</sup>

We revise the crystal structure of UCl<sub>6</sub> in which the positions of the U and Cl atoms had been determined incorrectly. In addition, we present a novel low temperature polymorph of UCl<sub>6</sub>.<sup>[6]</sup>

We developed a novel synthesis for UBr<sub>5</sub> and also obtained a novel polymorph.<sup>[6]</sup>

We present the reaction of UI<sub>3</sub> with RbNH<sub>2</sub> in anhydrous NH<sub>3</sub> and the formation of Rb<sub>2</sub>[U(NH<sub>2</sub>)<sub>6</sub>] as well as some ammonolysis reactions occurring in and ammine complexes obtained from liquid ammonia.<sup>[7,8]</sup>

## References

1. Rudel, S. S.; Deubner, H. L.; Scheibe, B.; Conrad, M.; Kraus, F. Facile Syntheses of Pure Uranium(III) Halides: UF<sub>3</sub>, UCl<sub>3</sub>, UBr<sub>3</sub>, and UI<sub>3</sub>. *Z. Anorg. Allg. Chem.* **2018**, *644* (6), 323–329. <https://doi.org/10.1002/zaac.201700402>.
2. Rudel, S. S.; Kraus, F. Facile Syntheses of Pure Uranium Halides: UCl<sub>4</sub>, UBr<sub>4</sub> and UI<sub>4</sub>. *Dalton Trans.* **2017**, *46* (18), 5835–5842. <https://doi.org/10.1039/C7DT00726D>.
3. Scheibe, B.; Bruns, J.; Heymann, G.; Sachs, M.; Karttunen, A. J.; Pietzonka, C.; Ivlev, S. I.; Huppertz, H.; Kraus, F. UF<sub>4</sub> and the High-Pressure Polymorph HP-UF<sub>4</sub>. *Chem. Eur. J.* **2019**, *25*, 7366–7374. <https://doi.org/10.1002/chem.201900639>.
4. Scheibe, B.; Rudel, S. S.; Buchner, M. R.; Karttunen, A. J.; Kraus, F. A 1D Coordination Polymer of UF<sub>5</sub> with HCN as a Ligand. *Chem. Eur. J.* **2017**, *23* (2), 291–295. <https://doi.org/10.1002/chem.201605293>.
5. Rudel, S. S.; Pietzonka, C.; Hoelzel, M.; Kraus, F. [UCl<sub>4</sub>(HCN)<sub>4</sub>] – a Hydrogen Cyanide Complex of Uranium Tetrachloride. *Chem. Commun.* **2018**, *54* (10), 1241–1244. <https://doi.org/10.1039/C7CC09401A>.
6. Deubner, H. L.; Rudel, S. S.; Sachs, M.; Pietzonka, C.; Karttunen, A. J.; Ivlev, S. I.; Müller, M.; Conrad, M.; Müller, U.; Kraus, F. A Revised Structure Model for the UCl<sub>6</sub> Structure Type, Novel Modifications of UCl<sub>6</sub> and UBr<sub>5</sub>, and a Comment on the Modifications of Protactinium Pentabromides. *Chem. Eur. J.* **2019**, *25* (25), 6402–6411. <https://doi.org/10.1002/chem.201900389>.
7. Rudel, S. S.; Karttunen, A. J.; Kraus, F. Rb<sub>2</sub>[U(NH<sub>2</sub>)<sub>6</sub>], a Rubidium Hexaamidouranate(IV) Obtained from the Reaction of UI<sub>3</sub> with RbNH<sub>2</sub> in Anhydrous Ammonia. *Z. Anorg. Allg. Chem.* **2020**, *646*, 1023–1029. <https://doi.org/10.1002/zaac.202000086>.
8. Rudel, S. S.; Baer, S. A.; Woidy, P.; Müller, T. G.; Deubner, H. L.; Scheibe, B.; Kraus, F. Recent Advances in the Chemistry of Uranium Halides in Anhydrous Ammonia. *Z. Kristallogr. - Cryst. Mater.* **2018**, *233* (12), 817–844. <https://doi.org/10.1515/zkri-2018-2066>.

\* Corresponding author. Tel.: +49-6421-28-26668.  
E-mail address: f.kraus@uni-marburg.de.

## Relativistic theory of pNMR and EPR

Stanislav Komorovsky<sup>a,\*</sup><sup>a</sup>*Institute of Inorganic Chemistry, Slovak Academy of Sciences, Dúbravská cesta 9, 84536 Bratislava, Slovakia*

---

**Abstract**

In the first part of this contribution, we will argue that the Helmholtz free energy and its derivatives are the proper starting point in developing the molecular properties at finite temperature. The Helmholtz free energy was, for the first time, used by Van den Heuvel and Soncini[1] in the development of the pNMR theory. This approach, however, significantly differs from the strategy applied in the theoretical development of the magnetic susceptibility tensor by Van Vleck [2] and of the pNMR tensor Kurland and McGarvey[3]. Furthermore, additional strategy was proposed by Moon and Patchkovskii[4] when developing the theory for the pNMR tensor calculations. Here we will unify all theories with the help of the Hellmann-Feynman theorem at a finite temperature[5].

The relativistic theory based on the Dirac–Coulomb–Breit (DCB) Hamiltonian with restricted kinetically and magnetically balanced basis sets is considered the gold standard for developing relativistic quantum chemical approaches. In the second part of this contribution, we revisit the basic aspects of the EPR theory and discuss their validity within the relativistic domain described by the DCB Hamiltonian. Because of the high-level of relativistic theory, the only tool available to us is the time-reversal symmetry. Some of the questions we will answer are: Is the *g*-tensor a tensor? Is the *g*-tensor an observable quantity? Can the *g*-tensor be diagonalized within the relativistic theory described by the DCB Hamiltonian? What is the connection of the principal axis system of the *g*- and *D*-tensors? What is the validity of the standard textbook EPR effective Hamiltonian within the relativistic theory? What is the fundamental difference between the Kramers and non-Kramers partners? Can the sign of the *g*-tensor eigenvalues be measured? Most of the theories necessary to answer these questions can the interested reader find in works by Chibotaru[6], Griffith[7], Abragam and Bleaney[8], and Bolvin and Autschbach[9].

If time allows, in the third part of this contribution, we will separate the pNMR tensor into the orbital and Curie terms in the framework of the exact-state theory (here, we follow the work of Moon and Patchkovskii [4]). Then we will map the exact-state pNMR theory to the parameters of the NMR and EPR effective Hamiltonians in a rigorous manner. In this improved mapping procedure, we reveal the correct form of the orbital contribution to the pNMR tensor, which can be further used as a starting point for implementing approximations typically used in currently available computational methodologies.

**References**

1. Van Den Heuvel, W.; Soncini, A. *J. Chem. Phys.* 2013, 138, 054113.
2. Gerloch, M.; McMeeking, R. F. *J. Chem. Soc., Dalton Trans.* 1975, 22, 2443–2451.
3. Kurland, R. J.; McGarvey, B. R. *J. Magn. Reson.* 1970, 2, 286–301.
4. Moon, S.; Patchkovskii, S. First-principles calculations of paramagnetic NMR shifts, in: M. Kaupp, M. Bühl, V. G. Malkin (Eds.), *Calculation of NMR and EPR Parameters. Theory and Applications*, Wiley-VCH, Weinheim, 2004, Ch. 20.
5. Pons, M.; Juliá-Díaz, B.; Polls, A.; Rios, A.; Vidaña, I. *The hellmann–feynman theorem at finite temperature*, *Am. J. Phys.* 2020, 88, 503–510.
6. Chibotaru, L. F. *Ab initio methodology for pseudospin hamiltonians of anisotropic magnetic complexes*, in: *Advances in Chemical Physics*, John Wiley & Sons, Inc., 2013, 397–519.
7. Griffith, J. S. *Phys. Rev.* 1963, 132, 316–319.
8. Abragam, A.; Bleaney, B. *Electron Paramagnetic Resonance of Transition Ions*, Oxford University Press, Oxford, 1970.
9. Bolvin, H.; Autschbach, J. *Relativistic methods for calculating electron paramagnetic resonance (EPR) parameters*, Springer Berlin Heidelberg, 2016.

---

\* Corresponding author. Tel.: +421-903-667-523; fax: +421-2-59410-444.  
*E-mail address:* stanislav.komorovsky@savba.sk.

# Speciation of An<sup>VI</sup> complexes in solution by combining pNMR and classical Molecular Dynamics simulations

Clovis Poulin-Ponnelle<sup>a,\*</sup>, Thomas Dumas<sup>a</sup>, Magali Duvail<sup>b</sup>, Claude Berthon<sup>a</sup>

<sup>a</sup> CEA, DES, ISEC, DMRC, University Montpellier, Marcoule France

<sup>b</sup> ICSM, University Montpellier, CEA, CNRS, ENSCM, Marcoule France

## Abstract

Paramagnetic Nuclear Magnetic Resonance (pNMR) plays an important role in structural determination of complexes in solution, particularly in biological systems where pNMR chemical shifts are induced by lanthanide(III) cations<sup>[1]</sup> (as probe in metalloproteins). The use of actinides (An) for complex structure determination has never really been employed while it could be useful in nuclear fuel research and environmental science since their toxicology can be investigated through the cation - peptide coordination chemistry owing to structural information studies<sup>[2]</sup>.

For AnO<sub>2</sub><sup>2+</sup> complexes (An = Np, Pu), chemical shifts in <sup>1</sup>H pNMR are mainly induced by the pseudocontact contribution, corresponding to the magnetic interaction between the 5*f* unpaired electron of the metallic cation and the proton nuclear spin<sup>[3]</sup>. This pseudocontact contribution depends on both the magnetic susceptibility anisotropy of the metal ion and a geometrical factor related to proton positions in the complex (Fig. 1.a). The aim of this work is to carry on investigations about the relationship between <sup>1</sup>H pNMR shifts and their coordinates within a complex taking into account molecular moves of the alkyl chains by classical molecular dynamics (MD) simulations.

To this end, MD simulations have been performed with AnO<sub>2</sub><sup>2+</sup> cations and diglycolamides (TEDGA) or amino acids (valine) as ligands (Fig. 1.b) and calculated paramagnetic shifts confronted to experimental <sup>1</sup>H pNMR chemical shifts (Fig. 1.a).

The relative flexibility of the TEDGA molecule gives, in the case of the 1:2 complex, two types of coordination mode, *i.e.*, either bidentate or tridentate, that corresponds either to 5 or 6 TEDGA oxygen atoms in the AnO<sub>2</sub><sup>2+</sup> first coordination sphere, which is experimentally confirmed by EXAFS experiments. Amino acid complexes exist in many conformations in solution, with broad peaks in <sup>1</sup>H pNMR due to the wide range of positions that the amino acid side chain nuclei can take. These broad peaks may be related to the distributions of geometric factors calculated from MD simulations.

This study provides important structural information on the An<sup>VI</sup> complexes, such as the speciation in solution, the different coordination modes and give access to the magnetic susceptibility anisotropy parameters of the paramagnetic cations.

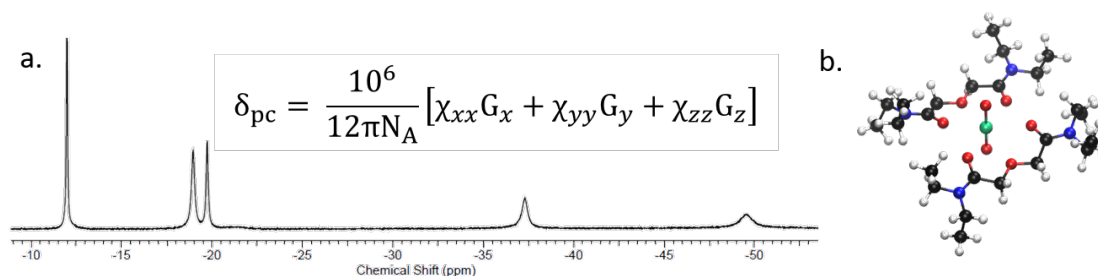


Figure 1: a. <sup>1</sup>H NMR spectrum of [PuO<sub>2</sub>(TEDGA)<sub>2</sub>]<sup>2+</sup> complex and the formula of the chemical shift pseudocontact contribution. b. Snapshot of [AnO<sub>2</sub>(TEDGA)<sub>2</sub>]<sup>2+</sup> complex issued from MD simulations.

## References

1. Bertini, I.; et al., NMR of paramagnetic molecules: applications to metalloproteins and models, 2016, Second edition, 25-60.
2. Jeanson, A.; et al., New J. Chem., 2009, 33, 976–985.
3. Autillo, M.; et al., Chem. Eur. J., 2019, 25, 4435–4451.

# Process development studies for the separation of trivalent actinides from used nuclear fuel solutions

Andreas Wilden<sup>a,\*</sup>, Andreas Geist<sup>b</sup>, Giuseppe Modolo<sup>a</sup>

<sup>a</sup>Forschungszentrum Jülich GmbH, Institut für Energie- und Klimaforschung – Nukleare Entsorgung (IEK-6), 52428 Jülich, Germany

<sup>b</sup>Karlsruhe Institute of Technology (KIT), Institute for Nuclear Waste Disposal (INE), 76021 Karlsruhe, Germany

---

## Abstract

For the future application of nuclear electricity production and improvements of sustainability, further advancements of the nuclear fuel cycle and innovative reactor concepts are considered.<sup>1</sup> In Europe, several research projects were funded by the European Commission and the German government, addressing innovative hydrometallurgical processes for the separation of actinides from used nuclear fuel.<sup>2,3</sup> The objectives included the development of processes for the separation of the trivalent minor actinides (An(III)) americium and curium from a PUREX (Plutonium Uranium Reduction Extraction) process raffinate. Due to the high radioactivity and share of spontaneous fission in the decay of curium isotopes, any fabrication of curium containing nuclear fuel would require special handling and a facility with high level of shielding. Therefore, the research recently focused on the even more challenging development of an effective method for separating Am(III) alone.

The processes are based on either the selective extraction of the desired metal ions, or their selective back-extraction from a loaded organic phase. Diglycolamides are often used for the complexation of trivalent actinides and lanthanides and provide high distribution ratios from process relevant nitric acid concentrations, beneficial kinetics, and stability against hydrolysis and radiolysis.<sup>4,5</sup> Nitrogen-donor ligands can provide the required selectivity for An(III) over Ln(III) or even Am(III) over Cm(III).<sup>6</sup> Understanding the fundamental complexation mechanisms and complex structures are crucial for successful process development.

This presentation will give an overview of the current state of process development in Europe. Examples of successful process demonstrations will be given.<sup>7-10</sup> They include the investigation of lipophilic and hydrophilic ligands for the (selective) complexation of actinide metal ions.

**Acknowledgements** Funding for this research was provided by the European Commission through the PATRICIA project (grant agreement number 945077), the German Ministry of Education and Research through the f-Char project (02NUK059D), as well as the German Ministry of Economic Affairs and Energy through the SEPAM project (02E11921A).

## References

1. OECD-NEA, *Strategies and Considerations for the Back End of the Fuel Cycle*, OECD Nuclear Energy Agency (NEA), Boulogne-Billancourt, France, 2021.
2. A. Geist, J.-M. Adnet, S. Bourg, et al., *Separ. Sci. Technol.*, 2021, **56**, 1866-1881.
3. T. L. Authen, J.-M. Adnet, S. Bourg, et al., *Separ. Sci. Technol.*, 2021, DOI:10.1080/01496395.2021.2001531.
4. Y. Sasaki, Y. Sugo, S. Suzuki, et al., *Solvent Extr. Ion Exch.*, 2001, **19**, 91-103.
5. S. A. Ansari, P. Pathak, P. K. Mohapatra, et al., *Chem. Rev.*, 2012, **112**, 1751-1772.
6. P. J. Panak and A. Geist, *Chem. Rev.*, 2013, **113**, 1199-1236.
7. A. Wilden, G. Modolo, C. Schreinemachers, et al., *Solvent Extr. Ion Exch.*, 2013, **31**, 519-537.
8. A. Wilden, G. Modolo, P. Kaufholz, et al., *Sep. Sci. Technol.*, 2015, **50**, 2467-2475.
9. A. Wilden, G. Modolo, P. Kaufholz, et al., *Solvent Extr. Ion Exch.*, 2015, **33**, 91-108.
10. A. Wilden, D. Schneider, Z. Paparigas, et al., *Radiochim. Acta*, 2022, DOI:10.1515/ract-2022-0014.

---

\* Corresponding author. Tel.: +49-2461-61-3965; fax: +49-2461-61-2450.  
E-mail address: a.wilden@fz-juelich.de

# Variability of crystal surface reactivity controls the migration and sorption of radionuclides

Tao Yuan<sup>a</sup>, Stefan Schymura<sup>a</sup>, Till Bollermann<sup>a</sup>, Konrad Molodtsov<sup>a</sup>, Paul Chekhonin<sup>a</sup>, Moritz Schmidt<sup>a</sup>, Thorsten Stumpf<sup>a</sup> & Cornelius Fischer<sup>a,\*</sup>

<sup>a</sup>Helmholtz-Zentrum Dresden-Rossendorf (HZDR), Institute of Resource Ecology, Dresden, Germany

## Abstract

Reactive transport models are an important tool for predicting radionuclide migration in the biosphere and geosphere. However, the predictive power of reactive transport models for sorption reactions is still limited by the parameterization of a so-called reactive surface. The problem of surface reactivity of crystalline solids is also currently under discussion for growth and dissolution reactions<sup>1</sup>. The variability of the density of specific reactive sites across the nanotopography of the crystal surface represents an "energetic landscape" responsible for the heterogeneous sorption efficiency, which is not captured mechanistically and quantitatively in current reactive transport modelling approaches.

In this study, we investigate the spatially heterogeneous sorption behavior of Eu(III), as an analog of trivalent actinides, on a polycrystalline nanotopographic calcite surface and quantify the sorption efficiency as a function of surface nanoroughness. Based on experimental data from micro-focus time-resolved laser-induced luminescence spectroscopy ( $\mu$ TRLFS)<sup>2</sup>, vertical scanning interferometry (VSI)<sup>1</sup>, and electron back-scattering diffraction (EBSD), we parameterize a surface complexation model (SCM) using surface nanotopography data (Fig. 1).

Experimental validation of quantitatively predicted spatial sorption heterogeneity suggests that retention reactions can be significantly affected by nanotopographic surface features, such as kink sites, surface steps, and complex etch pit topographies. Our study demonstrates a way to implement heterogeneous surface reactivity into a predictive SCM to improve the general prediction of radionuclide retention<sup>3</sup>.

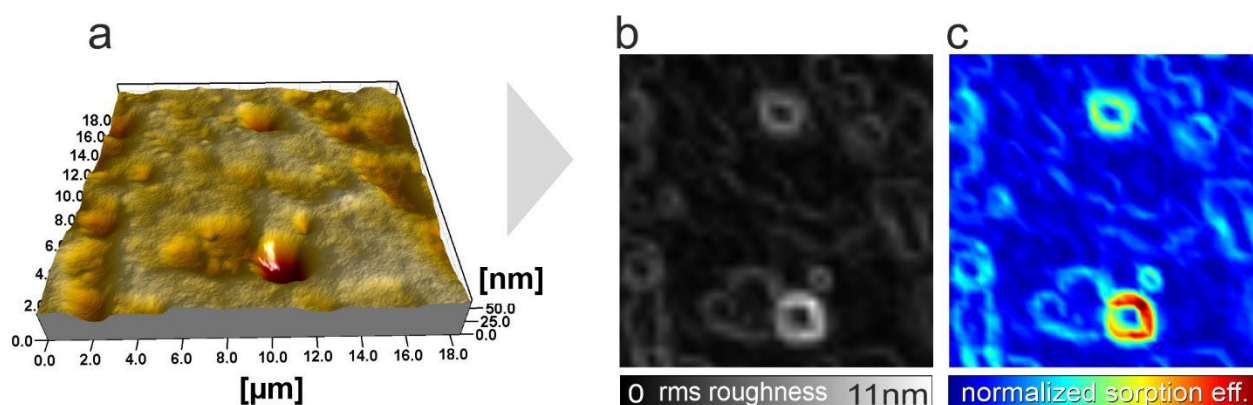


Figure 11. Numerical simulation (surface complexation modeling, SCM) of the sorption efficiency of a crystal surface applied to a nanotopographic data set measured by phase shifting interferometry microscopy (a). The variability in surface reactivity, based on different crystallographic surface building blocks is quantified by the proxy parameter rms surface roughness (b). Conceptually, this parameter is used for novel parameterization of SCM calculations (c).

## References

1. Fischer, C.; Luttge, A., Pulsating dissolution of crystalline matter. *PNAS* **2018**, *115* (5), 897-902.
2. Stumpf, T.; Bauer, A.; Coppin, F.; Fanghänel, T.; Kirn, J. I., Inner-sphere, outer-sphere and ternary surface complexes: a TRLFS study of the sorption process of Eu(III) onto smectite and kaolinite. *Radiochim. Acta* **2002**, *90*, 345-349.
3. Yuan, T.; Schymura, S.; Bollermann, T.; Molodtsov, K.; Chekhonin, P.; Schmidt, M.; Stumpf, T.; Fischer, C., Heterogeneous Sorption of Radionuclides Predicted by Crystal Surface Nanoroughness. *Environmental Science & Technology* **2021**, *55* (23), 15797-15809.

\* Corresponding author. Tel.: +49-352-260-4660  
E-mail address: c.fischer@hzdr.de

# Masked Uranium(II) Delivery by a Diuranium(III) complex for Multi-Electron Transfer

Dieuwertje K. Modder<sup>1</sup>, Chad T. Palumbo<sup>1</sup>, Iskander Douair<sup>2</sup>, Rosario Scopelliti<sup>1</sup>, Farzaneh Fadaei-Tirani<sup>1</sup>, Laurent Maron<sup>2</sup>, Marinella Mazzanti<sup>\*1</sup>

<sup>1</sup>Institut des Sciences et Ingénierie Chimiques, École Polytechnique Fédérale de Lausanne (EPFL), 1015 Lausanne, Switzerland.

<sup>2</sup>Laboratoire de Physique et Chimie des Nano-objets, Institut National des Sciences Appliquées, 31077 Toulouse, Cedex 4, France.

## Abstract

One of the main challenges chemistry currently faces in the transition to a sustainable economy is the activation and functionalization of small molecules, such as N<sub>2</sub>, CO and CO<sub>2</sub>, which requires multi-electron transfer processes. Low-oxidation state uranium compounds have shown high reactivity in these transformations, but need to be designed carefully, as uranium predominantly undergoes single electron transfer. To overcome this, monouranium complexes could be tuned to transfer more electrons, uranium could be combined with redox-active ligands, or multimetallic complexes could be employed. Recently in our group, the use of siloxide ligands allowed the isolation of two diuranium(III) complexes, showing remarkable small molecule reactivity.<sup>[1]</sup> The linker was shown to have an important influence on the reactivity.

In this work, we studied the influence of the ancillary ligands by investigating silylamide supported complexes, resulting in the isolation of an oxide-bridged diuranium(III) complex.<sup>[2]</sup> Reactivity studies showed that the U–O bond is easily broken upon substrate addition, resulting in the delivery of a masked U(II) and a U(IV) terminal oxo co-product (Figure 1). The masked U(II) can effect cooperative single electron reductions of pyridine and bipyridines, affording unique examples of diuranium(III) complexes bridged by redox-active ligands. Furthermore, the masked U(II) is also able to effect multi-electron reductions of diphenylacetylene by two electrons and of azobenzene by four electrons.<sup>[3]</sup> This reactivity was also observed for the previously reported corresponding U(II) complex<sup>[4]</sup>, showing the first example of an unambiguous single metal four-electron transfer in f-element chemistry.

These results provide new insight into how uranium can be used in multi-electron transfer processes, essential in the activation of small molecules.

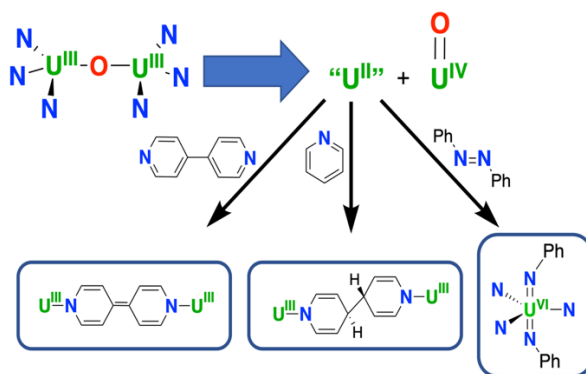


Figure 12 A diuranium(III) oxo-bridged complex acts as masked U(II) and can transfer two electrons cooperatively to (bi)pyridine and four electrons to azobenzene.

## References

1. Falcone, M.; Barluzzi, L.; Andrez, J.; Fadaei-Tirani, F.; Zivkovic, I.; Fabrizio, A.; Corminboeuf, C.; Severin, K.; Mazzanti, M. *Nature Chem.*, **2019**, *11*, 154.
2. Modder, D. K.; Palumbo, C. T.; Douair, I.; Fadaei-Tirani, F.; Maron, L.; Mazzanti, M. *Angew. Chem. Int. Ed.*, **2021**, *60*, 3737.
3. Modder, D. K.; Palumbo, C. T.; Douair, I.; Scopelliti, R.; Maron, L.; Mazzanti, M. *Chem. Sci.*, **2021**, *12*, 6153.
4. Ryan, A. J.; Angadol, M. A.; Ziller, J. W.; Evans, W. J. *Chem. Commun.*, **2019**, *55*, 2325.

\* Corresponding author.

E-mail address: marinella.mazzanti@epfl.ch

# Unusual Building Units and Properties of Actinide Metal-Organic Frameworks

Sara E. Gilson<sup>a,\*</sup>, Melissa Fairley<sup>a</sup>, Jennifer E.S. Szymanowski<sup>a</sup>, Sylvia Hanna<sup>b</sup>, Patrick Julien<sup>a</sup>, Zhijie Chen<sup>b</sup>, Peng Li<sup>b</sup>, Jacob White<sup>c</sup>, Debmalya Ray<sup>c</sup>, Allen G. Oliver<sup>a</sup>, Laura Gagliardi<sup>c</sup>, Omar K. Farha<sup>b</sup>, Peter C. Burns<sup>a</sup>

<sup>a</sup>University of Notre Dame, Notre Dame, IN, 46556 USA

<sup>b</sup>Northwestern University, Evanston, IL, 60208 USA

<sup>c</sup>University of Minnesota, Minneapolis, MN, 55455 USA

## Abstract

Metal-organic frameworks (MOFs) are modular, three-dimensional structures consisting of metal secondary building units (SBUs) and organic linkers. Numerous transition metal MOFs have been reported, but actinide-bearing MOFs remain relatively underexplored, especially for the subset of transuranic MOFs. To expand this area of actinide materials, MOFs with actinide-bearing SBUs were targeted. The structures and properties of three actinide MOFs are illustrated in Figure 1.

All MOFs were studied with single-crystal diffraction and Raman spectroscopy. Two of these structures contain Np<sup>5+</sup> polyhedra bonded together to give unprecedented SBUs. In [C<sub>34</sub>O<sub>8</sub>H<sub>18</sub>]<sub>3</sub>(F/OH)<sub>6</sub>(H<sub>2</sub>O)<sub>18</sub>(NpO<sub>2</sub>)<sub>18</sub> (NNS1) (Figure 1A),<sup>[1]</sup> double wheel-shaped clusters of eighteen neptunyl polyhedra connected through actinyl-actinyl interactions (AAIs) are stabilized by tetratopic linkers. NNS1 displays the rare (4,12)-connected **shp** topology.

In [(CH<sub>3</sub>)<sub>2</sub>NH<sub>2</sub>]<sub>4</sub>[(NpO<sub>2</sub>)<sub>4</sub>(C<sub>53</sub>O<sub>8</sub>H<sub>32</sub>)(HCOO)<sub>4</sub>] (NSM), Np<sup>5+</sup> neptunyl pentagonal bipyramids connect through integral AAIs and bridging formate ligands to give SBUs that are infinite, helical chains.<sup>[2]</sup> The connectivity of SBUs and organic linkers gives a new MOF topology termed the **nsm** topology. NSM also exhibits notable radiation resistance. Diffraction and spectroscopic analyses imply that the radiation resistance of the framework is greater than the linker building block. Additionally, single-crystal X-ray diffraction was used to assess changes in atomic connectivity of irradiated single-crystals of NSM.

The structure of Th<sub>6</sub>O<sub>4</sub>(OH)<sub>4</sub>(H<sub>2</sub>O)<sub>6</sub>(C<sub>22</sub>O<sub>6</sub>H<sub>12</sub>)<sub>6</sub> (TOF-16) is shown in Figure 1C.<sup>[3]</sup> Hexamers of Th<sup>4+</sup> polyhedra are connected by binaphthol linkers. TOF-16 displays exceptional radiation resistance, as it does not become completely X-ray amorphous until application of a He<sup>2+</sup> ion beam to a dose of about 25 MGy. Radiation resistance of this framework is attributed to the functional groups of the organic linkers as well as the strong Lewis acidity of the Th atoms.

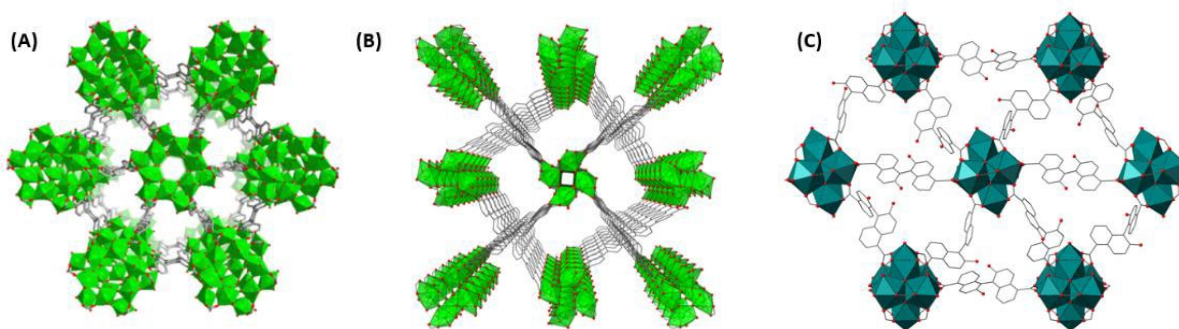


Figure 13 The structures of (A) NNS1 (B) NSM and (C) TOF-16. Green for Np, blue for Th, grey for C, and red for O.

## References

- Gilson, S.E.; Li, P.; Szymanowski, J.E.S.; White, J.; Ray, D.; Gagliardi, L.; Farha, O.K.; Burns, P.C. *J. Am. Chem. Soc.*, **2019**, *141*, 11842-11846.
- Gilson, S.E.; Fairley, M.; Hanna, S.L.; Szymanowski, J.E.S.; Julien, P.; Chen, Z.; Farha, O.K.; LaVerne, J.A.; Burns, P.C. *J. Am. Chem. Soc.*, **2021**, *143*, 17354-17359.
- Gilson, S.E.; Fairley, M.; Julien, P.; Oliver, A.G.; Hanna, S.L.; Arntz, G.; Farha, O.K.; LaVerne, J.A.; Burns, P.C. *J. Am. Chem. Soc.*, **2020**, *142*, 13299-13304.

\* Corresponding author. Tel.: +1-856-264-8840  
E-mail address: s.gilson@hzdr.de

# Calix[4]arenes with phosphoryl and salicylamide functional groups: synthesis, complexation and selective extraction of f-element cations

Berthold Kersting<sup>a,\*</sup>, Florian Gasneck<sup>a</sup>, Quirina I. Roode-Gutzmer<sup>b</sup>, Thorsten Stumpf<sup>b</sup>

<sup>a</sup>Institute of Inorganic Chemistry, Leipzig University, Johannisallee 29, 04103 Leipzig, Germany.

<sup>b</sup>Institute of Resource Ecology, Helmholtz-Zentrum Dresden-Rossendorf, Bautzner Landstrasse 400, 01328 Dresden, Germany

## Abstract

Rare-earth elements (REE) are important metals used in various areas such as production of permanent magnets, luminescent materials, catalysts for petroleum cracking, de-oxygenation of steel, and many other areas. To manage the turnaround in the energy policy, the demand for permanent magnets for wind turbines and electric vehicle technology is expected to increase significantly. Circumventing possible supply bottlenecks of REEs necessitates the development of better recycling technologies.<sup>[1]</sup> REEs from primary resources are generally contaminated with traces of radioactive uranium and thorium. Producers of rare-earths are required to adhere to radiation protection measures. It is therefore essential to ensure radioactive decontamination prior to recovering the REEs.

The potential for calixarenes to be employed as an extracting agent for the separation and purification of lanthanides was first demonstrated in 1987.<sup>[2]</sup> Since then many other calix[4]arenes have been utilized as extracting agents in liquid-liquid-extraction processes. Herein, we present a series of tetra-substituted bifunctional calixarene ligands bearing phosphoryl and salicylamide functional groups appended to the lower rim of the *p-tert*-butylcalix[4]arene scaffold. Ligand interactions with lanthanide cations (light: La<sup>3+</sup>, Pr<sup>3+</sup>; intermediate: Eu<sup>3+</sup> and Gd<sup>3+</sup>; and heavy: Yb<sup>3+</sup>), as well as the uranyl cation (UO<sub>2</sub><sup>2+</sup>) have been examined in the solution and solid state, respectively with spectrophotometric titration and single crystal X-ray diffractometry. The solvent extraction behaviour was examined for cation selectivity and extraction efficiency. The ligands were found to be effective extracting agent for UO<sub>2</sub><sup>2+</sup> over La<sup>3+</sup> and Yb<sup>3+</sup> cations.<sup>[3]</sup> Herein, we report on our findings.

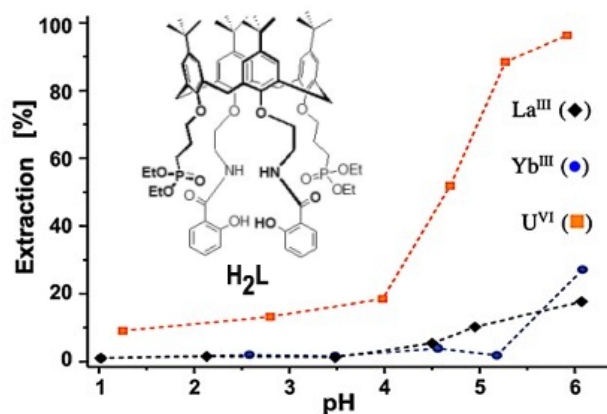


Figure 14 Extraction of single metal cations with **H<sub>2</sub>L** as a function of pH at T = 298 K. Organic phase: [**H<sub>2</sub>L**] = 10<sup>-2</sup> mol/L in CHCl<sub>3</sub>. Aqueous phase: [La<sup>3+</sup>], [Yb<sup>3+</sup>], [UO<sub>2</sub><sup>2+</sup>] each with a concentration of 10<sup>-4</sup> mol/L buffered with H<sub>3</sub>BO<sub>3</sub>/Na<sub>2</sub>B<sub>4</sub>O<sub>7</sub> (10<sup>-2</sup> mol/L in H<sub>2</sub>O). Extraction: 15 min. Equilibration: 30 min..

## References

1. T. Lorenz, T.; Bertau, M.; *J. Clean. Prod.* **2019**, *215*, 131-143.
2. McKerverve, A.; Arnaud-Neu, F.; Schwing-Weill, M.-J. in *Comprehensive Supramolecular Chemistry* (Ed.: G. W. Gokel), Pergamon, Oxford, **1996**
3. Gasneck, F.; Roode-Gutzmer, Q. I.; Stumpf, T.; Kersting, B. *Chem. Eur. J.* **2022**, *28*, e202104301

\* Corresponding author. Tel.: +49-341-973-6143; fax: +49-341-973-6160.  
E-mail address: b.kersting@uni-leipzig.de

## Actinium Chemistry in Silico

Georg Schreckenbach<sup>a,\*</sup>, Yang Gao<sup>a,b</sup>, Cen Li<sup>a</sup>, Josef Tomeček<sup>a,c</sup>, Payal Grover<sup>a</sup><sup>a</sup>Department of Chemistry, University of Manitoba, Winnipeg, MB, R3T 2N2, Canada<sup>b</sup>Institute of Fundamental and Frontier Sciences, University of Electronic Science and Technology of China, Chengdu, Sichuan 610054, China<sup>c</sup>Department of Chemistry, Imperial College London, London, SW7 2AZ, United Kingdom

## Abstract

<sup>225</sup>Ac-based radiopharmaceuticals have the potential to become novel agents for the treatment of cancer. However, due to the radioactivity and scarcity of all actinium isotopes, there is limited knowledge about the chemistry of this element. To fill some of these knowledge gaps, we have studied a range of different actinium complexes. In this presentation, we will give an overview of our work in this area:

- (i) binding of  $\text{Ac}^{3+}$  with a range of small mono- and bidentate ligands;<sup>1</sup>
- (ii) geometric and electronic structural properties of hydrated  $\text{Ac}^{3+}$  cations including the first and second hydration shells in aqueous solution and gas phase;<sup>2</sup>
- (iii) bonding in Ac-DOTA Complexes;<sup>3</sup>
- (iv) complexation of  $\text{Ac}^{3+}$  with a variety of chelating ligands – such as derivatives of the HOPO ligand – of interest for the development of radiopharmaceuticals.

We will discuss bonding in these systems (for instance, we find that the aquo complex adopts a closed-shell 18-electron configuration ( $1S^21P^61D^{10}$ ) of a superatom state) and outline challenges and considerations for the computational study of these systems.

## References

1. J. Tomeček, C. Li, ‡ G. Schreckenbach, *J. Comp. Chem.*, submitted.
2. Y. Gao, P. Grover, G. Schreckenbach, *Chem. Sci.* **2021**, *12*, 2655–2666.
3. Y. Gao, E. Varathan, P. Grover, G. Schreckenbach, *Inorg. Chem.* **2021**, *60*, 6971–6975.

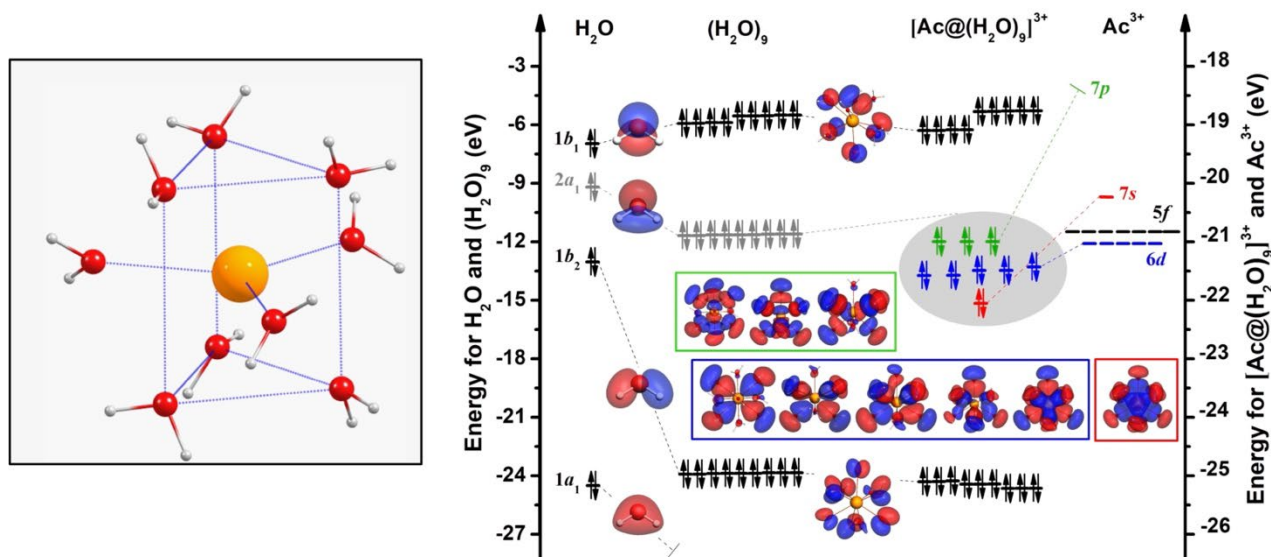


Figure 15.  $[\text{Ac}(\text{H}_2\text{O})_9]^{3+}$  complex (left) and its frontier orbitals showing the closed-shell superatom states (right).

# Resonance ionization spectroscopy on $^{254,255}\text{Es}$ and $^{255}\text{Fm}$ with a “boostered” sample

S. Berndt<sup>a,\*</sup>, Th.E. Albrecht-Schönzart<sup>b</sup>, M. Block<sup>a,c,d</sup>, H. Dorrer<sup>a</sup>, Ch.E. Düllmann<sup>a,c,d</sup>,  
 J.G. Ezold<sup>e</sup>, M. Kaja<sup>a</sup>, T. Kieck<sup>c,d</sup>, N. Kneip<sup>a</sup>, U. Köster<sup>f</sup>, J. Lantis<sup>a</sup>, C. Mokry<sup>a,c</sup>,  
 D. Münzberg<sup>a,c,d</sup>, S. Nothhelfer<sup>a,c,d</sup>, S. Raeder<sup>c,d</sup>, D. Renisch<sup>a,c</sup>, J. Runke<sup>a,d</sup>, M. Stemmler<sup>a</sup>,  
 D. Studer<sup>a</sup>, P. Thörle-Pospiech<sup>a,c</sup>, N. Trautmann<sup>a</sup>, J. Warbinek<sup>d</sup>, F. Weber<sup>a</sup>, K. Wendt<sup>a</sup>

<sup>a</sup>Johannes Gutenberg University Mainz, 55099 Mainz, Germany

<sup>b</sup>Florida State University, 32306 Tallahassee, FL, USA

<sup>c</sup>Helmholtz-Institut Mainz, 55099 Mainz, Germany

<sup>d</sup>GSI Helmholtzzentrum für Schwerionenforschung GmbH, 64291 Darmstadt, Germany

<sup>e</sup>Oak Ridge National Laboratory, Oak Ridge, 37831 Oak Ridge, TN, USA

<sup>f</sup>Institut Laue-Langevin, 38042 Grenoble, France

---

## Abstract

Einsteinium ( $Z = 99$ ) and fermium ( $Z = 100$ ) are the heaviest synthetic actinide elements which can be produced in macroscopic quantities. This is possible via neutron capture in high-flux reactors like the High Flux Isotope Reactor (HFIR) at Oak Ridge National Laboratory (ORNL), Oak Ridge, TN, USA [1]. Resonant laser ionization spectroscopy is an efficient and sensitive technique to study the atomic and nuclear structure of transuranium elements by measuring atomic transitions including their hyperfine structure splitting and isotope shift. In this contribution we will present recent activities at the RISIKO mass separator [2] at Johannes Gutenberg University Mainz (JGU) regarding laser resonance ionization spectroscopy on  $^{254,255}\text{Es}$  and  $^{255}\text{Fm}$ . For this, we used a sample produced by irradiating targets consisting of  $^{244-248}\text{Cm}$  with thermal neutrons at HFIR. After the irradiation, which took place in 2019, the targets were chemically separated into fractions of the individual elements at ORNL’s Radiochemical Engineering Development Center [3]. A sample of  $^{253-255}\text{Es}$  was shipped to JGU, where these isotopes were studied by laser resonance ionization spectroscopy at the RISIKO mass separator. Investigating the atomic structure of neutral einsteinium and the hyperfine structure of optical transitions yielded information on new atomic energy levels as well as on the nuclear moments for these isotopes with  $^{255}\text{Es}$  being at the very edge of sensitivity [4]. These experiments consumed only part of the sample and in 2021 the remaining sample contained still about  $6.8 \cdot 10^{11}$  atoms of  $^{254}\text{Es}$  ( $t_{1/2} = 275.7$  d), whereas the shorter-lived  $^{253,255}\text{Es}$  were largely decayed. This  $^{254}\text{Es}$  sample was then sent to the Institut Laue-Langevin (ILL) Grenoble, France, for a second irradiation with thermal neutrons to produce  $^{255}\text{Es}$  ( $t_{1/2} = 39.8$  d). This irradiation took place from October 4 to October 11, 2021. The sample was returned to JGU and subsequently used as a generator system for the production of  $^{255}\text{Fm}$  ( $t_{1/2} = 20.1$  h). From this generator system,  $^{255}\text{Fm}$  atoms were separated with a  $\alpha$ -hydroxyisobutyric acid ( $\alpha$ -HIB) based actinide separation by cation exchange on Mitsubishi CK10Y resin. This separation was performed at  $70^\circ\text{C}$  using a  $0.14$  M  $\alpha$ -HIB solution at pH 4.8. After the first separation, which took place on November 2, 2021, the Es was fully eluted, reprocessed, and again placed on top of the resin to allow ingrowth of the  $^{255}\text{Fm}$  daughter. Three more separations were performed until November 22, 2021 and a total of  $1.9 \cdot 10^7$  atoms of  $^{255}\text{Fm}$  were thus made available for laser spectroscopic studies of this isotope. With these samples optical transitions reported by Sewtz *et al.* [5] and Backe *et al.* [6] were recorded with higher spectral resolution and investigated for their lifetime despite the 3 orders of magnitude lower sample sizes compared to [6]. After conclusion of the measurements of  $^{255}\text{Fm}$ , the remaining “boostered” sample still contained  $\sim 2 \cdot 10^8$   $^{255}\text{Es}$  atoms as determined from the  $^{255}\text{Fm}$  activity. This enabled additional investigations of  $^{254,255}\text{Es}$ . In  $^{255}\text{Es}$  the 411 nm ground state transition ( $5f^{11}7s^2, J = 15/2 \rightarrow 5f^{11}7s7p, J = 15/2$ ) was measured for its hyperfine structure with suitable statistics. The same transition was then remeasured in  $^{254}\text{Es}$  with high resolution ( $\sim 100$  MHz) by using the Perpendicularly Illuminated Laser Ion Source and Trap (PI-LIST) [7]. At the workshop, the isotope production, separation, and laser spectroscopy studies will be presented.

## References

- [1] Robinson, S.M. *et al.*, *Radiochim. Acta*, 2020, **108(9)**, 737.
- [2] Kieck, T. *et al.*, *Rev. Sci. Instrum.*, 2019, **90**, 053304.
- [3] Roberto, J.B. *et al.*, *Nucl. Phys. A*, 2015, **944**, 99.
- [4] Nothhelfer, S. *et al.*, *Phys. Rev. C*, 2022, **105**, L021302.
- [5] Sewtz, M. *et al.*, *Phys. Rev. Lett.*, 2003, **90**, 163002.
- [6] Backe, H. *et al.*, *Hyperfine Interact*, 2005, **162**, 3.
- [7] Heinke, R. *et al.*, *Hyperfine Interact*, 2017, **236**, 6.

---

\* Corresponding author. Tel.: +49-6131-39-28614.

E-mail address: sberndt@uni-mainz.de

# High-Valent U, Np, and Pu Imidophosphorane Mono-Oxo Complexes

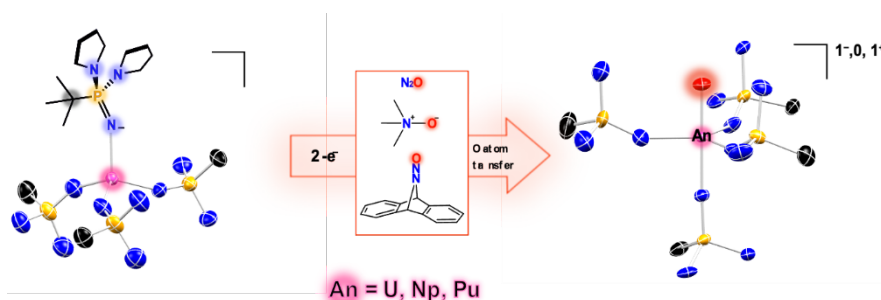
Henry S. La Pierre<sup>a,b,\*</sup>, and Julie E. Niklas<sup>a</sup>

<sup>a</sup>School of Chemistry and Biochemistry, Georgia Institute of Technology, Atlanta, Georgia 30332-0400, United States

<sup>b</sup>Nuclear and Radiological Engineering and Medical Physics Program in the School of Mechanical Engineering  
Georgia Institute of Technology, Atlanta, Georgia 30332-0400, United States

## Abstract

In this talk, I will present the synthesis of tetrahomoleptic, imidophosphorane complexes of U, Np, and Pu in several formal oxidation states ( $[\text{An}(\text{NP}(t\text{-Bu})(\text{pyrr}_2)_4)]^q$ , where An = U, Np, and Pu and q can be -1, 0, or +1, pyrr = pyrrolidiny) and the reactivity of these complexes with two-electron oxygen atom transfer reagents to form high-valent mono-oxo complexes ( $[\text{An}(\text{O})(\text{NP}(t\text{-Bu})(\text{pyrr}_2)_4)]^q$ , Scheme 1).<sup>1,2</sup> These studies build on my group's recently reported synthesis of hexavalent uranium mono-oxo and mono-imido complexes via two-electron atom transfer reactions.<sup>3</sup> This discussion will include the examination of several oxygen-atom transfer reagents including (nitrous oxide, trimethylamine N-oxide, dioxygen, and DBABH-NNO (9,10-dihydro-11-nitroso-anthracen-9,10-imine)), the description of ligand design processes to afford high-quality single crystals of the mono-oxo complexes in good yield and on small-scale (10-40 mg of isotope) and the one-electron oxidation and reduction chemistry of the mono-oxo complexes.<sup>4-6</sup> Detailed spectroscopic and solution and solid-state structural analyses will address changes in the inverse trans-influence across the mid-actinides – a phenomenon which is uniquely addressable by this series of complexes.<sup>1-3</sup> Additional topics to be covered may include electrochemistry, magnetism, and EPR spectroscopy of selected complexes.



**Scheme 1:** Reaction scheme for the oxidation of tetra-actinide homoleptic complexes with two-electron, oxygen atom transfer reagents to form mono-oxo products. The complexes are shown as molecular structures as determined by SC-XRD and thermal ellipsoids are plotted at 50%. The ligands are truncated to core N and C atoms to reveal connectivity at the metal. A single ligand on the homoleptic complex (left) is drawn to depict the full ligand connectivity.

## References

1. Niklas, J.E.; Barker, T.B.; Ramanathan, A.; Bacsá, J.; Popov, I. A.; and La Pierre, H.S.; “Inverse-*trans* Influence in an Isostructural Valence Series of Neptunium ( $\text{Np}^{5+}$ ,  $\text{Np}^{6+}$ , and  $\text{Np}^{7+}$ ) Mono-oxo Complexes,” *in preparation* 2022.
2. Niklas, J.E.; Barker, T.B.; Ramanathan, A.; Bacsá, J.; Popov, I. A.; La Pierre, H.S.; “Reactivity of Homoleptic Plutonium Imidophosphorane Complexes,” *in preparation* 2022.
3. Rice, N.T.; McCabe, K.; Bacsá, J.; Maron, L.; La Pierre, H.S.; “Two-Electron Oxidative Atom Transfer at a Homoleptic, Tetravalent Uranium Complex,” *J. Am. Chem. Soc.* 2020, *142*, 16, 7368–7373.
4. Niklas, J.E.; Barker, T.B.; Bacsá, J.; Popov, I. A.; and La Pierre, H.S.; “Crystal Engineering of Hexavalent Uranium Mono-oxo Complexes,” *in preparation* 2022.
5. Aguirre Quintana, L.M.; Niklas, J.E.; Jiang, N.; Bacsá, J.; Maron, L.; La Pierre, H.S.; “Elemental Chalcogen Reactions of a Tetravalent Uranium Imidophosphorane Complex: Cleavage of Dioxgen,” *in preparation* 2022.
6. Niklas, J.E.; Barker, T.B.; Ramanathan, A.; Bacsá, J.; Popov, I. A.; La Pierre, H.S.; “Inverse-*trans* influence and weak-field paramagnetism in a pentavalent uranium mono-oxo complex,” *in preparation* 2022.

\* Corresponding author. Tel.: +49-6131-39-28614.  
E-mail address: sberndt@uni-mainz.de

# Uranium Going the Soft Way: Studies of the Electronic Structure of U(III)-Complexes with a Series of new S-based Chelating Ligands

Benedikt Kestel<sup>a</sup>, Daniel Pividori<sup>a</sup>, Matthias E. Mielich<sup>a</sup>, Frank W. Heinemann<sup>a</sup>, Andreas Scheurer<sup>a</sup>, Michael Patzschke<sup>b</sup>, Karsten Meyer<sup>a,\*</sup>

<sup>a</sup>Friedrich-Alexander-University Erlangen-Nürnberg (FAU), Department of Chemistry and Pharmacy, Inorganic Chemistry, Egerlandstraße 1, 91058 Erlangen, Germany.

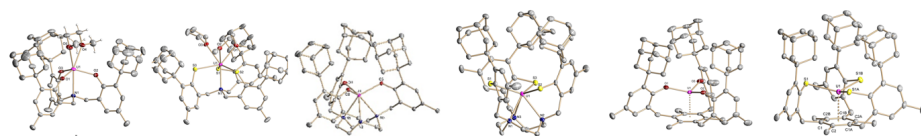
<sup>b</sup>Institute of Resource Ecology, Helmholtz-Zentrum Dresden-Rossendorf, Bautzner Landstraße 400, 01328 Dresden, Germany.

## Abstract

While uranium complexes with classical O- and N-based donor ligands were thoroughly studied throughout the years, the coordination chemistry of uranium with the heavier group 16 elements trailed behind. It is mostly limited to simple reactivity studies and despite those revealing interesting trends in bond covalency and -strength, sulfur-based ligand design is limited to little exceptions.

To overcome that gap, and to further study properties of low-valent uranium centers in the coordination spheres of soft donor ligands, we accomplished the synthesis of a series of tripodal, thiophenolate-based ligands and their corresponding complexes  $[(N^{(Mc,Ad)ArS})_3U^{III}(DME)(THF)]$  (**L1-U**),  $[U^{III}((SAr^{Ad,Mc})_3tacn)]$  (**L2-U**) and  $[U^{III}((OAr^{Ad,Mc})_3mes)]$  (**L3-U**). Particular features of the molecular structures obtained by single-crystal X-ray diffraction analysis – such as wide-opened axial cavities – are discussed. <sup>1</sup>H NMR, UV/Vis-NIR electronic absorption and EPR spectroscopies as well as SQUID magnetometry and cyclic voltammetry confirm the U(III) oxidation states and provide a comprehensive picture of the complexes' electronic structure.

In that regard, differences and similarities with the well-studied analogues  $[((^{Mc,Ad}ArO)_3N)U^{III}(DME)]$ ,  $[U^{III}((OAr^{Ad,Mc})_3tacn)]$  and  $[U^{III}((OAr^{Ad,Mc})_3mes)]$  are observed (see **Figure 1**). Comparisons of the results indicate partially drastic changes in the electronic structure when moving from phenolate-based to sulfur-based ligands **L1-L3**, suggesting different reactivity in small molecule activation chemistry, which is part of ongoing studies. For **L3-U**, computational studies (NBO, DFT, and QTAIM) complete the electronic structure discussion.



	$U^{III}((OAr)_3N)$	$U^{III}((SAr)_3N)$ <b>L1-U</b>	$U^{III}((OAr)_3tacn)$	$U^{III}((SAr)_3tacn)$ <b>L2-U</b>	$U^{III}((OAr)_3mes)$	$U^{III}((SAr)_3mes)$ <b>L3-U</b>
high temp $\mu_{eff}$	2.98 $\mu_B$ (300 K)		2.82 $\mu_B$ (300 K)	3.07 $\mu_B$ (300 K)	1.84 $\mu_B$ (300 K)	2.89 $\mu_B$ (300 K)
low temp $\mu_{eff}$	1.65 $\mu_B$ (5 K)		1.42 $\mu_B$ (2 K)	1.78 $\mu_B$ (2 K)	1.17 $\mu_B$ (5 K)	2.00 $\mu_B$ (2 K)
$g$ values		$g_x = 2.96$	$g_{  } = 2.42$	$g_{  } = 2.33$	$g_x = 1.58$	$g_x = 3.06$
		$g_y = 2.39$	$g_{\perp} = 1.91$	$g_{\perp} = 1.62$	$g_y = 1.46$	$g_y = 2.85$
		$g_z = 1.50$			$g_z = 1.20$	$g_z = 0.96$

Figure 16 Molecular structures and selected properties of complexes  $[((^{Mc,Ad}ArO)_3N)U^{III}(DME)]$ , **L1-U**,  $[U^{III}((OAr^{Ad,Mc})_3tacn)]$ , **L2-U**,  $[U^{III}((OAr^{Ad,Mc})_3mes)]$  and **L3-U**.

## References

- Pividori, D.; Mielich, M.E.; Kestel, B.; Heinemann, F.W.; Scheurer, A.; Patzschke, M.; Meyer, K. *Inorganic Chemistry* **2021**, *60*, 16455–16465.
- Kestel, B.; Meyer, K. unpublished results.
- Lam, O. P.; Bart, S. C.; Kameo, H.; Heinemann, F.W.; Meyer, K. *Chemical Communications* **2010**, *46*, 3137–3139.
- Halter, D.; Heinemann, F.W.; Maron, L.; Meyer, K. *Nature Chemistry* **2018**, *10*, 259–267.
- La Pierre, H.S.; Scheurer, A.; Heinemann, F.W.; Hieringer, W.; Meyer, K. *Angewandte Chemie International Edition* **2014**, *53*, 7158–7162.

\* Corresponding author. Tel.: +49 9131 85-27360; fax: +49 9131 85-27367.  
E-mail address: karsten.meyer@fau.de

# [An(acac)<sub>4</sub>] complexes revisited

Robert Gericke\*, Peter Kaden

*Helmholtz-Zentrum Dresden-Rossendorf, Institute of Resource Ecology, Bautzner Landstraße 400, 01328 Dresden, Germany*

---

**Abstract**

Actinides (An) play an important role in chemical research and environmental science related to the nuclear industry or nuclear waste repositories.<sup>1</sup> Investigating their coordination chemistry can function as a tool to obtain fundamental understanding of actinide binding. Due to the radiotoxicity of actinide complexes, special care in handling those material need to be employed in form of working in a controlled area lab. Therefore, the understanding of complexation properties of the actinides, in particular the transuranium (TRU) elements, is lacking behind those of the *d*- or 4*f*-elements, which can be handled in ordinary laboratories.

For the early actinides possible oxidation states are typically ranging from +II to +VII. A suitable approach to explore fundamental physico-chemical properties of the actinides is to study series of isostructural An compounds in which the An is in the same oxidation state.<sup>2</sup> Therefore our investigations are directed towards the synthesis of actinide complexes (An = Th, U, Np and Pu) with the *f*-element in the oxidation state IV, the dominant oxidation state particularly under anoxic environmental conditions. Observed changes in e.g., the binding situation or magnetic effects along such a series deliver insight into the elements' unique electronic properties mainly originating from the *f*-electrons. One important question in the field of An chemistry is the degree of "covalency" in compounds across the An series,<sup>3</sup> which may be addressed by systematic studies on series of An compounds, including transuranium (TRU) elements.

An-complexes using pure O-donor ligand systems can act as molecular mimic for related An-O-systems, e.g. UO<sub>2</sub> used as fuel in nuclear reactors. In these studies, we investigate the coordination chemistry of tetravalent actinides (An(IV)), using an organic monoanionic ligand with O-donor atoms of the acetylacetonate (acac) type. Since 1958, actinide complexes of the type [An(acac)<sub>4</sub>] have structurally been characterized at ambient temperature.<sup>4-8</sup> However, spectroscopic data is limited to vibrational spectroscopy especially for the transuranium complexes, leaving open questions of the actinide bonding. The [An(acac)<sub>4</sub>] complexes are typically synthesized via salt metathesis reactions under strict exclusion of moisture and air. Single crystal X-ray diffraction analysis at 100 K provides insight into isostructural complex series, which were achieved in each case. In order to obtain further insight into the electronic structure of these complexes, the compounds were further analysed by NMR, IR, UV-vis-NIR, and EPR spectroscopy. The redox chemistry of the series of [An(acac)<sub>4</sub>] complexes in NCMe was further investigated with cyclic voltammetry. These results are used as a basis to further analyse bonding trends along the actinide series by means of quantum chemical calculations.

From the results, trendlines along the actinides An = Th, U, Np and Pu in this complex series were obtained, which shed some light on the ongoing debate of covalency in actinide bonding.

**References**

1. L. S. Natrajan, A. N. Swineburn, M. B. Andrews, S. Randall, S. L. Heath, *Coord. Chem. Rev.* **2014**, 266-267, 171-193.
2. M. B. Jones, A. J. Gaunt, J. C. Gordon, N. Kaltsoyannis, *Chem. Sci.* **2013**, 4, 1189-1203.
3. M. P. Kelley, J. Su, M. Urban, M. Luckey, E. R. Batista, P. Yang, J. C. Shafer, *J. Am. Chem. Soc.* **2017**, 139, 9901-9908.
4. D. Grdenić, B. Matković, *Nature* **1958**, 182, 465-466.
5. D. Grdenić, B. Matković, *Acta Cryst.* **1959**, 12, 817-817.
6. B. Allard, *Acta Chem. Scand.* **1972**, 26, 3492-3504.
7. D. Brown, B. Whittaker, J. Tacon, *J. Chem. Soc., Dalton Trans.* **1975**, 1, 34-39.
8. B. Allard, *J. Inorg. Nucl. Chem.* **1976**, 38, 2109-2115.

---

\* Corresponding author. Tel.: +49 351 260 2011.  
E-mail address: r.gericke@hzdr.de.

# Applications of $^{238}\text{Pu}$ are Out of this World

David L Clark<sup>a,\*</sup>

<sup>a</sup>Los Alamos National Laboratory, National Security Education Center, MS-T001, Los Alamos, NM 87545

---

## Abstract

The first isotope of plutonium to be discovered was  $^{238}\text{Pu}$ , produced in 1940 by bombarding uranium with deuterons. Its short half-life (87.7 yr) was conducive to tracer studies that allowed its separation and identification. Today,  $^{238}\text{Pu}$  is readily obtained by neutron bombardment of  $^{237}\text{Np}$ , and separated by solvent extraction techniques.

$^{238}\text{Pu}$  has found important application in radioisotope power systems – nuclear power systems that derive their energy from the heat produced by spontaneous decay, as distinguished from nuclear fission. Most radioisotope power systems use  $^{238}\text{Pu}$  as an isotope heat source. I will present an overview of the production, purification, component fabrication, applications, and disposal of this very important isotope.

By far, the most prevalent application has been for space and interplanetary exploration. For this application, heat source fuel is enriched to 83.5% in  $^{238}\text{Pu}$  isotope, and oxygen atoms in  $^{238}\text{PuO}_2$  are enriched in  $^{16}\text{O}$  to reduce the neutron emission rate to as low as 6000 n/s/g. The  $^{238}\text{Pu}$  isotope provides 99.9% of the thermal power in heat source fuel. Radioisotope Thermoelectric Generators (RTGs) have been used in the United States to provide electrical power for spacecraft since 1961 in Space Nuclear Auxiliary Power (SNAP) units to power satellites and remote instrument packages on the moon. The current systems employ General Purpose Heat Sources (GPHS) of hot pressed 150g pellets of  $^{238}\text{PuO}_2$  (Figure 1). These have found widespread application as power sources for exploration of the planets through satellite probes such as Galileo (Jupiter), Cassini (Saturn), and New Horizons (Pluto), and more recently, to power instrumentation on a series of Mars Rovers (Figure 2). The use of  $^{238}\text{Pu}$  in future NASA space missions will be described.



Figure 1. 150g sintered  $^{238}\text{PuO}_2$  General Purpose Heat Source pellet.



Figure 2. The 2011 Curiosity Mars rover was the first to use a Multi Mission Radioisotope Thermoelectric Generator (MMRTG)

**Acknowledgements** This work was supported by the U.S. Department of Energy through the Los Alamos National Laboratory, LA-UR-16-23561. Los Alamos National Laboratory is operated by Triad National Security, LLC, for the National Nuclear Security Administration of U.S. Department of Energy under Contract No. 89233218CNA000001.

# PSMA-Macropa-Conjugates for Radiolabeling with Actinium-225 and Iodine-123

Ritchie Kranzen<sup>a</sup>, Falco Reissig<sup>a</sup>, Hans-Jürgen Pietzsch<sup>a</sup>, Klaus Kopka<sup>a</sup>, Constantin Mamat<sup>a,\*</sup>

<sup>a</sup> Helmholtz-Zentrum Dresden-Rossendorf, Institut für Radiopharmazeutische Krebsforschung, Bautzner Landstraße 400, D-01328 Dresden, Germany

## Abstract

Due to its favorable nuclear physical properties, actinium-225 belongs to the alpha emitters for therapeutic applications. Over ten clinical trials are displayed for actinium-225-DOTA-based conjugates. A trial of [<sup>225</sup>Ac]Ac-PSMA-617 in men with PSMA-positive prostate cancer is projected to start. Actinium-225 can easily be chelated with the standard DOTA chelator, but requires high temperatures (80–95°C) or microwave assistance. With macropa as alternative chelator, owing perfect characteristics for [<sup>225</sup>Ac]Ac<sup>3+</sup> chelation, mild labeling conditions, low reaction temperature and high *in vivo* stability is provided. The major drawback of macropa derivatives is the weak complexation and *in vivo* stability of diagnostically applied radionuclides like technetium-99m, gallium-68, indium-111, or scandium-43/-44.

To overcome this obstacle and to further improve the tumor uptake, precursors of albumin binding units based on the 4-iodophenylbutyrate moiety were introduced to perform the radiolabeling with iodine-123/-124 and to elongate the blood residence time of the radiotracer, leading to a higher tumor uptake.

The prostate-specific membrane antigen (PSMA) is expressed in most cases of prostate cancer at considerably higher levels in tumor cells compared to healthy tissues. Its upregulation occurs in all stages of the disease. Therefore, PSMA has emerged as an attractive target for molecular imaging and especially targeted radionuclide therapy (endoradiotherapy) of metastatic castration-resistant prostate cancer (mCRPC).

Two new radioconjugates were prepared containing the PSMA binding moiety and the albumin binding moiety connected one time or two times to the macropa chelator. First radiolabeling procedures were performed with both conjugates using with [<sup>225</sup>Ac]Ac<sup>3+</sup> at up to 5 MBq/nmol with >99% radiochemical purity. Stability tests showed that both radioconjugates are stable (>95%) up to 5 days.

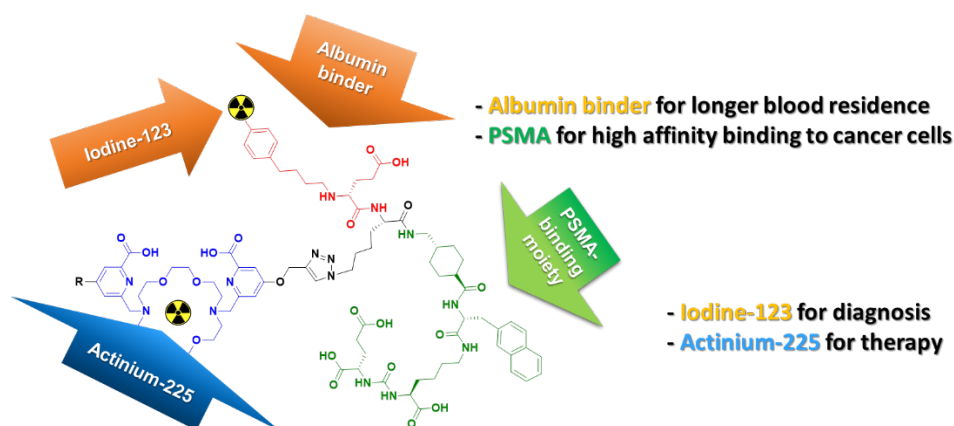


Figure 17 Radioconjugate containing the PSMA-binding moiety, the Albumin binder and the macropa chelator for radiolabelling with Ac<sup>3+</sup>.

## References

1. F. Reissig, D. Bauer, K. Zarschler, Z. Novy, K. Bendova, K. Kopka, H.-J. Pietzsch, M. Petrik, C. Mamat, *Cancers* **2021**, *13*, 1974.

\* Corresponding author. Tel.: +49-351-260 2805; fax: +49-351-260 2915.  
E-mail address: c.mamat@hzdr.de.

# Exploring excited state potential energy profile and luminescence properties of uranyl-based complexes by TRLFS and *ab initio* method

Valérie Vallet<sup>a,\*</sup>, Hanna Oher<sup>a,b</sup>, Florent Réal<sup>a</sup>, Thomas Vercoüter<sup>b</sup>,  
André Severo Pereira Gomes<sup>a</sup>, Richard E. Wilson<sup>c</sup>

<sup>a</sup> Université Lille, CNRS, UMR8523-PhLAM- Physique des Lasers Atomes et Molécules, F-59000 Lille

<sup>b</sup> DEN-Service d'Etudes Analytiques et de Réactivité des Surfaces (SEARS), CEA, Université Paris-Saclay, F-91191 Gif-sur-Yvette, France

<sup>c</sup> Chemical Sciences and Engineering Division, Argonne National Laboratory, Argonne Illinois USA

## Abstract

Uranyl complexes have been the subject of many research works for fundamental chemistry of actinides, environmental issues, or nuclear fuel cycle processes. The formation of various uranyl complexes, with organic and inorganic ligands in solution must be characterized for a better understanding of U(VI) speciation. As uranyl-ligand interactions and the symmetry of the complexes affect the electronic structure of U(VI) and thus its luminescence properties, time-resolved laser induced fluorescence spectroscopy (TRLFS) is one of the major techniques to characterize U(VI) complexes, with high sensitivity and selectivity. However, most of the relevant systems have complex chemical composition in solution and the identification of each species from spectroscopic data is challenging.

In our study, the synergy between TRLFS and *ab initio*-based interpretation appears as a promising route for complexation data. Luminescence spectra of uranyl complexes in solution show in general a narrow energetical range about 6000 cm<sup>-1</sup> and we can identify a single electronic transition between the initial and target states with the vibrationally resolved band [1]. The main challenge consists in exploiting a computationally cheap and effective theoretical approach, in a relativistic context, to characterize the main spectral parameters of the ground and luminescent states of symmetrical uranyl compounds (*i.e.* UO<sub>2</sub>Cl<sub>4</sub><sup>2-</sup>, UO<sub>2</sub>F<sub>5</sub><sup>3-</sup>, UO<sub>2</sub>(CO<sub>3</sub>)<sub>3</sub><sup>4-</sup>, UO<sub>2</sub>(NO<sub>3</sub>)<sub>2</sub>) with different organic or inorganic counter ions after the photo-excitation. We will illustrate that TD-DFT with the CAM-B3LYP functional is able to provide accurate excitation/emission energies for these systems, together with accurate vibronic progressions allowing the assignment of experimental data.

As a benchmark system serving the purpose of assessing the accuracy of our theoretical protocol, the uranyl tetrachloride UO<sub>2</sub>Cl<sub>4</sub><sup>2-</sup> was selected because of the extensive amount of structural and spectroscopic data available [2]. A good agreement was found between ours and previously obtained theoretical data (structural parameters, orbitals nature, excitation energies) [3]; the final luminescence spectrum is in remarkable agreement with our TRLFS measurements [4]. We will also quantify the effects of organic or inorganic counterions [5, 6], along with that of first-sphere ligands that might perturb the uranyl(VI) moiety.

This work showcases how one can predict vibrationally resolved spectra to assign the recorded TRLFS data, and shed light on the relationship between the uranyl coordination and its luminescence properties.

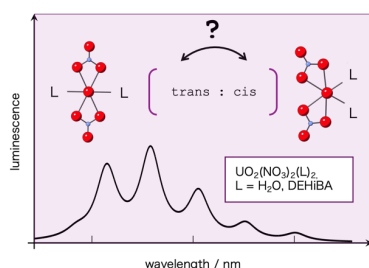


Figure 18 Vibronic spectra of cis and trans-UO<sub>2</sub>(NO<sub>3</sub>)<sub>2</sub>L<sub>2</sub>

## References

1. Visnak, H. et al., EPJ Web Conf., 2016, 28, 02002.
2. Denning, R. G. et al., Chem. Phys. Lett., 1991, 180, 101.
3. Pierloot, K. et al., J. Chem. Phys. 2005, 123, 204309.
4. Oher, H. Oher et al., Inorg. Chem., 2020, 59, 5896; *ibid.* Inorg. Chem., 2020, 59, 15036; *ibid.* Inorg. Chem., 2022, 61, 890.

\* Corresponding author. Tel.: +33-32033-5985.

E-mail address: valerie.vallet@univ-lille.fr

# Solubility limits and structural properties in the thorite-zircon pseudo-binary system for nuclear waste storage

Volodymyr Svitlyk<sup>a,b\*</sup>, Stephan Weiss<sup>a</sup>, Salim Shams<sup>a</sup>, Christoph Hennig<sup>a,b</sup>

<sup>a</sup> Helmholtz-Zentrum Dresden-Rossendorf, Institute of Resource Ecology, 01314 Dresden, Germany

<sup>b</sup> Rossendorf Beamline (BM20), European Synchrotron Radiation Facility, 38000 Grenoble, France

## Abstract

Spent nuclear waste (SNW) usually contains a large palette of highly radio-toxic transuranium elements like Np, Pu, Cm and Am. As a result, integrity of buried SNW should not be compromised by dissolution and internal irradiation over a period of  $10^6$  years. Strict physico-chemical requirements should be satisfied before final deposition of SNW in deep geological repositories. This requires development of universal and robust matrix materials with strong affinity to the above-mentioned species. In this context derivatives of zircon,  $ZrSiO_4$ , are of great interest since their natural analogs, which contain up to 5 %  $Th^{4+}$  and  $U^{4+}$ , are known to remain stable in geological cycles of up to  $10^9$  years.<sup>1</sup> In this work we investigate pseudo-binary thorite-zircon ( $ThSiO_4$  -  $ZrSiO_4$ ) system.  $Th(IV)$  was selected for this study because it represents a typical oxidation state of IV commonly found in nuclear waste containing transuranium elements.

Phases in the  $Th_{1-x}Zr_xSiO_4$  system were synthesized from precursor salts using hydrothermal method for  $x = 0 - 1$  in fine steps. Initially, synthesis at  $pH = 8$  was performed using  $HNO_3$  acid and  $NHCO_3$  stabilizing buffer. This  $pH$  was used in order to obtain phases with high concentration of Th. For the second batch of samples  $HCl$  was used to obtain  $pH = 1$  for the final solutions. This procedure was used to synthesize phases rich in Zr. Obtained solutions were sealed in autoclaves and placed in an oven at  $250^\circ C$  for 12 h for hydrothermal treatment. After the synthesis the obtained precipitates were separated and dried at  $200^\circ C$  for 12 h. High resolution XRD experiments were performed at the BM20 ROBL station at ESRF, Grenoble.<sup>2</sup> *In situ* high pressure (HP) XRD data were collected for selected samples as well.

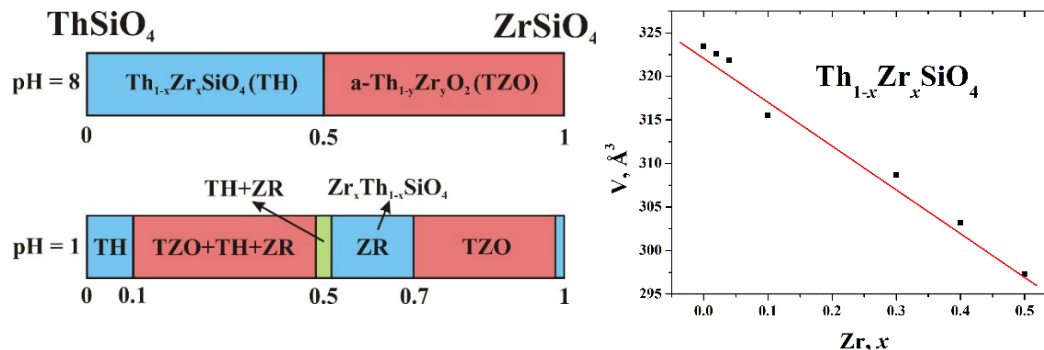


Figure 19 (left) Phase compositions in  $ThSiO_4$ - $ZrSiO_4$  system synthesized at  $pH = 8$  (top) and  $pH = 1$  (bottom); (right) reduction in unit-cell volume of  $ThSiO_4$  upon introduction of smaller Zr atoms.

As expected, synthesis at  $pH = 8$  successfully yielded phases situated on the Th-rich side of the phase diagram (Fig. 2, left, top). Continuous Th-Zr solubility was observed upto 50 at.% Zr (Fig. 1, right). For synthesis at  $pH = 1$  both  $ThSiO_4$  and  $ZrSiO_4$  end-members were formed (Fig. 1, left, bottom). Interestingly, they were separated from the  $Zr_xTh_{1-x}SiO_4$  limited solid solutions ( $x = 0.5 - 0.7$ ) by miscibility gaps. This phase behavior could be dictated by kinetic barriers and thermodynamic stabilities of corresponding phases under specific values of  $pH$ . The  $Th_{0.9}Zr_{0.1}SiO_4$  phase subjected to HP exhibited structural changes around  $P = 14$  GPa while other studied phases were more resistant to HP. More details on structural evolutions in the  $ThSiO_4$ - $ZrSiO_4$  system both as a function of Th content and external pressure will be presented. Affinity of tetravalent actinides with  $ZrSiO_4$  host matrix and associated potential for utilization of  $ZrSiO_4$ -based systems for long-term storage of SNW will be discussed.

## References

1. Heaman, L. M. *et al. Chem. Geol.* **110**, 95–126 (1993).
2. Scheinost, A. C. *et al. J. Synchr. Rad.* **28**, 333–349 (2021).

\* Corresponding author. Tel.: +33476882232  
E-mail address: svitlyk@esrf.fr

## Actinide bonding trends through the eye of the theoretician

Michael Patzschke<sup>a,\*</sup>, Benjamin Scheibe<sup>b</sup>, Roger Kloditz<sup>a</sup>, Thomas Radoske<sup>a</sup>,  
Juliane März<sup>a</sup>, Peter Kaden<sup>a</sup>, Luisa Köhler<sup>a</sup>, Moritz Schmidt<sup>a</sup>, Thorsten Stumpf<sup>a</sup>

<sup>a</sup>Institute of Resource Ecology, Helmholtz-Zentrum Dresden-Rossendorf, Bautzner Landstraße 400, 01328 Dresden, Germany

<sup>b</sup>Institute of Inorganic Chemistry, Philipps-Universität Marburg, Hans-Meerwein-Straße 4, 35032 Marburg, Germany

## Abstract

Actinides are a very interesting group of elements, both for the experimentalist and the theoretician. One reason being scalar relativistic effects, which lead to  $5f$  electrons participating in bonding. To make matters more interesting, the  $5f$  orbitals compete with the  $6d$  orbitals to make bonding rather dependent on the structure of the ligand scaffold. Consequently, spin-orbit coupling is important to understand the spectroscopic properties of An-containing compounds, but might not be relevant for bond distances and other structural parameters. Theoretical tools based on molecular orbitals and the electron density exist to analyze the ligand-actinide bond, but due to the open-shell nature of most An compounds, multi-reference calculations may be necessary in order to get a valid density to analyze. Checking for multi-reference cases is therefore important. In combination with the large number of electrons each actinide adds to the calculation such studies of actinide bonding become computationally extremely demanding. There is one additional effect that is sometimes overlooked: Actinide-ligand bonds are still highly ionic and the resulting complexes can therefore be structurally rather flexible. This can and should be checked by molecular dynamics calculations.

Collaborating closely with experimentalists is highly beneficial, the field of metal-organic actinide chemistry is no exception here. Together experimentalists and theoreticians can devise systems to probe the An-ligand bond with different ligating atoms and changes to oxidation state of the metal to illuminate important concepts like the HSAB principle.

We will present results from systems with ligating atoms with different bonding properties: Fluorine, a very good  $\sigma$ -donor, and a good  $\pi$ -acceptor, “hard” oxygen, “softer” nitrogen, and mixed  $N, O$  ligands. With these sets of ligands it is possible to probe the actinide bonding and gain deeper understanding in the involved orbitals. Special care will be taken to demonstrate the validity of the performed DFT calculations. To this end multi-reference calculations will be presented, revealing the necessary active space with the help of entanglement diagrams (see Figure 1) and the influence of such a calculation on the electron density will be demonstrated.<sup>1-4</sup>

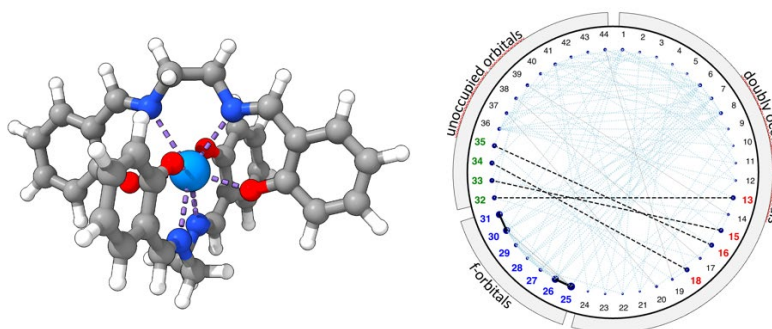


Figure 20. Molecular structure (left) and entanglement diagram (right) for  $[U(\text{salen})_2]$ .

## References

1. T. Radoske, R. Kloditz, S. Fichter, J. März, P. Kaden, M. Patzschke, M. Schmidt, T. Stumpf, O. Walter, A. Ikeda-Ohno, *Dalton Trans.*, **2020**,49, 17559-17570
2. B. Scheibe, M. Patzschke, J. März, M. Conrad, F. Kraus, *Eur. J. Inorg. Chem.*, **2020**, 3753-3759.
3. R. Kloditz, T. Radoske, M. Schmidt, T. Heine, T. Stumpf, M. Patzschke, *Inorg. Chem.* **2021**, 60 (4), 2514-2525.
4. L. Köhler, M. Patzschke, M. Schmidt, T. Stumpf, J. März, *Chem. Eur. J.* **2021**, 27, 18058–18065.

\* Corresponding author. Tel.: +xx-xxx-xx-xxxx; fax: +xx-xxx-xx-xxxx.  
E-mail address: your.name@institution.xxx.

# Insights at the molecular level into the formation of oxo-bridged trinuclear uranyl complexes

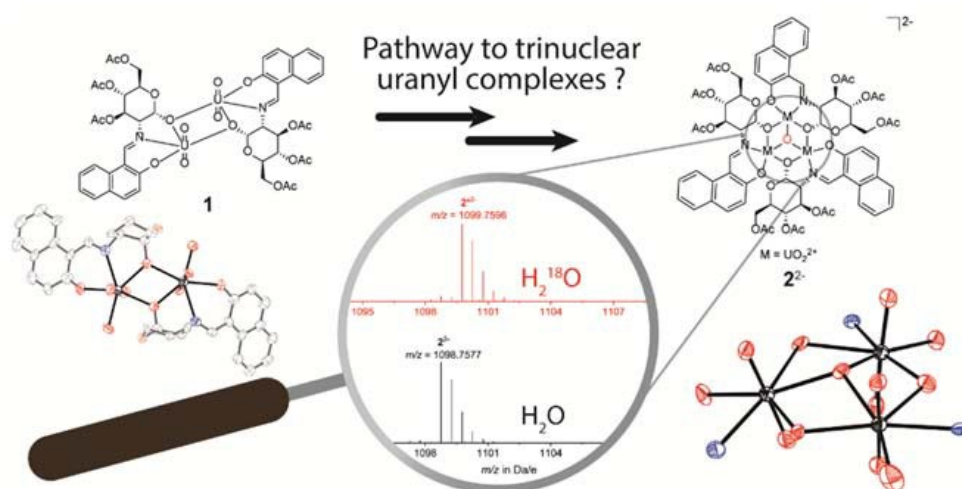
Gerrit Schaper<sup>a</sup>, Marco Wenzel<sup>a</sup>, Uwe Schwarzenbolz<sup>b</sup>, Johannes Steup<sup>a</sup>, Felix Hennersdorf<sup>a</sup>, Thomas Henle<sup>b</sup>, Jan J. Weigand<sup>a,\*</sup>

<sup>a</sup>Chair of Inorganic Molecular Chemistry, TU Dresden, 01062 Dresden, Germany

<sup>b</sup>Chair of Food Chemistry, TU Dresden, 01062 Dresden, Germany

## Abstract

As the most pervasive form of uranium in the natural environment, the coordination chemistry of the uranyl cation  $U^{VI}O_2^{2+}$  is of ongoing widespread interest.[1] The good solubility of most uranyl species and their subsequent high environmental mobility poses a significant threat to both human health and the ecosystem.[2] With this in mind, the coordination behaviour towards biologically relevant ligand systems is of special interest in relation to assessing potential contamination pathways.[3] Frequently the formation of multinuclear uranyl complex species is observed for such systems.[4] However, very few investigations have been undertaken regarding the formation details of such polynuclear uranyl complexes. In the present work we employed the glucosamine-derived Schiff base to investigate the formation of oxo-bridged trinuclear uranyl complex.[5] The reaction of the ligand with uranyl acetate results in the formation of the dinuclear uranyl complex **1**, which can be quantitatively transferred into the trinuclear oxo-bridged complex anion **2<sup>2-</sup>**. Single crystal X-ray analyses of a solvent adduct as well as of a protonated intermediate give insights into the different coordination modes of the uranyl ions during the conversion. Detailed examination of this transformation in solution using UV/Vis- and NMR-spectroscopy allowed details of the reaction pathway to be elucidated. Furthermore, the results of experiments employing isotope-enriched water to selectively introduce  $^{18}O$  into the  $\mu_3$ -bridge will be presented.



**Acknowledgement:** We thank the German Federal Ministry of Education and Research (FENABIUM project 02NUK046A) for financial support.

## References

1. Arnold, P. L.; Love, J. B.; Patel, D. *Coord. Chem. Rev.*, 2009, 253, 1973–1978.
2. Giannardi, C.; Dominici, D. *J. Environ. Radioact.* 2003, 64, 227–236.
3. Götzke, L.; Schaper, G.; März, J.; Kaden, P.; Huittinen, N.; Stumpf, T.; Kammerlander, K. K. K.; Brunner, E.; Hahn, P.; Mehnert, A.; Kersting, B.; Henle, T.; Lindoy, L. F.; Zanoni, G.; Weigand, J. J. *Coord. Chem. Rev.*, 2019, 386, 267-309.
4. Schaper, G.; Wenzel, M.; Hennersdorf, F.; Lindoy, L. F.; Weigand, J. J. *Chem. Eur. J.* 2021, 27, 8484–8491.
5. Schaper, G.; Wenzel, M.; Schwarzenbolz, U.; Steup, J.; Hennersdorf, F.; Henle, T.; Lindoy, L. F.; Weigand, J. J. *Chem. Commun.*, 2022, 58, 1748–1751.

\* Corresponding author. Tel.: +49 (351) 463-42800; fax: +49 (351) 463-3147.

E-mail address: jan.weigand@tu-dresden.de (J. J. Weigand)

DFT +  $U$  study of  $\text{UO}_2$  and  $\text{PuO}_2$  with Occupation Matrix ControlJiali Chen<sup>a,\*</sup>, Nikolas Kaltsoyannis<sup>a</sup><sup>a</sup>Department of Chemistry, University of Manchester, Oxford Road, Manchester, M13 9PL, UK**Abstract**

In the actinide series of elements, many of the chemical and physical properties display a turning point at plutonium. The actinide dioxides, which are the subject of this work, change from Mott-Hubbard insulators to charge transfer insulators at  $\text{PuO}_2$ .<sup>1-2</sup>  $\text{UO}_2$  and  $\text{NpO}_2$  have antiferromagnetic (AFM) ground states,<sup>3-4</sup> while a nonmagnetic (NM) ground state, which has been established by various experiments over a wide temperature range (4 - 1000K),<sup>5-8</sup> is found for  $\text{PuO}_2$ . However, previous DFT +  $U$  simulations have predicted an AFM ground state for  $\text{PuO}_2$ .<sup>9</sup> The inconsistency between experiment and DFT +  $U$  simulation over the correct magnetic ground state of  $\text{PuO}_2$  needs to be clarified. As  $\text{PuO}_2$  is a product of the recycling of spent  $\text{UO}_2$  nuclear fuel, detailed understanding of  $\text{PuO}_2$  is clearly essential not just at a fundamental level, but also to inform its safe current and long-term storage.

There are typically many different ways in which the actinide  $f$  orbitals may be populated, and use of the Hubbard  $U$  parameter in DFT calculations can lead to the location of meta-stable states arising from those electronic configurations.<sup>10</sup> The occupation matrix control (OMC) method in VASP, developed by Allen and Watson, is able to impose initial occupation matrices (OMs) on the orbitals of interest.<sup>11</sup> By considering all possible occupations of the actinide  $5f$  orbitals, the true ground state is the OM state with lowest energy. There are OMs for FM and  $1k$  colinear AFM  $\text{UO}_2$ , OMs for NM  $\text{UO}_2$ , OMs for FM and  $1k$  colinear AFM  $\text{PuO}_2$ , and OMs for NM  $\text{PuO}_2$ .

We initially tested the OMC on  $\text{UO}_2$  bulk, as  $\text{UO}_2$  is much better studied than  $\text{PuO}_2$ , with a wide range of  $U$  values (0.0 – 7.0 eV in 0.5 eV steps). Our DFT +  $U$  + OMC study of AFM  $\text{UO}_2$  shows that magnetic arrangements Type C (along the [100] direction), Type G (along the [110] direction) and Type A (along the [111] direction), have negligible influence on the energy. When the  $U$  value not too small ( $> 1.5$  eV), the [0000101], [00000101] and [0000200] OMs are always found to be the lowest energy state of AFM, FM and NM  $\text{UO}_2$ , while the AFM ground state is found for  $\text{UO}_2$  with  $U > 2.5$  eV. After locating the ground state of  $\text{UO}_2$ , various properties (lattice parameter, Bader charge, magnetic moment, band gap and densities of states) have been compared over a wide range of  $U$ . No  $U$  value perfectly predicts all the above mentioned properties, and we conclude that  $3.5 \text{ eV} \leq U \leq 4.5 \text{ eV}$  gives a good overall balance of agreement with experiments. Similar to  $\text{UO}_2$ , when  $U$  is not too small ( $> 1.5$  eV), the same OM states of  $\text{PuO}_2$  are found to have the lowest energy for the AFM, FM and NM states, these are [1010101], [1010101] and [0000202], respectively. The NM ground state is found for  $\text{PuO}_2$  with  $U > 2$  eV for the first time, in agreement with experimental results.  $3 \text{ eV} \leq U \leq 4 \text{ eV}$  is a good compromise for the simulation of the studied  $\text{PuO}_2$  bulk properties, i.e. lattice parameter, Bader charge, magnetic moment, band gap and densities of states.

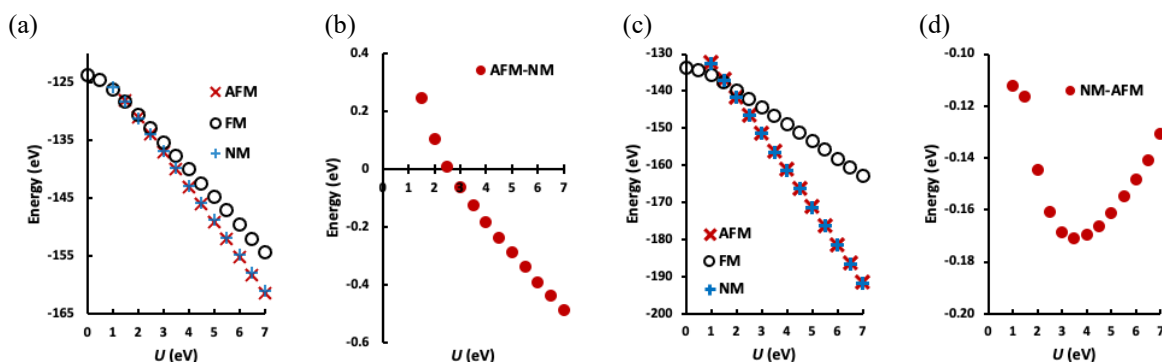


Figure 22 (a) energy of the most stable AFM, FM and NM OM state of  $\text{UO}_2$  (b) energy difference between the most stable AFM and NM state of  $\text{UO}_2$  (c) energy of the most stable AFM, FM and NM OM state of  $\text{PuO}_2$  and (d) energy difference between the most stable AFM and NM state of  $\text{PuO}_2$ .

**References**

- Chen, J.-L.; Kaltsoyannis, N. *The Journal of Physical Chemistry C* 2019, 123, 15540-15550.
- Chen, J.-L.; Kaltsoyannis, N. *Journal of Nuclear Materials* 2022, 560, 153490.

\* Corresponding author. Tel.: +44-0-7410377766.  
 E-mail address: jiali.chen@manchester.ac.uk.

3. Osborn, R.; Taylor, A. *Journal of Physics C: Solid State Physics* 1988, 21, L931.
4. Kern, S.; Morris, J. *Journal of Applied Physics* 1988, 63, 3598-3600.
5. Raphael, G.; Lallement, R. *Solid State Communications* 1968, 6, 383-385.
6. Kern, S.; Loong, C. K. *Journal of Physics: Condensed Matter* 1990, 2, 1933-1940.
7. Kern, S.; Robinson, R. *Physical Review B* 1999, 59, 104.
8. Yasuoka, H.; Koutroulakis, G. *Science* 2012, 336, 901-904.
9. Sun, B.; Zhang, P. *The Journal of chemical physics* 2008, 128, 084705.
10. Larson, P.; Lambrecht, W. R. *Physical Review B* 2007, 75, 045114.
11. Allen, J. P.; Watson, G. W. *Physical Chemistry Chemical Physics* 2014, 16, 21016-21031.

## Chemistry of Uranium Halides in liquid Ammonia

T. Graubner<sup>a,\*</sup>, A. Barba<sup>a</sup>, F. Kraus<sup>a</sup>AG Fluorchemie, Fachbereich Chemie, Philipps-Universität Marburg, Hans-Meerwein-Str. 4, 35032 Marburg, Germany

## Abstract

The chemistry of uranium halides and uranyl halides in anhydrous liquid ammonia is presented herein, following the recent achievements which were made in this field.<sup>[1–3]</sup> The synthesis of multi-nuclear uranium complexes is currently the focus of our attention. We therefore present the newly synthesized compound  $[\text{Th}_2(\text{NH}_3)_6][\{\text{UO}_2\text{F}_2(\text{NH}_3)\}_2(\mu\text{-F})_2]$ , which contains the already reported  $[\text{Th}_2(\text{NH}_3)_6]^{2+}$  cation and shows thalophilic interactions.<sup>[4]</sup> The synthesis was conducted at 40 °C using the bomb tube technique. The fluorine-bridged  $[\{\text{UO}_2\text{F}_2(\text{NH}_3)\}_2(\mu\text{-F})_2]^{2-}$  anion (figure 1) has two U(VI) central atoms, which are bridged by two fluorine atoms. This compound is an example that even fluorides can be dissolved in liquid ammonia, which is known to be quite a task.<sup>[5]</sup>

- [1] S. S. Rudel, S. A. Baer, P. Woidy, T. G. Müller, H. L. Deubner, B. Scheibe, F. Kraus, *Z. Kristallogr. - Cryst. Mater.* **2018**, *233*, 817–844.  
 [2] P. Woidy, F. Kraus, *Acta Crystallogr. Sect. E Crystallogr. Commun.* **2016**, *72*, 1710–1713.  
 [3] F. Kraus, S. A. Baer, *Chem. - Eur. J.* **2009**, *15*, 8269–8274.  
 [4] S. S. Rudel, T. Graubner, A. J. Karttunen, S. Dehnen, F. Kraus, *Inorg. Chem.* **2021**, *60*, 15031–15040.  
 [5] F. Kraus, *Bioinorg. React. Mech.* **2012**, *8*, 29–39.

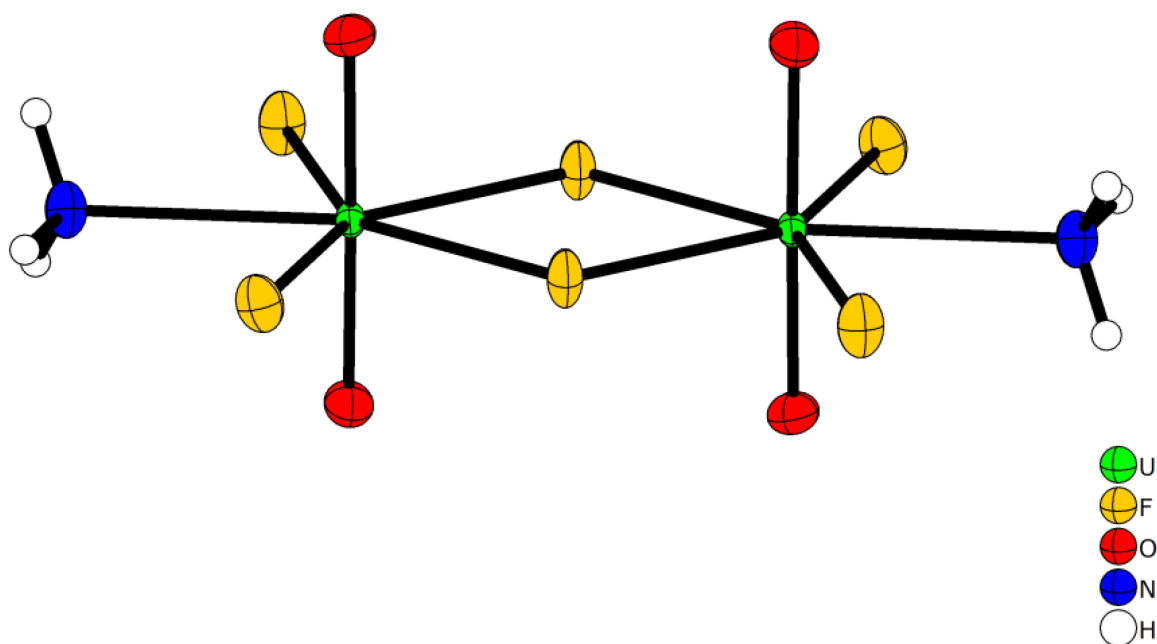


Figure 23 The  $[\{\text{UO}_2\text{F}_2(\text{NH}_3)\}_2(\mu\text{-F})_2]^{2-}$  anion. Displacement ellipsoids at 70% probability at 100 K, hydrogen atoms isotropic with arbitrary radius.

## Abstracts – Poster

# Insights into the solution structure of hydrated uranium and thorium ions from neutron scattering experiments

Samuel J. Edwards<sup>a</sup>, Daniel T. Bowron<sup>b</sup>, Robert J. Baker<sup>a\*</sup>

<sup>a</sup>*School of Chemistry, Trinity College Dublin, Dublin 2, Ireland*

<sup>b</sup>*Institution/University, Institute, Address, Country*

## Abstract

The solution structure of actinides is an important topic that is difficult to study in detail.<sup>1</sup> We report a study on a 1.0 M Uranyl Chloride solution that has been determined by the EPSR modelling of a combination of neutron scattering and previously reported EXAFS data. The experimental data shows an equilibrium in solution between  $[\text{UO}_2(\text{H}_2\text{O})_5]^{2+}$  and  $[\text{UO}_2\text{Cl}(\text{H}_2\text{O})_4]^+$  with a stability constant of  $0.23 \pm 0.03 \text{ mol}^{-1} \text{ dm}^3$ . A much smaller fraction of the neutral  $[\text{UO}_2\text{Cl}_2(\text{H}_2\text{O})_3]$  ion is also observed. The data also show, for the first time in solution, that the uranyl ion is a very poor hydrogen bond acceptor, but the coordinated waters show enhanced hydrogen bond ability compared to the bulk water. Further experiments on the increasing  $[\text{Cl}]^-$  concentrations of hydrated uranyl chloride will be discussed. To expand the results to other oxidation states,  $[\text{UCl}_4(\text{H}_2\text{O})_x]$  has been studied and again equilibria noted and stability constants extracted from the modelling. Furthermore, the solid state X-ray structure of  $[\text{Et}_4\text{N}][\text{UO}_2\text{Cl}_3(\text{H}_2\text{O})_2]$  will be presented and discussed in relation to the solution structures. Finally, hydrated  $\text{ThCl}_4$  and  $\text{ThBr}_4$  have been studied using the same technique and inner sphere vs outer sphere equilibria have again been noted.

We believe that the use of neutrons to interrogate light atoms in actinide compounds is an under-utilised technique that can give structural information that is generally complementary to EXAFS, but with the advantage that the model is not so dependent on built in assumptions that can render the errors in coordination numbers around an actinide metal centre. Using the combination of techniques, both the bulk and local structure can be extracted into a robust model. DFT calculations can follow the trends in hydration behaviour, but AIM analysis gives a deeper insight into the hydrogen bonding in the bulk phase.<sup>2</sup>

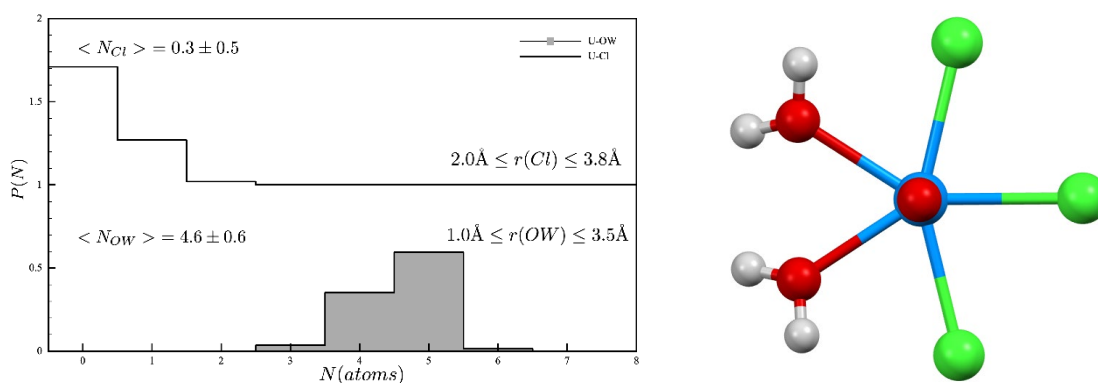


Figure 24 (left) Results of EPSR modelling of 1.0M Uranyl Chloride showing the Cl<sup>-</sup> and OH<sub>2</sub> coordination numbers; (right) X-ray structure of

## References

1. Knope, K.E.; Soderholm, L. Solution and Solid-State Structural Chemistry of Actinide Hydrates and Their Hydrolysis and Condensation Products. *Chem. Rev.*, 2013, 113, 944-994.
2. Baker, R.J.; Platts, J. A. Non-covalent interactions of uranyl complexes: a theoretical study. *Phys. Chem. Chem. Phys.*, 2018, 20, 15380

\* Corresponding author. Tel.: +353-1-8963501.

E-mail address: baker@tcd.ie

# In situ HERFD-XAS experiments on uranium state under high temperature

Elena Bazarkina<sup>a,b\*</sup>, Stephen Bauters<sup>a,b</sup>, Jean-Louis Hazemann<sup>c</sup>, Denis Testemale<sup>c</sup>,  
Kristina Kvashnina<sup>a,b</sup>

<sup>a</sup>Rossendorf Beamline at ESRF – The European Synchrotron, CS40220, 71 Avenue des Martyrs, 38043 Grenoble Cedex 9, France

<sup>b</sup>Helmholtz Zentrum Dresden-Rossendorf (HZDR), Institute of Resource Ecology, PO Box 510119, 01314 Dresden, Germany

<sup>c</sup>Université Grenoble Alpes, CNRS, Institut Néel, 25 Avenue des Martyrs, F-38042 Grenoble Cedex 9, France

## Abstract

Experiments under high temperature ( $T$ ) involving uranium (U) are of high importance for our knowledge of  $T$ -dependent chemical transformations of U compounds and the properties of final products under conditions typical for planet interiors or in nuclear accidents. With the help of a synchrotron radiation facility, oxidation state and local structure can be probed in situ by powerful techniques such as high-energy resolution fluorescence detection spectroscopy HERFD-XAS. The solid uranium state can be probed under high temperatures at the U  $M_4$  edge using a recently developed cell (Fig. 1., left) at ROBL [1]. The aqueous U species can be studied at the U  $L_3$  edge using an internal-cell hydrothermal autoclave (Fig. 1, right) at FAME-UHD [2].

The in-situ experiments under elevated  $T$  with the tender X-rays (i.e. near U  $M_4$  edge, 3728 eV) are extremely delicate due to the high absorption of the incident and emitted X-rays by the air and materials in the optical path. However, the HERFD-XANES method at the U  $M_4$ -edge spectra [3, 4] is extremely powerful since it allows accurate determination of  $U^{4+}$ ,  $U^{5+}$ , and  $U^{6+}$  fractions as a function of  $T$  and time. In the case of experiments in aqueous solutions at the  $L_3$  edge (17166 eV), our spectra prove the high stability of chloride complexes of uranyl at high  $T$  under oxidizing conditions. In the presence of glassy carbon, all dissolved U is reduced. Both types of in situ cells show a high sensitivity of U chemistry to temperature. With the help of thermodynamic approaches and electronic structure calculations, these types of experiments are very promising and need to be more explored.

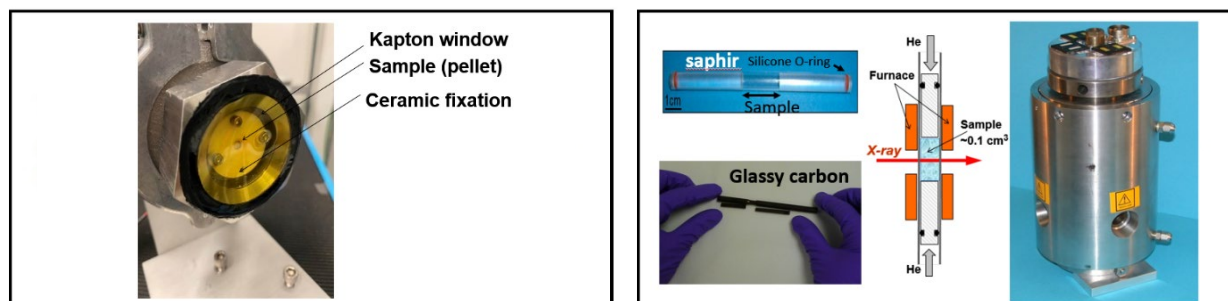


Figure 25. Left: The photo of the in-situ cell used in the experiment at  $M_4$ -edge of U. Right: photos and schema of internal heating cell and high-pressure autoclave used for aqueous speciation experiments at  $L_3$ -edge of U.

*This work was supported by ERC grant 759696.*

## References

1. Scheinost A. C.; Claussner J.; Exner J.; Feig M., Findeisen S.; Hennig C.; Kvashnina K. O.; Naudet D.; Prieur D.; Rossberg A.; Schmidt M.; Qiu C.; Colomp P.; Cohen C.; Dettona E.; Dyadkin V.; Stumpf T. *Journal of Synchrotron Radiation*, 2021, 28, 333–349.
2. Proux O.; Lahera E.; Del Net W.; Kieffer I.; Rovezzi M.; Testemale D.; Irar M.; Thomas S.; Aguilar-Tapia A.; Bazarkina E.F.; Prat A.; Tella M.; Auffan M.; Rose J.; Hazemann J.-L. *Journal of Environmental Quality*, 2017, 46, 1146–1157.
3. Kvashnina K.O.; Butorin S. M.; Martin P.; Glatzel P. *Physical Review Letters*, 2013, 111, 253002.
4. Kvashnina K.O.; Butorin S. M.; *Chemical Communications*, 2022, 58, 327–342.

\* Corresponding author. Tel.: +33-476-88-4578; fax: +33-476-88-2020.

E-mail address: elena.bazarkina@esrf.fr.

# Quantification of the impact of defect density on $\text{Eu}^{3+}$ sorption efficiency on alpha particle irradiated biotite crystals

M.A. Cardenas Rivera<sup>a,\*</sup>, S. Akhmadaliev<sup>b</sup>, C. Fischer<sup>a</sup>

<sup>a</sup>Institute of Resource Ecology, Helmholtz-Zentrum Dresden-Rossendorf, Dresden, Germany

<sup>b</sup>Institute of Ion Beam Physics and Materials Research, Helmholtz-Zentrum Dresden-Rossendorf, Dresden, Germany

## Abstract

Alpha particles emitted from actinides can cause lattice defects in crystalline solids. These affect surface reactivity of various reactions such as dissolution, growth or sorption<sup>1</sup>. Biotite is an important rock-forming mineral in a variety of igneous and metamorphic rocks that are considered for use as deep geological repositories. The frequent occurrence of biotite in host-rocks can quantitatively influence the retention of migrating radionuclides in the far field<sup>2</sup>. Therefore, understanding and quantifying the effects exposure to radionuclides can have on the sorbing capabilities of a crystal, will lead to an improved predictability of the far-field natural barriers upon which safe waste disposal relies.

In this study, as part of the H2020 EURAD project WP FUTURE, we investigate the formation of crystal defects in biotite and their influence on surface reactivity. For this study, two pristine biotite sampled were irradiated with and  $^4\text{He}^{3+}$  focused ion beam in order to induce crystal structural damage. This is an analogue to the situation of radionuclide release in the repository. The irradiation parameters were chosen to avoid amorphization and to focus on crystal defect development. The samples are then surface-controlled dissolved to finally quantify the defect density by using vertical scanning interferometry (VSI)(Figure 1). Subsequently, the surface-modified biotite samples are used for sorption experiments with actinide analogues such as  $^{152}\text{Eu}^{3+}$ . Comparison of the anticipated results will provide conclusions to be drawn about the quantitative changes in reactive transport processes of actinide migration in sheet-bearing host rocks.

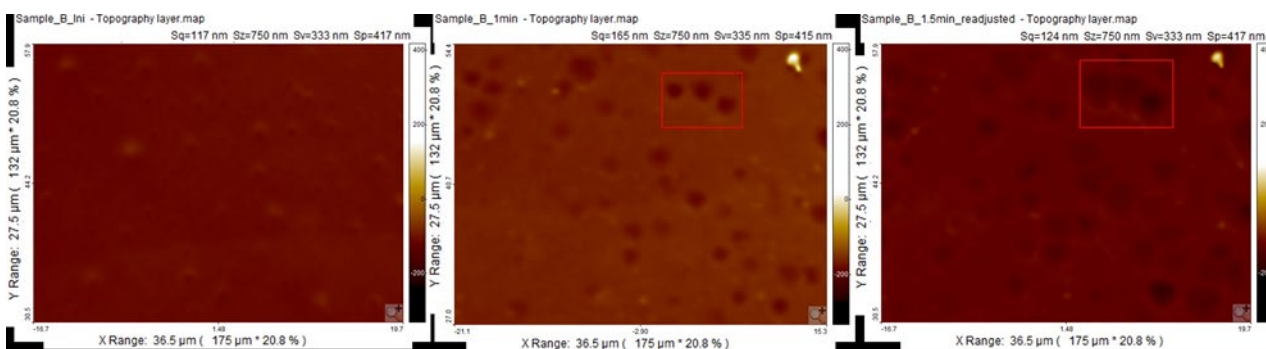


Figure 26 Sequence of identified defects under interferometric microscopy after 1 minute (centre) and 1.5 minutes (right) of controlled dissolution, compared to the initial pristine biotite crystal (left). The dissolution of the biotite allows to increase the visibility of the structural damages caused by irradiation, an enables the quantification of the dissolution rates by measuring both the horizontal and vertical increase of the of the identified surface defects (highlighted features in red box).

## References

1. Yuan, T. *et al.* Heterogeneous Sorption of Radionuclides Predicted by Crystal Surface Nanoroughness. *Environmental Science & Technology*, **55**, (2021).
2. Bower, W. R. *et al.* Radiation damage in biotite mica by accelerated  $\alpha$ -particles: A synchrotron microfocus X-ray diffraction and X-ray absorption spectroscopy study. *American Mineralogist*, **101**, 928–942 (2016).

\* Corresponding author.

E-mail address: m.cardenas-rivera@hzdr.de.

# Synthetic Organometallic Pathways to Produce Uranium Cermet Materials via Laser Decomposition

Bradley C. Childs<sup>a,\*</sup>, Michelle M. Greenough<sup>a</sup>, Maryline G. Ferrier<sup>a</sup>, Aiden A. Martin<sup>a</sup>,  
Kiel S. Holliday<sup>a</sup>, Jason R. Jeffries

<sup>a</sup>Physical and Life Sciences Directorate, Lawrence Livermore National Laboratory, Livermore, California 94550, USA

## Abstract

Metallic and cermet type materials containing uranium lack multiple routes to production due to the ease in which they have been made for over half a century. As new routes have been studied to observe the chemical behavior of advanced uranium compounds, further processing and decomposition to desirable binary and cermet uranium material has not been fully studied. Synthesis of complex uranium compounds with favorable decomposition temperatures were identified through volume based thermodynamic calculations.

Uranium organometallic compounds were then synthesized under air- and water-free conditions. Careful attention was placed on the following conditions:

1. The desired oxidation states of the core uranium atom are U(III) or U(IV).
2. Molar ratios of carbon and nitrogen in the surrounding ligands to achieve desired stoichiometries after irradiation under the laser.
3. At high temperatures (>2500K), compounds containing oxygen or oxygen bearing ligands can produce uranium oxides which are not desired.
4. Focus was placed on the halides bonded to the central uranium atom, especially on the chemistry of iodine and chlorine to understand if these leaving groups play a major role in processing.

Thermal analysis was performed on the compound through thermal gravimetric analysis and was also irradiated with an enclosed laser system. The products were confirmed based on X-ray diffraction, scanning electron microscopy and energy-dispersive X-ray spectroscopy.

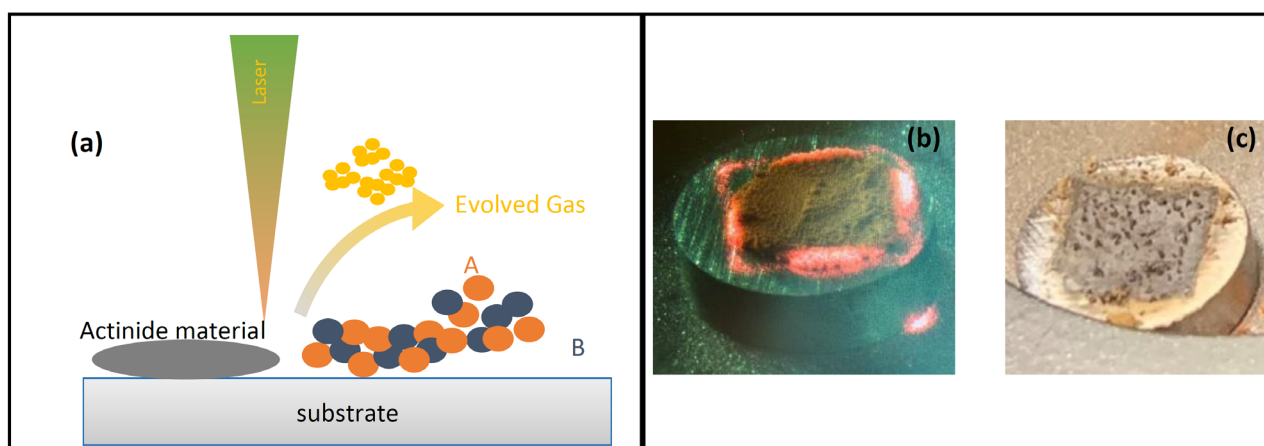


Figure 1: (a) Illustrates a schematic of a laser interacting with actinide material. (b) Displays an uranium organometallic under the guide beam of the laser system. (c) A uranium sample post 10-watt laser irradiation.

This work was performed under the auspices of the U.S. Department of Energy by Lawrence Livermore National Laboratory under Contract DE-AC52-07NA27344.

\* Corresponding author. Tel.: +1-925-424-4043.  
E-mail address: childsa4@llnl.gov

# Computational Studies of Iron-Actinide Chemistry of Importance to UK Nuclear Waste Clean-up

Ryan Dempsey<sup>a,\*</sup>, Samuel Shaw<sup>b</sup>, Katherine Morris<sup>b</sup>, Nikolas Kaltsoyannis<sup>a</sup>

<sup>a</sup>University of Manchester, Department of Chemistry, Manchester, M13 9PL, United Kingdom

<sup>b</sup>University of Manchester, Williamson Research Centre, School of Earth and Environmental Sciences, Manchester, M13 9PL, United Kingdom

## Abstract

The Enhanced Actinide Removal Plant (EARP) at Sellafield's nuclear decommissioning and fuel reprocessing site in Cumbria is one of the UK's most important radioactive effluent treatment plants. The EARP feed consists of highly acidic, ferrous conditions which is exploited by inducing a base hydrolysis process whereby the iron in solution crashes out rapidly forming a metastable ferrihydrite floc which transform into hematite or goethite. During this process there is a large uptake of actinides allowing for separation of radioactive effluent by some unknown mechanism. Recently, fuel reprocessing at Sellafield ended, the Thermal Oxide Reprocessing Plant (THORP) closed in 2018 as did the Magnox reprocessing plant in 2021. The EARP, however, will not close. As the reprocessing plants transition into post-operational clean out (POCO) the EARP feed will become more diverse than ever.

Smith et al. showed evidence of unique Pu-O bonding when Pu(IV) is sequestered in EARP conditions through L<sub>3</sub>-edge EXAFS and thermodynamic modelling. The results suggest that Pu may bind within a "square window" surrounded by four octahedrally coordinated [FeO<sub>6</sub>] units.<sup>1</sup> Prior to this work one would expect a nanoparticulate PuO<sub>2</sub> phase to dominate yet this was observed as a minor product. The EXAFS data is consistent with a Fe<sub>13</sub> Keggin unit which has also been confirmed as a precursor to nanoparticulate ferrihydrite formation.<sup>2</sup> If true, this process underpinning actinide removal is occurring at the molecular level prior to the floc formation leading to ferrihydrite. The need to develop our understanding of the molecular interactions prior to the flocculation process is more important now than ever before.

To investigate further, Density Functional Theory (DFT) has been used to assess the feasibility of a  $\alpha$ -Fe<sub>13</sub> Keggin cluster interacting with molecular Pu(IV), first binding to the "square window" and replacing the capping Na<sup>+</sup> in solution. Thermodynamically corrected reaction energies calculated at the def2-TZVP/PBE0 level show that such a process is favourable with the optimised geometries consistent with Smith's EXAFS data. This study also plans to explore similar chemistry across a series of actinides which are removed at the EARP.

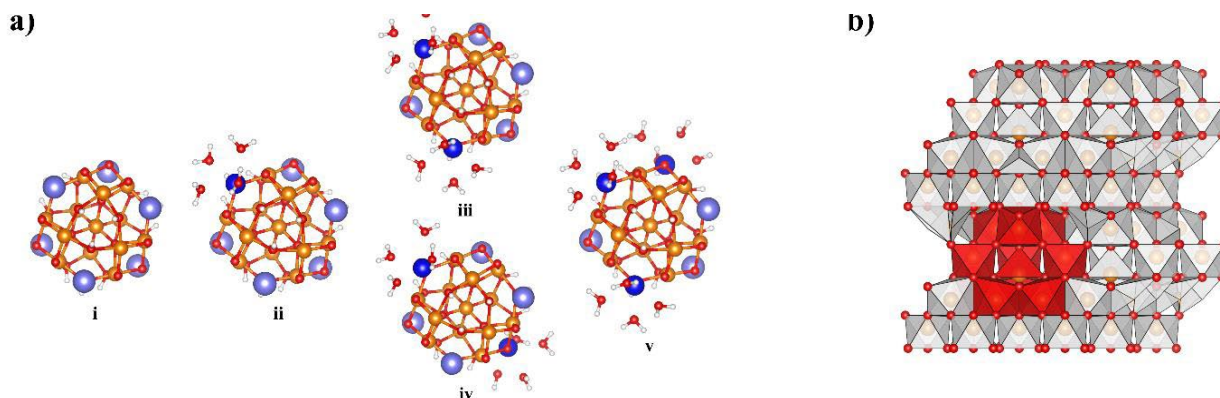


Figure 27. a) Optimised  $\alpha$ -Fe<sub>13</sub> Keggin clusters: from i to v the number of Pu(IV)(H<sub>2</sub>O)<sub>4</sub> substitutions increases where iii and iv are *cis*- and *trans*-disubstituted isomers and v is the *mer*-trisubstituted isomer (Fe = Orange, O = Red, H = White, Na = Purple and Pu = Blue). b) Polyhedral representation of 2-line Ferrihydrite with the  $\delta$ -Fe<sub>13</sub> Keggin unit emphasised in red.

## References

1. Smith, K. F.; **Morris, K.**; Law, G. T. W.; Winstanley, E. H.; Livens, F. R.; Weatherill, J. S.; Abrahamsen-Mills, L. G.; Bryan, N. D.; Mosselmans, J. F. W.; Cibin, G.; Parry, S.; Blackham, R.; Law, K. A.; **Shaw, S.**, *ACS Earth and Space Chemistry*, 2019, **3**, 2437-2442.
2. Weatherill, J. S.; **Morris, K.**; Bots, P.; Stawski, T. M.; Janssen, A.; Abrahamsen, L.; Blackham, R.; **Shaw, S.**, *Environmental Science and Technology*, 2016, **50**, 9333-9342.

\* Corresponding author. Tel.: +44-755-712-4958  
E-mail address: ryan.dempsey@postgrad.manchester.ac.uk.

# Influence of organic complexing agents on the sorption of Eu(III) to C-S-H phases: a TRLFS study

Sophie Dettmann<sup>a</sup>, Michael U. Kumke<sup>a,\*</sup>

<sup>a</sup>University of Potsdam, Institute of Chemistry, Karl-Liebknecht-Str. 24-25, 14476 Potsdam (Germany)

---

## Abstract

The sorption of radionuclides to technical barriers, such as cement phases, is an important retention mechanism in a deep geological repository for radioactive waste. However, the presence of organic complexing agents in the waste may influence the sorption behavior of the radionuclides and potentially increase their mobility, e.g., due to the formation of soluble complexes.[1,2] Therefore, the interactions between radionuclides, organic complexants and the technical barriers need to be understood under conditions present in the repository.

For this purpose, first the complexation of Eu(III), which can be considered as a non-radioactive analog for the trivalent Actinides Am(III) and Cm(III), with the two complexing agents NTA and gluconate was studied at pH 10 and 12. In the next step, ternary systems were analyzed. Here, the influence of NTA and gluconate on the sorption of Eu(III) to calcium silicate hydrate phases (C-S-H phases), which represent the major components of cement, was investigated over a large concentration range of the organic compounds ( $5 \mu\text{M} \leq [\text{organics}] \leq 150 \text{ mM}$ ). The experiments aimed to i) determine the complexant concentration, at which an alteration of the sorption can be observed and ii) to further develop the molecular understanding of the interaction and shed light on the mechanisms over which the sorption behavior is impacted. To reflect the different aging stages of cement in the repository, two different Ca:Si-ratios (C/S = 1.65 and 0.80) were used, corresponding to the alteration stages II and III respectively.[3]

Time-resolved laser fluorescence spectroscopy (TRLFS) combined with a parallel factors analysis was used to determine the speciation of Eu(III) both in the solid and aqueous phase. Based on the data qualitative and quantitative information on the species distribution and its changes due to the presence of the organics were derived. In addition, effects on the formation kinetics of the different species were obtained. Depending on the Ca:Si-ratio two to three sorption sites were identified, which may correspond to surface sorption and incorporation processes respectively.[4-6] However, different sorbed Eu(III) species were found for the two Ca:Si-ratios, subsequently reflecting the structural differences of the two C-S-H phases. At both Ca:Si-ratios, NTA only had a small influence on the quantitative sorption of Eu(III), while gluconate was able to drastically reduce the sorption at high Ca:Si-ratio and alter the relative amounts of each sorption species at low Ca:Si-ratio. Furthermore, Eu(III)-gluconate complexes were observed in the solid phase, suggesting a potential sorption of the complexes to the C-S-H surface. SEM imaging also revealed morphological changes of the C-S-H phases in the presence of high gluconate concentrations, indicating that the sorption may be influenced both by complexation of Eu(III) and alteration of the C-S-H properties.

## References

3. Keith Roach, M.; Shahkarami, P. Organic Materials with the Potential for Complexation in SFR, the Final Repository for Short-Lived Radioactive Waste, Stockholm, Sweden, 2021, R-21-03.
4. Dario, M.; Molera, M.; Allard, B. Effect of Organic Ligands on the Sorption of Europium on TiO<sub>2</sub> and Cement at High pH, Stockholm, Sweden, 2004, TR-04-04.
5. Tits, J.; Wieland, E. Actinide Sorption by Cementitious Materials, 2018, R-18-02.
6. Poiteau, I.; Piriou, B.; Fedoroff, M.; Barthes, M. G.; Marmier, N.; Fromage, F. J. Colloid Interface Sci. 2001, 236, 252-259.
7. Tits, J.; Stumpf, T.; Rabung, T.; Wieland, E.; Fanghänel, T. Environ. Sci. Technol. 2003, 37, 3568-3573.
8. Mandaliev, P.; Stumpf, T.; Tits, J.; Dähn, R.; Walther, C.; Wieland, E. Geochim. Cosmochim. Acta, 2011, 75, 2017-2029.

---

\* Corresponding author. Tel.: +49-331-977-5209; fax: +49-0331-977-6137.  
E-mail address: kumke@uni-potsdam.de

# Solvent extraction studies of different diastereomers of modified diglycolamide ligands for An(III) and Ln(III) extraction

Laura Diaz Gomez<sup>a,\*</sup>, Andreas Wilden<sup>a</sup>, Giuseppe Modolo<sup>a</sup>, Wim Verboom<sup>b</sup>

<sup>a</sup>Forschungszentrum Jülich GmbH, Institut für Energie- und Klimaforschung – Nukleare Entsorgung und Reaktorsicherheit (IEK-6), 52428 Jülich, Germany

<sup>b</sup>Mesa+ Institute for Nanotechnology, Laboratory of Molecular Nanofabrication, University of Twente, 7500 AE Enschede, The Netherlands

## Abstract

Solvent extraction is currently the preferred technique for the separation of actinides (An) from fission products (FP), and especially lanthanides (Ln), as constituents of Spent Nuclear Fuel (SNF) or PUREX raffinate. A special interest is on the separation of Am from Cm, Ln and other FP by testing various ligands to upgrade the current methods. Diglycolamide (DGA) derivatives have shown promising results as extractants for trivalent Ln and An, such as, *N,N,N',N'*-tetra-*n*-octyl diglycolamide (TODGA), which usually have a higher affinity for Cm(III) over Am(III). Wilden et al. [1] reported a change on Am(III) selectivity over Cm(III) with methyl substitutions with different orientation in the backbone of Me<sub>2</sub>-TODGA. Here, we study the selectivity and affinity of related extractants (TODGA and *N,N,N',N'*-tetra-*n*-decyl diglycolamide, TDDGA) with dipropyl and ethyl-methyl substitutions in the molecule backbone, and their respective diastereomers (*syn* or *anti*) in *n*-dodecane. The chemical structures are shown in Figure 1 An inverse selectivity is observed for Am(III) over Cm(III) and other Ln(III) at high nitric acid concentration (7 - 10 mol L<sup>-1</sup> HNO<sub>3</sub>). The steric hindrance gives low distribution ratios ( $D < 1.5$ ) for the trivalent metal ions at 0.1 mol L<sup>-1</sup> ligand concentration, as shown in Figure 2. Besides trivalent ions, Pu(IV) was also tested with the interest on the complexation behavior with tetravalent ions, which shows remarkably higher distribution ratios at the same HNO<sub>3</sub> concentrations ( $D > 10$ ). This is unlike methyl and dimethyl-TODGA, which present similar distribution ratios between trivalent and tetravalent metal ions. The *syn*-ethyl-methyl substitutions for both analogues showed the highest  $D$  values for Am(III) among the tested ligands, giving a promising molecule for further studies. The results of the extraction studies will be presented and discussed in the poster.

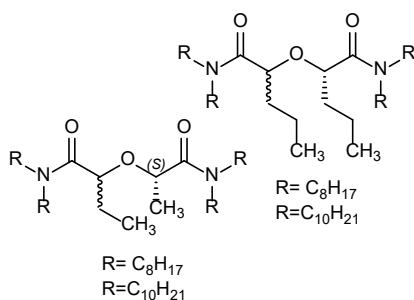


Figure 28. Chemical structures of the tested diglycolamides

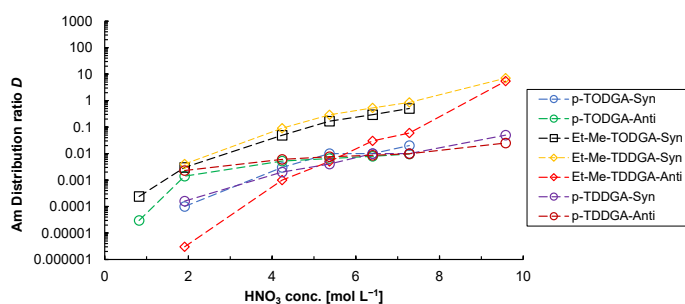


Figure 29. Comparison of the tested ligands. Am distribution ratios as a function of HNO<sub>3</sub> concentration. (Exp. 22°C, 30 min shaking time, [Ligand]: 0.1 mol L<sup>-1</sup> in *n*-dodecane)

## References

1. Wilden, A., et al., *Unprecedented Inversion of Selectivity and Extraordinary Difference in the Complexation of Trivalent f-Elements by Diastereomers of a Methylated Diglycolamide*. Chem. Eur. J., 2019. **25**(21): p. 5507-5513.

# Synthesis and Coordination Chemistry of N-Donor Ligands with early Actinides

T. Duckworth<sup>a,\*</sup>, J. März<sup>a</sup>, P. Kaden<sup>a</sup>, M. Patzschke<sup>a</sup>, N. Schwarz<sup>b</sup>, G. Greif<sup>b</sup>, T. Stumpf<sup>a</sup>

<sup>a</sup>Helmholtz-Zentrum Dresden-Rossendorf, Institute of Resource Ecology, Bautzner Landstraße 400, 01328 Dresden, Germany

<sup>b</sup>Karlsruhe Institute of Technology (KIT), Institute for Inorganic Chemistry, 76131 Karlsruhe, Germany

## Abstract

Understanding the subtle differences between lanthanide and actinide complexation chemistry with different ligand systems is an ongoing field of research. Soft donor ligands, especially ligands containing nitrogen, have shown to be promising for the investigation of the small differences in bonding behavior of actinides compared to lanthanides particularly with regards to the covalent contribution within the bond.

BTP type ligands have been used as an extracting ligand for the separation of lanthanides from actinides.<sup>1</sup> Therefore, new soft nitrogen donor ligands based on the BTP type ligand (2,6-Bis(1,2,4-Triazin-3-yl)Pyridine) or Schiff base ligands have been synthesized to explore the fundamental chemistry of the early 5f-elements. In order to investigate the coordination environment, ligand selectivity, bonding trends and electronic properties a series of actinide complexes ranging from thorium to plutonium has been characterized in solid state as well as in solution.

In the present study the synthesis of the new soft donor ligand **L1** was carried out via a copper mediated click reaction of the corresponding alkyne and azide. The bipyridine based ligand **L2** was obtained in a three step synthesis starting from bipyridine via the corresponding N-oxide and cyanide to give the tetrazine.

Both ligands **L1** and **L2** were successfully applied in the complexation reaction with trivalent lanthanides e.g. Er and Sm. In this contribution the investigation of the coordination chemistry of these soft N-donor ligands is extended to the early actinides in their tri- and tetravalent oxidation state.

First experimental results show the formation of a 3:1 complex in the case of trivalent Er. In contrast, the same ligand system **L1** forms a 2:1 complex with U(IV) including methanolato and iodo ligands for charge compensation. Further results including first structural characterization as well as results from quantum chemical calculations to elucidate the binding situation, will be presented in this contribution.

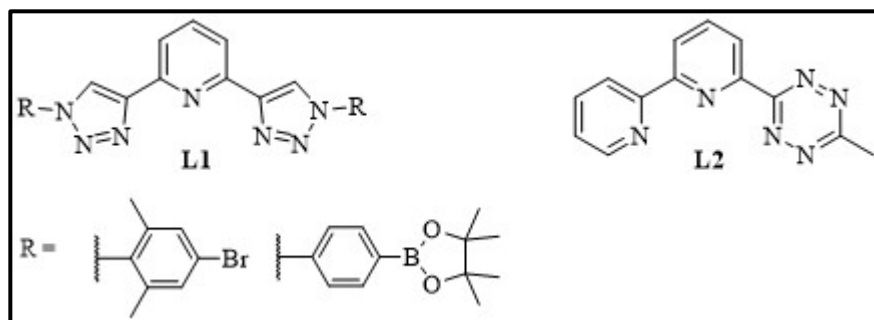


Figure 30 N-donor ligands used in this study

## References

1. Z. Kolarik, U. Müllich, F. Gassner, Solvent Extr. Ion Exch. 1999, 17, 23–32.

## Acknowledgement

This work was supported by the German Federal Ministry of Education and Research (BMBF) under project number 02NUK059 (f-char).

\* Corresponding author. Tel.: +49 351 260 2438

E-mail address: t.duckworth@hzdr.de

# Complexation of Eu(III) and Cm(III) by aminopolycarboxylic acids related to EGTA

Sebastian Friedrich<sup>a\*</sup>, Linus Holtmann<sup>b</sup>, Jérôme Kretschmar<sup>a</sup>, Björn Drobot<sup>a</sup>, Thorsten Stumpf<sup>a</sup>, Astrid Barkleit<sup>a</sup>

<sup>a</sup>Institute of Resource Ecology, Helmholtz-Zentrum Dresden-Rossendorf, Bautzner Landstraße 400, 01328 Dresden, Germany

<sup>b</sup>Institute for Radioecology and Radiation Protection, Leibniz Universität Hannover, Herrenhäuser Straße 2, 30419 Hannover, Germany

## Abstract

For purposes of chelation therapy and radiation protection, aminopolycarboxylic acids like ethylenediaminetetraacetic acid (EDTA) or diethylenetriaminepentaacetic acid (DTPA) are clinical approved decorporation agents against lanthanides (Ln) and actinides (An). This well known group of chelating agents shows promising results in complexation of Ln(III)/An(III). For EDTA and DTPA related compound ethylene glycol-bis(β-aminoethyl ether)-N,N,N',N'-tetraacetic acid (EGTA), complexes with trivalent europium (Eu) have been characterized by NMR spectroscopy and x-ray diffraction. In these complexes, EGTA acts as an octadentate ligand.<sup>[1][2]</sup> In this work the knowledge on the Eu-EGTA-system is extended by time-resolved laser-induced fluorescence spectroscopy (TRLFS), electrospray ionization mass spectrometry (ESI-MS) and isothermal titration calorimetry (ITC). These speciation studies on Eu(III) show promising results for EGTA as complexing agent (Figure 1).

To expand this ligand group, EGTA related ligands are synthesized. With these compounds, the complexation behaviour towards Eu(III) and curium(III) are determined and comprehensively characterised from both the ligands and metals perspective with TRLFS, NMR spectroscopy, single crystal x-ray diffraction and fourier-transform infrared spectroscopy. The overall goal is a better understanding between ligand design and affinity to trivalent lanthanides and actinides. Hence, in the future these ligands may contribute to chelation therapy as decorporation agents.

This work is funded by the German Federal Ministry of Education and Research (BMBF) under grant number 02NUK057A and part of the joint project RADEKOR.

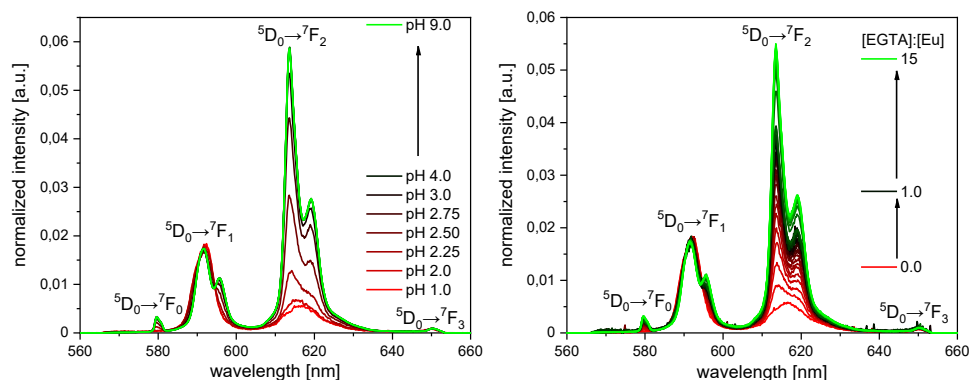


Figure 31: Emission spectra of Eu<sup>3+</sup> with EGTA obtained by TRLFS. Left: Influence of the pH value. pH = 1.0 to 9.0, [Eu<sup>3+</sup>] = 1 μM, [EGTA] = 10 μM, I<sub>NaClO<sub>4</sub></sub> = 100 mM. Right: Influence of concentration. pH = 3.0, [Eu<sup>3+</sup>] = 1 to 0.63 μM, [EGTA] = 0 to 9.4 μM, I<sub>NaClO<sub>4</sub></sub> = 100 mM.

## References

- [1]. S. Aime, A. Barge, A. Borel, M. Botta, S. Chemerisov, A. E. Merbach, U. Müller, D. Pubanz, *Inorg. Chem.* **1997**, 36, 5104.
- [2]. R. Xu, D. Li, J. Wang, Y. X. Kong, B. X. Wang, Y. M. Kong, T. T. Fan, B. Liu, *Russ. J. Coord. Chem.* **2010**, 36, 810.

\* Corresponding author. Tel.: + 49 351 260 3154.

E-mail address: s.friedrich@hzdr.de.

# Electron Paramagnetic Resonance Spectroscopy of Early d- and f-Block Metal(III)-Silanides

Gemma K. Gransbury<sup>a</sup>, Benjamin L. L. Réant<sup>a</sup>, Ashley J. Wooles<sup>a</sup>, Jack Emerson-King<sup>a</sup>, Nicholas F. Chilton<sup>a</sup>, Stephen T. Liddle<sup>a,\*</sup>, David P. Mills<sup>a,\*</sup>

<sup>a</sup> Department of Chemistry, The University of Manchester, Oxford Road, Manchester, M13 9PL, U.K.

## Abstract

f-Block silicon chemistry is a rapidly growing area, with potential applications including the use of uranium silicides as high density nuclear fuels and lanthanide silanides as polymerization catalysts.<sup>1,2</sup> However, f-element complexes containing metal-silicon bonds are relatively unexplored compared to analogous f-element carbon chemistry.<sup>3</sup> Here we present an isostructural family of M(III) hypersilanide complexes,  $[M(\text{Cp}^{\prime\prime})_2\{\text{Si}(\text{SiMe}_3)_3\}]$  (**1-M**, M = Ti, Zr, La, Ce, Nd, U;  $\text{Cp}^{\prime\prime} = \{\text{C}_5\text{H}_3(\text{SiMe}_3)_{2-1,3}\}$ ), which includes the first structurally authenticated U(III) silanide complex. EPR spectroscopy, supported by UV-vis-NIR spectroscopy, SQUID magnetometry and complete active space self-consistent field (CASSCF) calculations, were used to characterize the electronic structures of **1-M**. We have observed and rationalized a change in anisotropy between  $nd^1$  and  $nf^1$  or  $nf^3$  electronic configurations, and we have probed the M(III) – Si bonding interactions with reference to structurally similar chloride complexes,  $[M(\text{Cp}^{\prime\prime})_2\text{Cl}]$  (M = Ti, Zr), and U(III)  $5f^3 \rightarrow 6d^15f^2$  electronic transitions.

We thank the European Research Council for supporting this work, the EPSRC UK National Electron Paramagnetic Resonance Service for access to the EPR facility and the SQUID magnetometer, the University of Manchester, and its Computational Shared Facility.

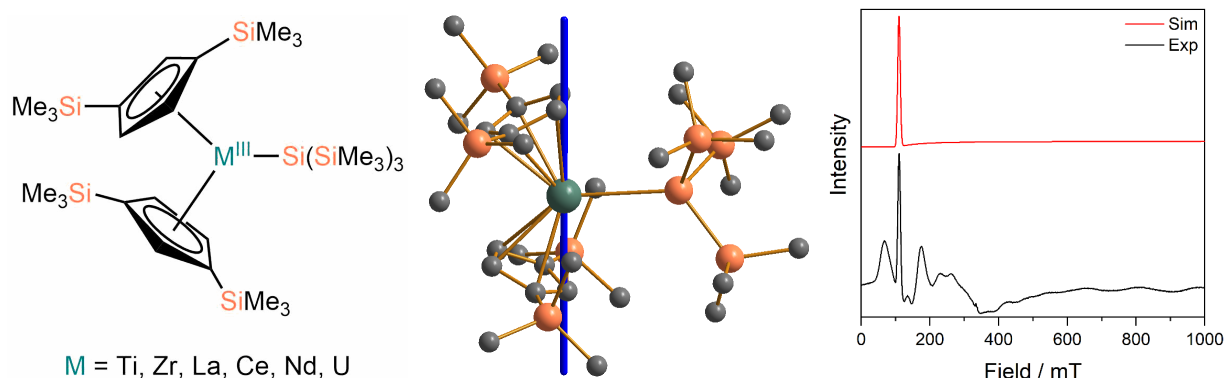


Figure 32. Metal complexes  $[M(\text{Cp}^{\prime\prime})_2\{\text{Si}(\text{SiMe}_3)_3\}]$  (**1-M**) (left), and calculated magnetic anisotropy axis in blue (centre) and powder continuous wave X-band EPR spectrum at 7 K (right) for **1-U**, with experimental data (Exp) in black and simulated data (Sim) in red.

## References

1. Wilson, T. L.; Moore, E. E.; Adorno Lopes, D.; Kocovski, V.; Sooby Wood, E.; White, J. T.; Nelson, A. T.; McMurray, J. W.; Middleburg, S. C.; Xu, P.; Besmann, T. M. *Adv. Appl. Ceram.*, **2018**, *117*, S76–S81.
2. I. Castillo, I.; Tilley, T. D. *Organometallics*, **2001**, *20*, 5598–5605.
3. Réant, B. L. L.; Liddle, S. T.; Mills, D. P. *Chem. Sci.*, **2020**, *11*, 10871–10886.

\* Corresponding author. Tel.: +44-(0)161-275-4702.  
E-mail address: gemma.gransbury@manchester.ac.uk

U value revisit of PuO<sub>2</sub> and its surface reactions with H<sub>2</sub>O and NOXiaoyu Han<sup>a,\*</sup>, Nikolas Kaltsoyannis<sup>a</sup><sup>a</sup>Department of Chemistry, The University of Manchester, Oxford Road, Manchester, M12 9PL, UK**Abstract**

As the major form in the spent nuclear fuel, the surface chemistry of PuO<sub>2</sub>, especially small molecules reactions, is of great interests.[1] Due to the intrinsic failure of DFT to describe the delocalised electron of the plutonium, DFT+U method offers an alternative to cost-effective solution. However, previous theoretical studies only focused on the matching the experimental data on the band gap of PuO<sub>2</sub> to justify the U value in the computational setting. Here, we revisit the U value on PuO<sub>2</sub> and its (111) surface. Our results shows that higher U values gives larger band gap, however, it lost the Pu 5f contribution on valence band (VB). This results controdicit with the ARPES observation where Pu 5f and O 2p hybridized on VB. Further, we also evaluated the U value on lattice paramenter, the peaks distance on VB, work function of (111) surface and the Bader charge of bulk and surface with experimental measurements. Collectively, we recommend U=3 preserved electronic characteristics of PuO<sub>2</sub>.

Further, individual H<sub>2</sub>O and NO molecules reactions was studied under 300K. For water molecules, our results reveal that adsorption energy single water molecule and dissociated water form is highly associated with f band center of Pu against Fermi level. This phenomenon is similar to the transition metal d-band theory driven catalytic properties.[2] For NO moelcules, the way NO approaching to the surface is direction-selective, with N pointing downwards energetically favorable. When NO parralle bonded to the surface, the Pu beneath the O<sub>NO</sub> atoms would exhibit defect states near Fermi level. However, it doesn't have any corrolation relationship with the adsorption and free energy. And this situation persistant when both H<sub>2</sub>O and NO co-reaction on the surfaces.

As the adsorption energy of H<sub>2</sub>O and NO is competitive on PuO<sub>2</sub>(111) surface. Two sequence reactions, A) NO, then H<sub>2</sub>O B) H<sub>2</sub>O, then NO were also investigated. The free energy of possible reaction pathways were considered with final products of NO<sub>2</sub>, HNO, and HNO<sub>2</sub>.

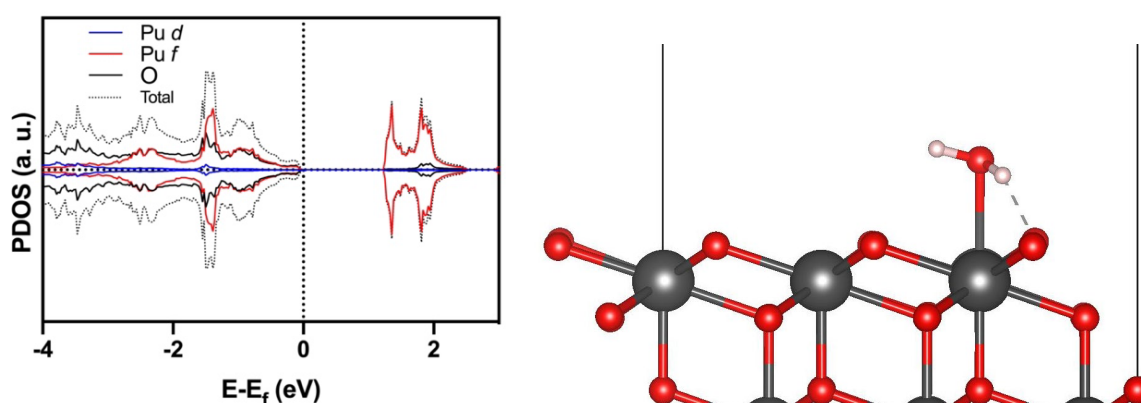
**Figures**

Figure 33 The projected Density of States (PDOS) of bulk PuO<sub>2</sub> with U value set to 3. The configuration of water adsorption on PuO<sub>2</sub>(111) surface.

**References**

1. M Fairweather, LS Tovey, C Boxall, AB Cundy, FJ Currell, JA Hriljac, NC Hyatt, N Kaltsoyannis, RJ Lunn, D Read, TB Scott, LJ Vandeperre, WM Symposia, Inc. 2020, INIS-US-21-WM-20106;
2. J. K. Norskov, F. Abild-Pedersen, F. Studt, and T. Bligaard, PNAS, 2011, 108(3), 937.

\* Corresponding author.

E-mail address: xiaoyu.han@manchester.ac.uk

# Two new Diffractometers for Actinide Research at the Rossendorf Beamline / ESRF

Christoph Hennig<sup>a,b,\*</sup>, Volodymyr Svitlyk<sup>a,b</sup>

<sup>a</sup> Helmholtz-Zentrum Dresden-Rossendorf, Institute of Resource Ecology, 01314 Dresden, Germany

<sup>b</sup> Rossendorf Beamline (BM20), European Synchrotron Radiation Facility, 38000 Grenoble, France

## Abstract

The Rossendorf Beamline was recently upgraded by two diffractometers which were added to the already existing spectroscopy station [1]. The two diffractometers allow measurements with high angular resolution for powder diffraction and measurements in a large segment of reciprocal space for single crystal diffraction and time-dependent studies. These diffractometers are accessible to the actinide community in the framework of joint research projects or ESRF proposals. Several recently obtained experimental results will be presented.

XRD-1, a 6-circle Huber diffractometer with Eulerian cradle geometry is used for high-resolution powder diffraction and surface diffraction (Fig. 1, left). The powder diffraction module uses an Eiger2 X CdTe 500k detector, the surface diffraction module is equipped with a Pilatus Si 100k detector. High-resolution powder diffraction data suitable for Rietveld refinement can be collected between 10 and 31 keV with a resolution of  $\delta d/d = 10^{-4}$ . The Bragg reflexes are extracted by radial integration using a recently developed modified pyFAI code [2].

XRD-2 consists of a heavy optical bench with an exchangeable goniometer and a Pilatus3 X 2M detector (Fig. 1, right). This diffractometer is used for single crystal diffraction and is applied mainly in the small-molecule field of chemistry and materials science. The high flux and the tunable energy support diffraction of actinide containing crystals which often suffer from remarkable absorption effects. The tunable energy makes the diffractometer suitable for the analysis of anomalous dispersion effects around X-ray absorption edges. It is also used for *in situ* or *operando* powder diffraction studies. A single-element Si drift detector can be installed on both diffractometers to combine diffraction measurements with spectroscopy (XAS and XRF), e.g. to determine the oxidation state of actinides directly on the same crystal which is used for diffraction.

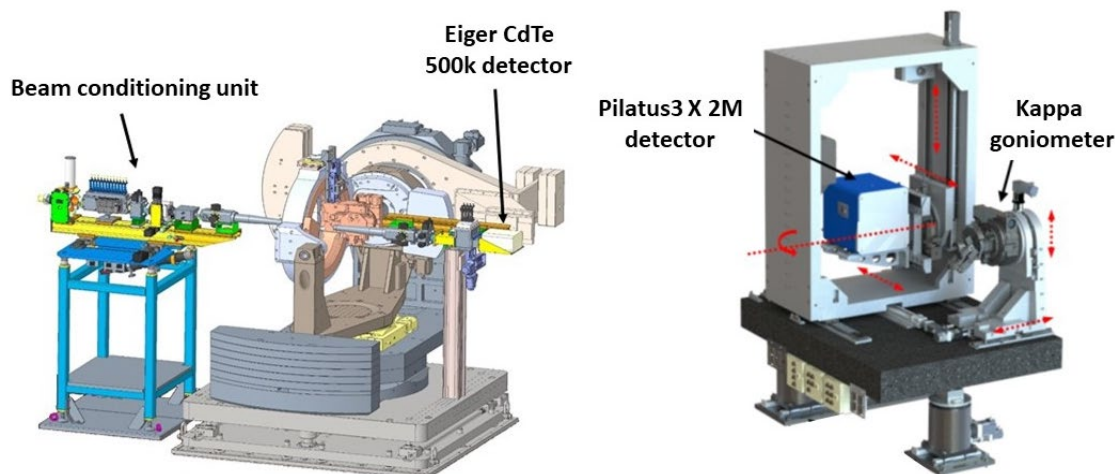


Figure 34 The two diffractometers at ROBL: XRD-1 (left) and XRD-2 (right).

## References

1. Scheinost, A. C. et al. ROBL-II at ESRF: a synchrotron toolbox for actinide research. *J. Synchrotron Rad.*, **28**, 333-349 (2021).
2. Kieffer J, Valls V, Blanc N, Hennig C. New tools for calibrating diffraction setups. *J. Synchrotron Rad.*, **27**, 558-566, (2020).

\* Corresponding author. Tel.: +33-476-88-2005.  
E-mail address: hennig@esrf.fr.

# Coordination Chemistry of Tri- and Tetravalent Actinides with Benzamidinate Ligands

Boseok Hong<sup>a,\*</sup>, Sebastian Fichter<sup>a</sup>, Adrian Näder<sup>a</sup>, Juliane März<sup>a</sup>, Peter Kaden<sup>a</sup>, Michael Patzschke<sup>a</sup>, Moritz Schmidt<sup>a</sup>, Thorsten Stumpf<sup>a</sup>

<sup>a</sup>Helmholtz-Zentrum Dresden-Rossendorf, Institute of Resource Ecology, Bautzner Landstrasse 400, 01328 Dresden, Germany

## Abstract

Because of their excellent properties of stabilizing transition metal complexes in various oxidation states, amidinate ligands have received considerable attention in the field of coordination chemistry over the last decades as versatile soft N-donor ligands. There have been a number of studies on transition metal amidinate complexes including lanthanides and some early actinides. Still, these studies are mainly limited to thorium (Th) and high valent (V, VI) uranyl complexes. Recently, the tetravalent actinide complexes with the chiral benzamidinate ((S)-PEBA) have been successfully synthesized in our group.<sup>1,2</sup> The present study is inspired by these precedent studies to synthesize a new series of benzamidinate compounds with An(III) and An(IV) to provide and expand a comprehensive understanding of the electronic properties of actinide compounds.

In this study, we succeeded to obtain a series of tetravalent actinide tris-benzamidinate chloro complexes [AnCl(amid)<sub>3</sub>] (An= Th, U, and Np; amid= *i*Pr<sub>2</sub>BA and (S)-PEBA).<sup>1</sup> The crystal structures of the model actinide complexes were determined by single-crystal XRD, showing three benzamidinates and one halide ligand coordinated to the actinide metal center in a mono-capped distorted octahedral coordination geometry. We also synthesized additional halide complex series (F, Br) by halogen exchange reactions on these chloro complexes to investigate the conformational stability of the complex.<sup>2</sup> The paramagnetic effects of these actinide complexes were investigated extensively in solution with NMR spectroscopy. Furthermore, the reduction of An(IV) to An(III) afforded the corresponding homoleptic benzamidinate complexes [An(amid)<sub>3</sub>] (An= U and Np; amid= *i*Pr<sub>2</sub>BA and (S)-PEBA), allowing the comparison of structural and chemical bonding situations with isostructural Ln(III) complexes via paramagnetic NMR studies.

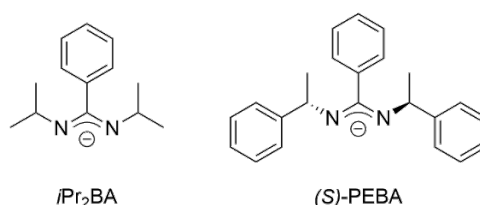


Figure 35: Chemical structure of benzamidinate ligands (*i*Pr<sub>2</sub>BA, (S)-PEBA)

## Acknowledgement

This study was supported by the German Federal Ministry of Education and Research (BMBF) funding under the project No. 02NUK046B (FENABIUM) and No. 02NUK059 (f-Char).

## References

1. Kloditz, R.; Fichter, S.; Kaufmann, S.; Brunner, T. S.; Kaden, P.; Patzschke, M.; Stumpf, T.; Roesky, P. W.; Schmidt, M.; März, *J. Inorg. Chem.* **2020**, *59* (21), 15670–15680.
2. Fichter, S.; Kaufmann, S.; Kaden, P.; Brunner, T. S.; Stumpf, T.; Roesky, P. W.; März, *J. Chem. - A Eur. J.* **2020**, *26* (41), 8867–8870.

# Spin Orbit Coupling Parameters for Semi-Empirical Methods: DFTB & GFN-xTB

Gautam Jha<sup>a,b,\*</sup>, Thomas Heine<sup>a,b,c</sup>

<sup>a</sup>Helmholtz-Zentrum Dresden-Rossendorf, Institut für Ressourcenökologie, Bautzner Landstraße 400, 01328 Dresden

<sup>b</sup>TU Dresden, Fakultät für Chemie und Lebensmittelchemie, Bergstraße 66c, 01062 Dresden, Germany

<sup>c</sup>Department of Chemistry, Yonsei University, Seodaemun-gu, Seoul 120-749, Republic of Korea

## Abstract

We present a consistent set of spin-orbit coupling (SOC) parameters for semi-empirical quantum mechanical (SQM) methods as in DFTB<sup>1</sup> and GFN-xTB<sup>2</sup>, covering elements throughout the periodic table. SOC is crucially important for correct description of the electronic structure of various materials as in van der Waals heterostructures, assessing the transport properties of Metal Organic Frameworks (MOF), and analyzing the topological properties of topological insulators<sup>3</sup>. The parameters are calculated from atomic SOC data at the Density Functional Theory (DFT) level. We tested parameters in various reference materials and molecules as in TMDC 2D crystals<sup>4</sup>, Topological Insulators, MOFs, III-V semiconductors<sup>5</sup>, and heavy element compounds. The parametrization opens the door to the incorporation of SOC in the calculations of large systems in SQM methods.

## References

- (1) Elstner, M.; Porezag, D.; Jungnickel, G.; Elsner, J.; Haugk, M.; Frauenheim, T. *Physical Review B – Condensed Matter and Materials Physics* **1998**, *58* (11), 7260.
- (2) Grimme, S.; Bannwarth, C.; Shushkov, P. *Journal of Chemical Theory and Computation* **2017**, *13* (5), 1989–2009.
- (3) Ma, Y.; Dai, Y.; Kou, L.; Frauenheim, T.; Heine, T. *Nano Letters* **2015**, *15* (2), 1083–1089.
- (4) Zibouche, N.; Kuc, A.; Musfeldt, J.; Heine, T. *Annalen der Physik* **2014**, *526* (9-10), 395–401.
- (5) Chadi, D. J. *Physical Review B* **1977**, *16* (2), 790.

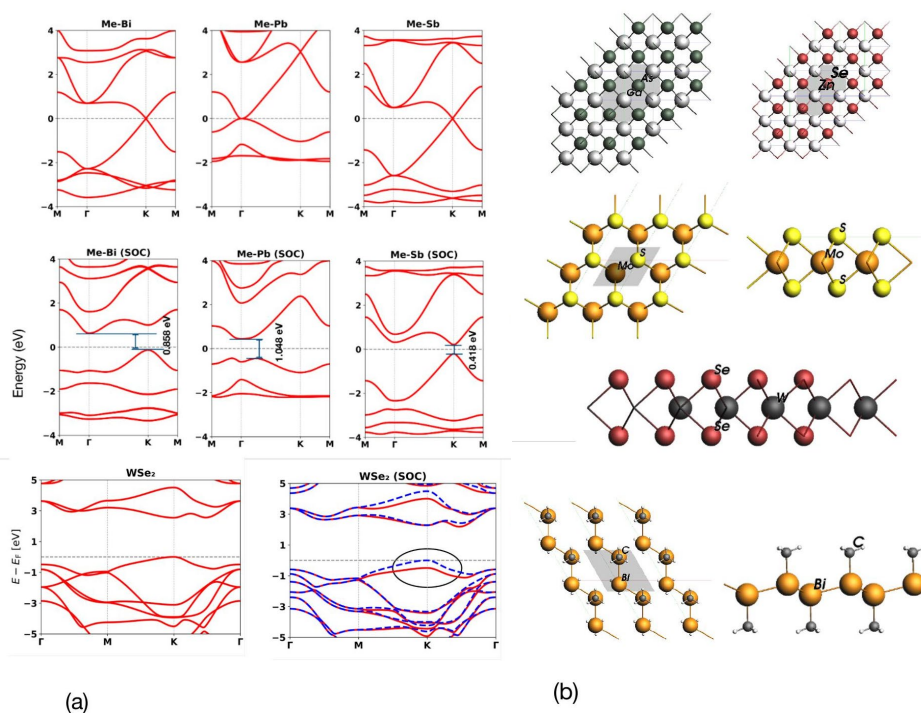


Figure 36 (a) Band structures calculated at DFTB level with and without the incorporation of SOC. (b) Optimized reference structures for Benchmark calculations.

\* Corresponding author. Tel.: +49-351-463-40838; fax: +49-351-463-35953.

E-mail address: g.jha@hzdr.de

*Ab initio* modelling of magnetite surfaces for radionuclide retentionAnita Katheras<sup>a,\*</sup>, Konstantinos Karalis<sup>a</sup>, Matthias Krack<sup>b</sup>, Andreas C. Scheinost<sup>c,d</sup>,  
Sergey V. Churakov<sup>a,e</sup><sup>a</sup>University of Bern, Institute of Geological Sciences, CH-3012 Bern, Switzerland<sup>b</sup>Paul Scherrer Institute, Laboratory for Scientific Computing and Modelling, CH-5232 Villigen PSI, Switzerland<sup>c</sup>Helmholtz-Zentrum Dresden-Rossendorf, Institute of Resource Ecology, D-01328 Dresden, Germany<sup>d</sup>European Synchrotron Radiation Facility, The Rossendorf Beamline at ESRF, F-38043 Grenoble Cedex 9, France<sup>e</sup>Paul Scherrer Institute, Laboratory for Waste Management, CH-5232 Villigen PSI, Switzerland**Abstract**

In many countries, spent nuclear fuel and high-level radioactive waste from the operation of nuclear power plants will be stored in deep geological repositories. This waste will be packed into thick-wall carbon steel casks to prevent the release of radionuclides into the environment. However, it is expected that steel corrodes over time and the corrosion products are expected to form mixed Fe<sup>2+</sup>/Fe<sup>3+</sup> oxides, mainly magnetite. After tens of thousands of years, casks may breach allowing leaching of the radiotoxic elements, such as Pu and Tc, by host rock pore-water. The dissolved radionuclides can then interact with the steel corrosion products and be adsorbed or incorporated into the solids [1]. But since these interaction mechanisms are poorly understood at the atomistic scale, our goal is to better understand them by using computer simulations alongside experiments [2][3].

In this computational study, we identified the dominant low index surfaces on nano-magnetite particles and their termination at the relevant conditions based on Kohn-Sham density functional theory (DFT). This was done using the open-source code CP2K. The DFT+U method was employed for the strongly correlated 3d and 5f electrons of Fe and Pu, respectively. The Hubbard U parameter was determined by comparing experimental cell parameters and band gaps to our results [4]. With this revised model, we examined the preferential magnetite crystal orientation plane (111) with different surface terminations (cf. fig. 1) as a function of oxygen fugacity and partial water pressure. Based on our modelling, we found the most stable magnetite (111) surfaces under real repository conditions. Subsequently, we used classical and *ab initio* molecular dynamics (MD) to investigate the interaction mechanisms of radionuclides with magnetite, especially the redox sensitive uptake of Tc and Pu under the incorporation of these elements into the magnetite structure.

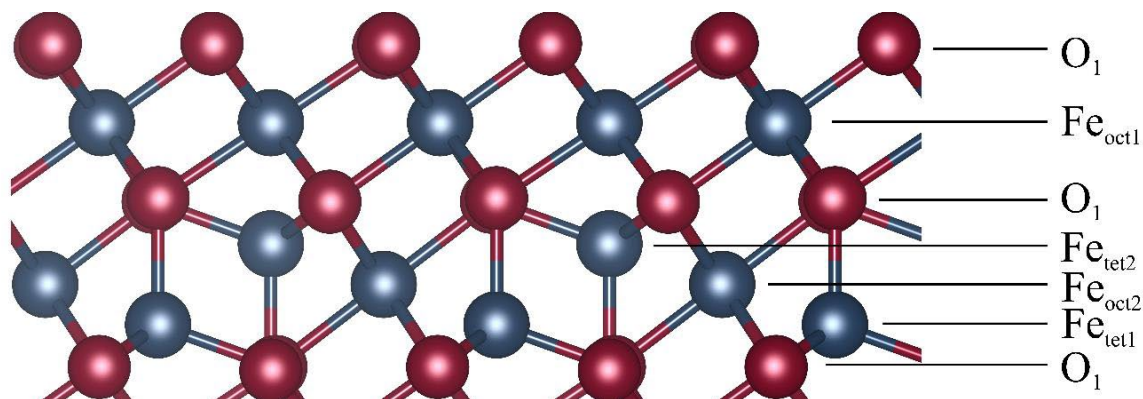


Figure 37 Side view of the magnetite (111) surface as cut from bulk crystal showing the six layers and possible inherent surface terminations. O atoms are red and Fe atoms are blue; the coordination of Fe is either octahedrally (Fe<sub>oct</sub>) or tetrahedrally (Fe<sub>tet</sub>).

**References**

1. Dumas, T.; Fellhauer, D.; Schild, D.; Gaona, X.; Altmaier, M.; Scheinost, A. C. *ACS Earth and Space Chemistry*, 2019, 3 (10), 2197–2206.
4. Kéri, A.; Dähn, R.; Krack, M.; Churakov, S. V. *Environmental Science & Technology* 2017, 51 (18), 10585–10594.
2. Kirsch, R.; Fellhauer, D.; Altmaier, M.; Neck, V.; Rossberg, A.; Fanghänel, T.; Charlet, L.; Scheinost, A. C. *Environmental Science & Technology* 2011, 45 (17), 7267–7274.
3. Yalçıntaş, E.; Scheinost, A. C.; Gaona, X.; Altmaier, M. *Dalton Transactions* 2016, 45 (44), 17874–17885.

\* Corresponding author. Tel.: +41-31-684-4564.

E-mail address: anita.katheras@geo.unibe.ch

# Discrete and Cationic Thorium-Incorporated Palladium(II)-Oxo Clusters

Saurav Bhattacharya and Ulrich Kortz\*

*Department of Life Sciences and Chemistry, Jacobs University, 28759 Bremen, Germany*

---

**Abstract**

Polyoxometalates are anionic polynuclear metal-oxo clusters that are constructed from early transition metal ions in high oxidation states, such as Mo<sup>VI</sup>, W<sup>VI</sup>, V<sup>V</sup>, Nb<sup>V</sup>, and Ta<sup>V</sup>, with oxo-linkers, resulting in a large class of compounds with an enormous variety of shapes, sizes and compositions.<sup>1</sup> Polyoxometalates (POMs) based exclusively on Pd<sup>2+</sup> ions (polyoxopalladates, POPs) were discovered in 2008.<sup>2</sup> The area of POP chemistry has developed rapidly ever since due to the fundamentally novel structural and compositional features of POPs resulting in unprecedented electronic, spectroscopic, magnetic, and catalytic properties.<sup>3</sup> In recent years efforts were made to modulate the POP structures along with their associated charges in order to try and control the structure-property relationship. This pursuit has recently led to the discovery of neutral palladium(II)-oxo clusters (POCs), such as [Pd<sub>16</sub>O<sub>8</sub>(OH)<sub>8</sub>((CH<sub>3</sub>)<sub>2</sub>AsO<sub>2</sub>)<sub>8</sub>] (**Pd<sub>16</sub>**), the chloro-derivative [Pd<sub>16</sub>Na<sub>2</sub>O<sub>10</sub>(OH)<sub>3</sub>Cl<sub>3</sub>((CH<sub>3</sub>)<sub>2</sub>AsO<sub>2</sub>)<sub>8</sub>] (**Pd<sub>16</sub>Cl**), the larger [Pd<sub>24</sub>O<sub>12</sub>(OH)<sub>8</sub>((CH<sub>3</sub>)<sub>2</sub>AsO<sub>2</sub>)<sub>16</sub>] (**Pd<sub>24</sub>**), and the very large [Pd<sub>40</sub>O<sub>24</sub>(OH)<sub>16</sub>{(CH<sub>3</sub>)<sub>2</sub>AsO<sub>2</sub>}<sub>16</sub>] (**Pd<sub>40</sub>**).<sup>4</sup> Here the synthesis and structure of the first examples of cationic POCs containing *f-metal ions* will be discussed.<sup>5</sup>

**References**

1. M. T. Pope, *Heteropoly and Isopoly Oxometalates*, Springer, 1983.
2. E. V. Chubarova, M. H. Dickman, B. Keita, L. Nadjo, M. Mifsud, I. W. C. E. Arends, U. Kortz, *Angew. Chem. Int. Ed.* **2008**, *47*, 9542.
3. (a) P. Yang, U. Kortz, *Acc. Chem. Res.* **2018**, *51*, 1599–1608; (b) N. V. Izarova, M. T. Pope, U. Kortz, *Angew. Chem. Int. Ed.* **2012**, *51*, 9492.
4. (a) S. Bhattacharya, U. Basu, M. Haouas, P. Su, M. F. Espenship, F. Wang, A. Solé-Daura, D. H. Taffa, M. Wark, J. M. Poblet, J. Laskin, E. Cadot, U. Kortz, *Angew. Chem. Int. Ed.* **2021**, *60*, 3632; (b) S. Bhattacharya, X. Ma, A. S. Mougharbel, M. Haouas, P. Su, M. F. Espenship, D. H. Taffa, H. Jaensch, A.-J. Bons, T. Stuerzer, M. Wark, J. Laskin, E. Cadot, U. Kortz, *Inorg. Chem.* **2021**, *60*, 17339.
5. S. Bhattacharya, A. Barba-Bon, T. A. Zewdie, A. B. Müller, T. Nisar, A. Chmielnicka, I. A. Rutkowska, C. J. Schürmann, V. Wagner, N. Kuhnert, P. J. Kulesza, W. M. Nau, U. Kortz, *Angew. Chem. Int. Ed.* **2022**, e202203114. <https://doi.org/10.1002/anie.202203114>

---

\* Corresponding author.

# A density functional investigation of dinuclear hydrolysis complexes $[(\text{AnO}_2)_2(\text{OH})]^q$ for $\text{An} = \text{U}$ and $\text{Np}$

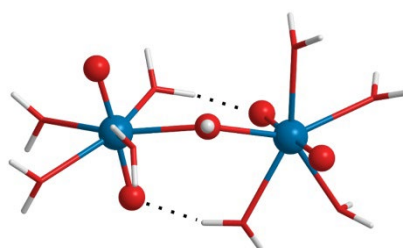
I. Chiorescu<sup>a</sup>, S. Krüger<sup>a,\*</sup>

*Department Chemie, Technische Universität München, 85748 Garching, Germany*

## Abstract

The characterization of hydrolysis complexes of actinides is of considerable interest as hydrolysis is the fundamental reaction of actinide ions in water. It determines their speciation in dependence of concentration and pH. Thus, a detailed knowledge of hydrolysis is a prerequisite to understand the interaction of actinide ions with other compounds in solution and at mineral surfaces as well as their solubility. All these processes are significant for safety considerations of geological disposal of radioactive waste. While a large number of hydrolysis complexes of U(VI) are known, the hydrolysis speciation of Np(VI), which should be similar to U(VI), and of Np(V) is less developed [1].

We used quantum mechanical calculations at the scalar-relativistic density functional level to investigate diactinyl monohydroxo complexes,  $[(\text{AnO}_2)_2(\text{OH})]^{3+/+}$ , for  $\text{An} = \text{U(VI)}$ ,  $\text{Np(VI)}$ , and  $\text{Np(V)}$  in aqueous solution. These complexes are the smallest examples of multinuclear oxo-hydroxo complexes of actinyls.  $[(\text{UO}_2)_2(\text{OH})]^{3+}$  is a known complex of U(VI) at low pH [1]. Although not yet found in experiments,  $[(\text{NpO}_2)_2(\text{OH})]^{3+}$  should exist due to the similarity between Np(VI) and U(VI) complexes.  $[(\text{NpO}_2)_2(\text{OH})]^+$  is a hypothetical species. Thus, this study contributes especially to the knowledge of the hydrolysis of Np(VI) and Np(V). We carefully modelled structures and energies of various isomers of these complexes. This allows a detailed characterization of the known species  $[(\text{UO}_2)_2(\text{OH})]^{3+}$  and sheds light on the possible contribution of  $[(\text{NpO}_2)_2(\text{OH})]^{3+/+}$  to the hydrolysis of neptunium. Our model calculations show that the An(VI) complexes favour a parallel orientation of actinyls, while for the Np(V) complex a perpendicular arrangement is stabilized by intramolecular hydrogen bonds. As expected, the Np(VI) diactinyl complex  $[(\text{NpO}_2)_2(\text{OH})]^{3+}$  features a similar structure and stability as its U(VI) analogue. Calculated formation constants for An(VI) diactinyl monohydroxo complexes show a qualitative agreement with the experiment for U(VI) and the very similar result for Np(VI) suggests the existence of  $[(\text{NpO}_2)_2(\text{OH})]^{3+}$  as a minority species. Both An(VI) complexes are only slightly less stable than their separate mononuclear constituents  $[\text{AnO}_2]^{2+}$  and  $[\text{AnO}_2(\text{OH})]^+$ . For the Np(V) complex  $[(\text{NpO}_2)_2(\text{OH})]^+$  we determined a considerably lower complexation constant than for its An(VI) analogues, in agreement with the weaker hydrolysis of Np(V). On the other hand, this complex is more stable against decay to its constituents. Thus,  $[(\text{NpO}_2)_2(\text{OH})]^+$  could exist at the onset of Np(V) hydrolysis ( $\text{pH} \approx 10$ ) for higher than trace concentrations of Np(V). This newly suggested complex might contribute to resolve open issues regarding the hydrolysis of Np(V) [1,2,3].



Exemplary structure of  $[(\text{AnO}_2)_2(\text{OH})]^q$ .

## References

1. Grenthe, I.; Gaona, X.; Plyasunov, A. V.; Rao, L.; Runde, W.; Grambow, B.; Konings, R. J. M.; Smith, A. L.; Moore, E. E. *Second update on the chemical thermodynamics of U, Np, Pu, Am and Tc*. OECD NEA 2020.
2. Petrov, V. G.; Fellhauer, D.; Gaona, X.; Dardenne, K.; Rothe, J.; Kalmykov, S. N.; Altmaier, M. *Radiochim. Acta* 2017, 105, 1.
3. Gray, A.; Chiorescu, I.; Krüger, S.; Rösch, N. *Eur. J. Inorg. Chem.* 2019, 4516.

\* Corresponding author. Tel.: +49 89 289 13619  
 E-mail address: krueger@ch.tum.de

# Crystal-chemical investigation of $MU_8S_{17}$ and $Ln_6U_{12}S_{31}I$ compounds ( $M = 3d$ metal; $Ln =$ lanthanide metal)

Marvin Michak<sup>a</sup>, Paula Huth<sup>b</sup>, Reinhard Denecke<sup>b</sup>, Holger Kohlmann<sup>a,\*</sup>

<sup>a</sup>Leipzig University, Institute for Inorganic Chemistry, Johannisallee 29, 04103 Leipzig, Germany

<sup>b</sup>Leipzig University, Wilhelm-Ostwald-Institute of Physical and Theoretical Chemistry, Linnéstr. 2, 04103 Leipzig, Germany

## Abstract

Solid-state uranium compounds show a fascinating crystal-chemical variety due to the actinides' ability to exist in many different oxidation states. This is especially true for uranium chalcogenides, which often exhibit mixed valency between the +III and +IV oxidation state, as for example shown in the binary compound  $U_3S_5$ .<sup>[1]</sup> Accordingly, this compound class provides intriguingly diverse properties, moving from metals to semiconductor materials to crystal structures containing polyanions with increasing chalcogenide content.

In our work, multiple ternary 3d metal uranium sulfides of the formula  $MU_8S_{17}$  were synthesized using either simple solid-state reactions of the respective binary sulfides or chemical vapour transport methods for growth of larger crystals. Especially since the compounds are already known from X-ray powder diffraction data, we were interested in single-crystal-data for their in-depth structural characterization. In other synthesis experiments by chemical transport, crystals of a new quaternary mixed lanthanide-actinide sulfide iodide  $Ln_6U_{12}S_{31}I$  were discovered and structurally characterised.

Single-crystal X-ray diffraction studies were performed on different crystals of the respective phases. The compounds  $MU_8S_{17}$  all crystallize in the  $CrU_8S_{17}$  structure type of monoclinic space group  $C2/m$ , which can be described by different intertwined networks of  $US_8$ -polyhedra and  $MS_6$ -octahedra (Figure 1, left). Typically, twinning by reticular merohedry is observed in the crystals, which can be rationalized by analysis of the crystal structure.

Likewise, the structure of the quaternary phases  $Ln_6U_{12}S_{31}I$  can be described as a dense polyhedral network of  $US_7$ -polyhedra, in which units of six edge-sharing  $LnS_6$ -prisms are embedded (Figure 1, right). Single-crystal X-ray diffraction reveals an unusual electron density distribution, which can be described by a disordered structure model. The iodine atoms are surrounded by uranium atoms in an unusually large distance of 3.58643(4) Å (for  $Ln = Lu$ ), raising the question of their interatomic interaction.

XPS-investigations hint toward a single oxidation state of U(IV) in  $TiU_8S_{17}$ , whereas in  $Lu_6U_{12}S_{31}I$  two main U4f-components are proposed, indicating either multiple oxidation states or other uranium-containing phases that might have formed upon surface oxidation.

## References

1. H. Kohlmann, H. P. Beck, *J. Solid State Chem.*, 2000, 150, 336–341.

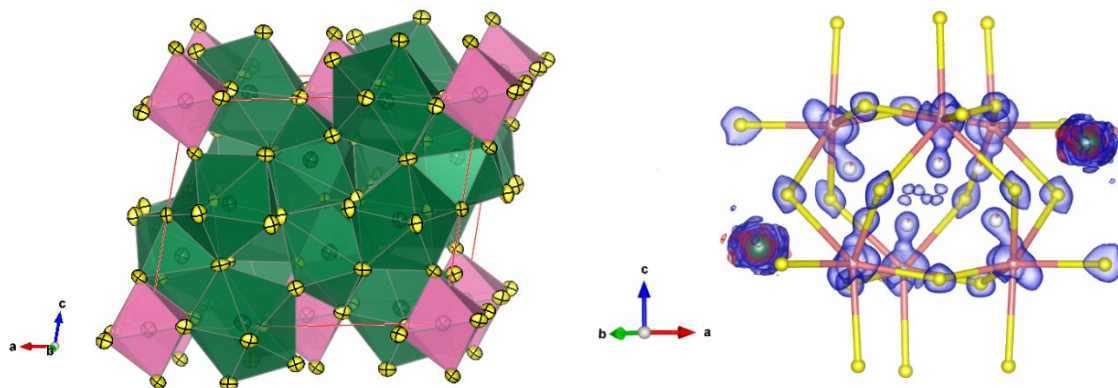


Figure 38: Crystal structure of  $TiU_8S_{17}$  (left) and the observed electron-density of the disordered lutetium partial structure in  $Lu_6U_{12}S_{31}I$  (right).

\* Corresponding author. Tel.: +49-341-97-36201; fax: +49-341-97-36199.  
E-mail address: holger.kohlmann@uni-leipzig.de.

## Magnetic Relaxation of Actinide-based Single Molecule Magnets

Meagan S. Oakley<sup>a,\*</sup>, Nicholas Chilton<sup>a</sup><sup>a</sup>Department of Chemistry, University of Manchester, Oxford Road, Manchester, M13 9PL**Abstract**

Single molecule magnets (SMMs) can remain magnetised upon the removal of a magnetic field allowing them to store magnetic information. Due to their small size, these molecules could be used in the next generation of high density information storage devices, ultimately reducing space and energy requirements of data centers. The main challenge is to design a SMM which can retain magnetic hysteresis and exhibit slow magnetic relaxation at high temperatures. Lanthanide ions are most commonly used as their large spin-orbit coupling and chemically inert 4f orbitals, along with tailored ligand fields, can give rise to a barrier for magnetisation reversal, leading to memory effects. Magnetisation is lost when the SMM traverses this barrier by coupling the SMMs' electronic spin to its vibrational degrees of freedom (spin-phonon coupling). Significant progress has been made by fine-tuning the ligand field and increasing the magnetic moment through magnetic exchange, but very few examples exhibit retention of the magnetic moment above 77 K.<sup>1,2</sup> In the case of high-performance lanthanide-based SMMs, loss of magnetisation at high temperature (usually >60 K) arises from Orbach relaxation over the barrier, whereas below this temperature two-phonon Raman mechanisms dominate. Actinides have been touted to have potential in increasing the size of the barrier, as they have inherently stronger spin-orbit coupling and more radially diffuse f orbitals than lanthanides and thus would, in theory, produce larger crystal field splitting. However, it has been shown that the loss of magnetisation in actinide-based SMMs may be dominated by the Raman mechanism, and not due to over-barrier processes.<sup>3</sup>

In this communication, we use our established spin dynamics protocol to probe the difference in magnetic relaxation between a series of isostructural lanthanide and actinide SMMs (shown in Figure 1).<sup>4</sup> Through modelling the spin dynamics, we can highlight features of the electronic and phononic structure that gives rise undesirable relaxation pathways, and hence begin to build design criteria for actinide-based SMMs.

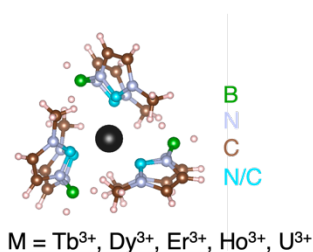


Figure 39. Dihydrobis(methylpyrazolyl)borate and dihydrobis(methylimidazolyl)borate lanthanide and actinide single molecule magnet structures.

**References**

1. Guo, F.; Day, B. M.; Chen, Y-C.; Tong, M-L; Mansikkamäki, A.; Layfield, R. A. *Science*, 2018, 362 (6421), 1400-1403.
2. Gould, C. A.; McClain, K. R.; Reta, D.; Kragoskow, J. G. C.; Marchiori, D. A.; Lachman, E.; Choi, E.-S.; Analytis, J. G.; Britt, R. D.; Chilton, N. F.; Harvey, B. G.; Long, J. R. *Science* 2022, 375 (6577), 198–202.
3. Meihaus, K. R.; Long, J. R. *Dalton Trans.*, 2015, 44, 2517-2528.
4. Meihaus, K. R.; Minasian, S. G; Lukens Jr., W. W.; Kozimor, S. A.; Shuh, D. K.; Tylliszczak, T.; Long, J. R. *J. Am. Chem. Soc.*, 2014, 136 (16), 6056-6068.

\* Corresponding author.

E-mail address: meagan.oakley@manchester.ac.uk.

# Characterization of *f*-element complexes with *soft-donor* ligands for selective Americium separation

Fynn Sören Sauerwein<sup>a,\*</sup>, Andreas Wilden<sup>a</sup>, Giuseppe Modolo<sup>a</sup>

<sup>a</sup>Forschungszentrum Jülich GmbH, Institut für Energie- und Klimaforschung – Nukleare Entsorgung (IEK-6), 52428 Jülich, Germany

## Abstract

In recent years, much effort has been invested in recycling of minor actinides from PUREX raffinate solutions. Hydrophilic N-donor ligands such as tetrasodium-3,3',3'',3'''-([2,2'-bipyridine]-6,6'-diylbis(1,2,4-triazine-3,5,6-triyl))tetrabenzenesulfonate (SO<sub>3</sub>-Ph-BTBP, Figure 1) were used for selective separation of Am(III) from Cm(III) and other trivalent fission lanthanides by smart combination with diglycolamide ligands as extractants such as *N,N,N',N'*-tetra-*n*-octyl diglycolamide (TODGA, Figure 1).<sup>1,2</sup> In this fundamental oriented work, the combination of SO<sub>3</sub>-Ph-BTBP with TODGA and its mono- and dimethylated derivatives Me-TODGA and Me<sub>2</sub>-TODGA (see Figure 1) was investigated for their extraction behavior in nitric acid solution. All systems showed a high selectivity of An(III) over Ln(III), and Am(III) over Cm(III). Separation factors decreased in the order TODGA > Me-TODGA > Me<sub>2</sub>-TODGA. Moreover, a significant drop in distribution ratios of heavier lanthanides (Tb-Lu) was observed in all three extraction systems. This effect was further elucidated by speciation studies of the formed complexes with several lanthanides using UV/Vis spectroscopy. The formation of 1:2 complexes (metal-to-ligand ratio) with SO<sub>3</sub>-Ph-BTBP was confirmed for the studied lanthanides and stability constants  $\log \beta$  of  $7.7 \pm 0.8$  for Nd(III) at  $10^{-3}$  mol L<sup>-1</sup> HNO<sub>3</sub> and  $6.1 \pm 0.4$  for Ho(III) at 3 mol L<sup>-1</sup> HNO<sub>3</sub> were determined. No complexation was observed for Nd(III) at 3 mol L<sup>-1</sup> HNO<sub>3</sub>. Therefore, the formation of complexes with a protonated form of SO<sub>3</sub>-Ph-BTBP seems to be possible with Ho(III), but not with Nd(III). The results of the solvent extraction experiments and speciation studies will be presented and discussed.

## Acknowledgements

Funding for this research was provided by the German Federal Ministry of Education and Research through the f-Char project under grant number 02NUK059D.

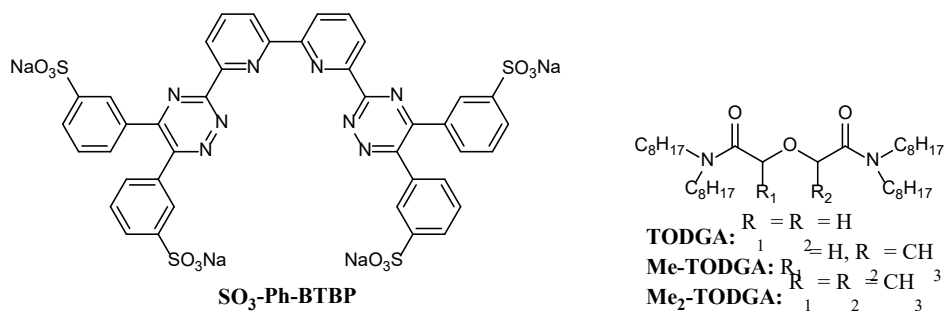


Figure 40: Chemical structures of SO<sub>3</sub>-Ph-BTBP, TODGA, Me-TODGA, and Me<sub>2</sub>-TODGA.

## References

1. C. Wagner et al., *Solvent Extr. Ion Exch.*, 2016. 34 (2): p. 103-113.
2. A. Geist and P. J. Panak, *Solvent Extr. Ion Exch.*, 2021. 39 (2): p. 128-151.

# Investigation of the ligand configuration in Th(IV) N-donor ligand complexes

Thomas Sittel<sup>a,b,\*</sup>, Michael Trumm<sup>a</sup>, Christian Adam<sup>a</sup>, Andreas Geist<sup>a</sup>, Petra Panak<sup>a,b</sup>

<sup>a</sup>Karlsruhe Institute of Technology (KIT), Institute for Nuclear Waste Disposal (INE), P. O. Box 3640, 76021 Karlsruhe, Germany

<sup>b</sup>Ruprecht-Karls-Universität Heidelberg, Physikalisch-Chemisches Institut, Im Neuenheimer Feld 253, 69120 Heidelberg, Germany

## Abstract

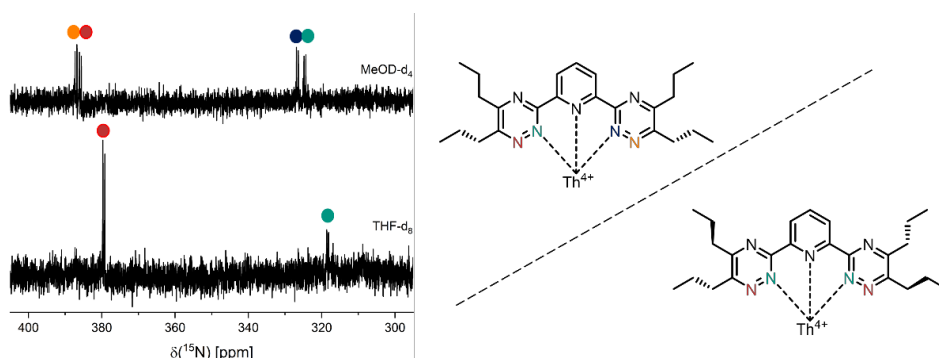


Figure 41  $^{15}\text{N}$  NMR spectra of  $[\text{Th}(\text{nPr-BTP})_3](\text{OTf})_4$  in  $\text{MeOD-d}_4$  and  $\text{THF-d}_8$ . A stronger solvent-complex interaction in  $\text{MeOD-d}_4$  results in a slightly different ligand configuration in the Th(IV) complex (upper structure) leading to twice as many  $^{15}\text{N}$  signals as expected.

For the separation of trivalent actinides and lanthanides highly selective ligands are required. Soft N-donor ligands such as bis(triazinyl)pyridines (BTPs) are known for their high selectivity.<sup>1,2</sup> The molecular origin of the selectivity still is a topic of fundamental scientific interest.

To probe the effect of the cation's nuclear charge on the bonding properties in actinide N-donor complexes, we extended our studies to tetravalent actinides. Here, we report a NMR spectroscopic and theoretical investigation on the complexation of Th(IV) with nPr-BTP. For the first time we observed the formation of different complex species for  $[\text{Th}(\text{nPr-BTP})_3](\text{OTf})_4$  depending on the solvent used. The higher charge compared to An(III) and Ln(III) results in a stronger complex-solvent interaction which leads to slightly different ligand configurations in the complex.<sup>3</sup> The ligand configuration highly depends on the solvent's ability to actively form H-bonds. This correlation was found by preparing  $[\text{Th}(\text{nPr-BTP})_3](\text{OTf})_4$  in a range of deuterated organic solvents as well as in binary solvent mixtures.

The figure above shows the results of the  $^{15}\text{N}$  NMR data analysis of  $[\text{Th}(\text{nPr-BTP})_3]^{4+}$  in  $\text{THF-d}_8$  (lower spectrum) and methanol- $\text{d}_4$  (upper spectrum). In  $\text{THF-d}_8$ , the symmetrical organization of the side chains results in a minimal repulsion between the three BTP ligands. This complex structure was also described for Am(III) and Ln(III) BTP complexes.<sup>3</sup> In methanol- $\text{d}_4$ , the symmetry is lifted due to a strong complex-solvent interaction. The side chains of one 1,2,4-triazinyl ring are organized in a way that prevents a fast solvent exchange resulting in twice as many signals in  $^1\text{H}$ ,  $^{13}\text{C}$  and  $^{15}\text{N}$  spectra as observed in  $\text{THF-d}_8$  or for the Am(III) and Ln(III) complexes. The experimental findings are supported by complementary calculations on the density functional theory level probing the effect of the torsion of triazine rings and nPr side chains. A possible torsion of an entire triazine ring as seen for the solvated nPr-BTP complex can be excluded, the calculations show that it is energetically not feasible for the Th complex system.

Summarizing, the results provide valuable information on the bonding mode and bonding differences in tetravalent actinide N-donor complexes compared to the trivalent lanthanide and actinide ions. Furthermore, this study serves as a valuable reference for future NMR studies of paramagnetic tetravalent actinides U(IV), Pu(IV), and Np(IV).

## References

1. Panak, P. J.; Geist, A. *Chem. Rev.*, 2013, **113**, 1199-1236.
2. Geist A.; Panak, P. J. *Solvent Extr. Exch.*, 2021, **39**, 128-151.
3. Adam, C. *et al. Dalton Trans.*, 2013, **42**, 14068-14074.

This work was funded by the German Federal Ministry for Research and Education (grant agreement No. 02NUK059A, 02NUK059C)

\* Corresponding author. Tel.: +49 721-608-24652

E-mail address: thomas.sittel@kit.edu

# Brewer's spent grain: A promising starting material for efficient uranyl ion adsorbents?

Yi Su<sup>a</sup>, Marco Wenzel<sup>a</sup>, Wendelin Böhm<sup>b</sup>, Silvia Paasch<sup>c</sup>, Markus Seifert<sup>a</sup>, Margret Acker<sup>d</sup>, Thomas Doert<sup>e</sup>, Eike Brunner<sup>c</sup>, Thomas Henle<sup>b</sup>, Jan J. Weigand<sup>a,\*</sup>

<sup>a</sup>Chair of Inorganic Molecular Chemistry, TU Dresden, 01062 Dresden, Germany

<sup>b</sup>Chair of Food Chemistry, TU Dresden, 01062 Dresden, Germany

<sup>c</sup>Chair of Bioanalytical Chemistry, TU Dresden, 01062 Dresden, Germany

<sup>d</sup>Central Radionuclide Laboratory, TU Dresden, 01062 Dresden, Germany

<sup>e</sup>Chair of Inorganic Chemistry II, TU Dresden, 01062 Dresden, Germany

## Abstract

Increasing concerns about uranium pollution in the environment require sustainable strategies for its removal from wastewater. On the base of cost-to-performance ratio, biosorbents are the most preferable and economically viable choices.[1] However, few studies have focused on biomass rich in both proteins and fibers, such as brewer's spent grain (BSG), a by-product from the beer brewery industry, which is suitable for adsorption of uranyl ions and can be further functionalized due to abundant functional groups on its surface.[2] This work aims to develop low-cost and efficient adsorbents from BSG with high adsorption capacity, fast kinetics, and reusability through different approaches, including thermal treatment, chemical oxidation and graft polymerization (Figure 1).

The results show that BSG can be converted into effective adsorbents for uranyl ions by mild hydrothermal treatment (150 °C, 16 h) and nitro-oxidation, with adsorption capacities increasing from 96 mg/g (BSG) to 221 mg/g (hydrothermal treatment)[3] and 242 mg/g (nitro-oxidation).[4] Furthermore, BSG can be converted into BSG-supported superabsorbent polymer by graft polymerization with acrylic acid and acrylamide, which has an excellent adsorption capacity (1465 mg/g) and can be used in continuous flow systems. Detailed characterizations of the adsorbents, the adsorption performance in various conditions, and the adsorption mechanisms are used to derive structure-affinity principles which will be discussed. In addition, preliminary results of a BSG-based material modified using surface ion-imprinting technology for enhanced selective U(VI) separation from lanthanides are presented.



Figure 42 Preparation of adsorbents for uranium adsorption from BSG through thermal treatment, oxidation, and graft polymerization.

**Acknowledgement:** We thank the German Federal Ministry of Education and Research (FENABIUM project 02NUK046A) and China Scholarship Council (CSC No. 201804910464) for financial support. We thank Lohrmanns Brauerei GmbH for providing the material used in this study.

## References

1. Rajasulochana, P.; Preethy, V. *Resource-Efficient Technologies*, 2016, 2, 175–184.
2. Mussatto, S. I.; Dragone, G.; Roberto, I. C. *Journal of Cereal Science*, 2006, 1, 1–14.
3. Su, Y.; Böhm, W.; Wenzel, M.; Paasch, S.; Acker, M.; Doert, T.; Brunner, E.; Henle, T.; Weigand, J. J. *RSC Advances*, 2020, 73, 45116–45129.
4. Su, Y.; Wenzel, M.; Paasch, S.; Seifert M.; Böhm, W.; Doert, T.; Weigand, J. J. *ACS Omega*, 2021, 30, 19364-19377.

\* Corresponding author. Tel.: +49 (351) 463-42800; fax: +49 (351) 463-3147.

E-mail address: jan.weigand@tu-dresden.de (J. J. Weigand)

# Improving computational methods for active elements: structures of mixed $d$ - and $f$ -elements oxides ( $MUO_4$ ) from experiment and first principles simulations

Rebekka Tesch<sup>a,b,c,\*</sup>, Gabriel L. Murphy<sup>d</sup>, Zhaoming Zhang<sup>e</sup>, Brendan J. Kennedy<sup>f</sup>,  
Piotr M. Kowalski<sup>a,b</sup>

<sup>a</sup>Forschungszentrum Jülich, Institute of Energy and Climate Research, Theory and Computation of Energy Materials (IEK-13), Wilhelm-Johnen-Straße, 52425 Jülich, Germany

<sup>b</sup>Jülich Aachen Research Alliance, JARA-CSD and JARA-ENERGY, 52425 Jülich, Germany

<sup>c</sup>RWTH Aachen University, Faculty of Georesources and Materials Engineering, Chair of Theory and Computation of Energy Materials, 52062 Aachen, Germany

<sup>d</sup>Forschungszentrum Jülich, Institute of Energy and Climate Research, Nuclear Waste Management and Reactor Safety (IEK-6), Wilhelm-Johnen-Straße, 52425 Jülich, Germany

<sup>e</sup>Australian Nuclear Science and Technology Organisation, Lucas Heights, NSW 2234, Australia

<sup>f</sup>The University of Sydney, School of Chemistry, Sydney, NSW 2006, Australia

---

## Abstract

Computing the electronic structure of materials that contain strongly correlated  $d$ - and  $f$ -electrons is a methodological challenge. With a combination of atomistic modeling and experimental methods we investigated a series of mixed  $d$ - and  $f$ -element oxides ( $MUO_4$ ,  $M = \text{Cd}, \text{Mn}, \text{Co}, \text{Mg}, \text{Ni}$ ). The X-ray (S-XRD), neutron powder diffraction (NPD) and X-ray absorption spectroscopy (XAS) data revealed formation of structure characterized by the lower-symmetry  $Ibmm$  space group [1]. These show distortion by tilting of the  $MO_6$  polyhedra for all  $M$  except Cd, which shows the high-symmetry structure of the  $Cmmm$  space group. Interestingly, standard DFT+ $U$  calculations wrongly predicted the  $Cmmm$  space group for all the  $M$  cations. We found that this discrepancy arises from a spurious Hubbard energy contribution [2], resulting from imperfect prediction of occupations of  $d$ - and  $f$ -orbitals, when the atomic orbitals are used as projectors in the standard DFT+ $U$  approach. We reconciled simulation and experimental results when applying a more realistic Wannier representation of  $d$ - and  $f$ -orbitals in the projection scheme. With this we were able to correctly reproduce structures of  $MUO_4$  compounds, including the size of the distortion. The high-quality experimental data on transition metal-actinide oxides gave us a unique opportunity to understand the shortcomings of the theoretical methods and propose a solution. This knowledge gain is of utmost importance for predictive computation of not only nuclear materials compounds, but materials of importance for energy transition, as these are mainly based on transition metal elements as active redox sites for electrochemical processes.

## References

1. Murphy, G. L. et al. Inorg. Chem., 2021, 60, 2246.
2. Cococcioni, M.; de Gironcoli, S. Phys. Rev. B, 2005, 71, 035105.

# Insight into the Separation of An(III) from Ln(III) Using Bis(2,4,4-trimethylpentyl)dithiophosphinic Acid

Guoxin Tian,<sup>a,b\*</sup> Qiling Guo<sup>a</sup>, Tuo Fang<sup>a</sup>, Tiantian Xia<sup>a</sup>, Qiaorui Sui<sup>a</sup>, Qing Deng<sup>a</sup>,  
Qian Liu<sup>a</sup>, Liyang Zhu<sup>a</sup>, Suliang Yang<sup>a</sup>

<sup>a</sup>Department of Radiochemistry, China Institute of Atomic Energy, Beijing, China

<sup>b</sup>Institute of Nuclear Energy and New Energy Technology, Tsinghua University, Beijing, China

---

## Abstract

The complexes of Nd(III) and Am(III) with bis(2,4,4-trimethylpentyl)dithiophosphinic acid (HA) are investigated spectroscopically and compositionally. With help of x-ray diffraction analysis on single crystals of Nd(H<sub>2</sub>O)<sub>10</sub>•3B (HB = bis(iso-butyl)dithiophosphinic acid), five complex species of Nd(III) with HA have been identified as NdA<sub>3</sub>, NdA<sub>3</sub>(HA), NdA<sub>3</sub>(HA)H<sub>2</sub>O, NdA<sub>3</sub>(H<sub>2</sub>O)<sub>3</sub>, and Nd(H<sub>2</sub>O)<sub>22</sub>•3A. Three of these five complexes, NdA<sub>3</sub>(HA)H<sub>2</sub>O, NdA<sub>3</sub>(H<sub>2</sub>O)<sub>3</sub>, and Nd(H<sub>2</sub>O)<sub>22</sub>•3A can be obtained from solvent extraction under varying conditions, while the other two, NdA<sub>3</sub>, NdA<sub>3</sub>(HA) can only be prepared under dry conditions. In single crystals of Nd(H<sub>2</sub>O)<sub>10</sub>•3B, the central Nd(III) ions are fully hydrated and the three B<sup>-</sup> anions do not directly bond to Nd(III) but present in the second coordination sphere just to balance the positive charge. The almost identical absorption spectra of the extracted species Nd(H<sub>2</sub>O)<sub>22</sub>•3A, and aqua Nd(III) as the reflectance spectrum of solid Nd(H<sub>2</sub>O)<sub>10</sub>•3B suggest the central Nd(III) ions in Nd(H<sub>2</sub>O)<sub>22</sub>•3A are also fully hydrated with similar coordination geometry as that Nd(H<sub>2</sub>O)<sub>10</sub>•3B. In comparison, for Am(III) only one complex AmA<sub>3</sub>(HA) is formed and identified in the corresponding extraction system

# Homoleptic Acetylacetonate (acac) and $\beta$ -Ketoimnate (acnac) Complexes of Uranium

Pablo Waldschmidt, Judith Riedhammer, Douglas Hartline, Frank W. Heinemann and Karsten Meyer\*

Friedrich-Alexander-Universität Erlangen-Nürnberg (FAU), Department of Chemistry and Pharmacy, Inorganic Chemistry, Egerlandstraße 1, 91058 Erlangen, Germany

## Abstract

Transmetalation of the potassium salts of differently substituted acetylacetonate (acac),  $\beta$ -ketoimnate (acnac) and  $\beta$ -diketiminato (nacnac) with  $[U(III)_3(\text{dioxane})_{1.5}]$  or  $[U(III)_4(\text{dioxane})_2]$  resulted in formation of homoleptic, octahedral complexes  $[U(\text{nacnac})_3]_1$  and  $[U(\text{tBuacnac})_3]$  in the oxidation states +III and +IV, the homoleptic, square prismatic  $[U(\text{Me-acnac})_4]$ , and the square antiprismatic complexes  $[U(\text{acacR})_4]$  (R = H, Me or Ph) in oxidation states +III to +V.

With the bulky version of the acnac ligand,  $\text{tBuacnac}$ , three ligands coordinate to the uranium center in a propeller-like fashion, similar to the earlier reported  $[U(\text{nacnac})_3]_1$  and supported by single-crystal structural studies on the oxidized complex  $[U(\text{tBuacnac})_3][\text{OTf}]$ . Since further oxidation of this anionic complex is not viable, the ligand system was changed to the less bulky  $\text{Meacnac}$  ligand, which allowed for the isolation of a neutral complex with four chelating ligands, namely  $[U(\text{Meacnac})_4]$ . The solid-state molecular structure reveals a heavily distorted, square prismatic coordination environment. This structure shows more similarity to the tetravalent, square antiprismatic  $[U(\text{acac})_4]$  complexes, which complete this series.

All complexes were characterized with a broad range of spectroscopic, electro- and magnetochemical techniques, including single-crystal X-ray diffraction analysis, a combination of UV/vis/NIR electronic absorption, NMR and IR spectroscopies, as well as solid-state SQUID magnetization studies and cyclic voltammetric analyses, and show overall well comparable data. Noteworthy is the strong temperature dependence of the magnetochemical data for  $[U(\text{tBuacnac})_3]$ , which is a very atypical behavior for trivalent uranium complexes. Electrochemical studies on the homoleptic uranium (IV) complexes with differently substituted acacR ligands reveal large electrochemical windows of up to 2.91 V, measured between the uranium(III) and the uranium(V) species, in addition to high stability towards repeated potential scans; thus, simulating charge-discharge processes.

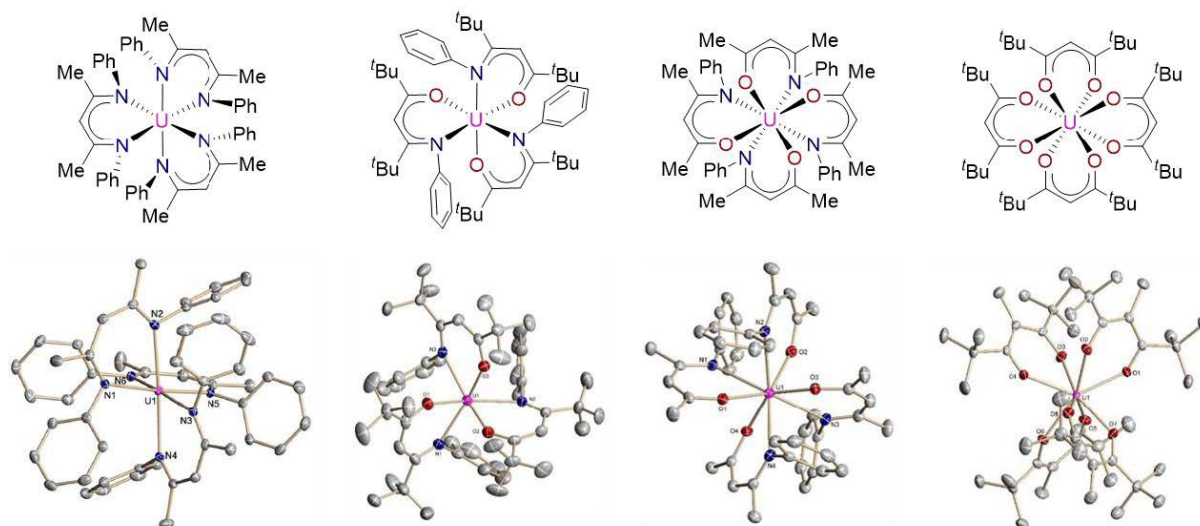


Figure 43 Overview of the molecular structures of  $[U(\text{nacnac})_3]$ ,  $[U(\text{tBuacnac})_3]$ ,  $[U(\text{Meacnac})_4]$  and  $[U(\text{acac}^{\text{Me}})_4]$  from left to right.

## References

- Riedhammer, J.; Aguilar-Calderon, J. R.; Miehlich, M.; Halter, D. P.; Munz, D.; Heinemann, F. W.; Fortier, S.; Meyer, K.; Mindiola, D. J., Werner-Type Complexes of Uranium(III) and (IV). *Inorganic Chemistry* **2020**, *59*, 2443-2449.

\* Corresponding author. Tel.: +49 9131 8527360; fax: +49 9131 8527367  
E-mail address: karsten.meyer@fau.de.

# Incorporation and diffusion of krypton and xenon in uranium mononitride; a density functional theory study

Lin Yang\*, Nikolas Kaltsoyannis

Department of Chemistry, School of Natural Sciences, The University of Manchester, Oxford Road, Manchester M13 9PL

## Abstract

Nitride fuels such as UN are considered as ideal candidates for Generation IV nuclear reactors, especially lead-cooled fast reactors, due to their high metal density and melting temperature, excellent thermal conductivity, and good compatibility with lead coolant. During irradiation of nuclear fuel, the fission of uranium generates a large number of products, e.g., 15% of the fission product in  $\text{UO}_2$  consists of noble gases (Ng) Xe and Kr [1]. These Ng atoms have low solubility in the fuel matrix and may migrate in the fuel, form bubbles inside and on the boundary of the grains, or escape to the fuel-clad gap, leading to fuel swelling and reduction in the thermal conductivity of the fuel rods[1]. Thus, for the safe and efficient use of nitride fuels, it is important to have a comprehensive understanding of the generation and migration of Ng atoms in the fuel matrix. Given the difficulty of experimentally studying radioactive materials, computational simulation is particularly valuable.

Based on the above considerations, we systemically studied the incorporation and diffusion behaviour of Kr and Xe in UN by density functional theory (DFT). We first calculated the solution energies of Kr and Xe in the UN interstitial site, U vacancy ( $V_U$ ), N vacancy ( $V_N$ ), and the bound Schottky defect (SD) sites, and found high stoichiometric dependence. Under U-rich and N-rich conditions, Kr and Xe have the lowest solution energy at SD and  $V_U$ , respectively, while under near-stoichiometric conditions, Kr and Xe behave differently with the former preferring a  $V_U$  and the latter preferring the SD (Figure 1, left).

Then, we calculated the diffusion coefficients of Kr and Xe in UN *via* the  $V_U$ -assisted and interstitial mechanisms. We found that the two mechanisms show opposite stoichiometric dependence, with the former increasing from U-rich to N-rich conditions and the latter decreasing. The reasonable agreement between our calculated  $V_U$ -assisted diffusion coefficient with experiment - similar to or better than existing theoretical and empirical models - indicates that the  $V_U$ -assisted mechanism governs Xe diffusion in UN (Figure 1, right). We believe our work provides a good theoretical basis to predict the diffusivity of Ng in UN grains, and that it will contribute to fission gas release models in UN.

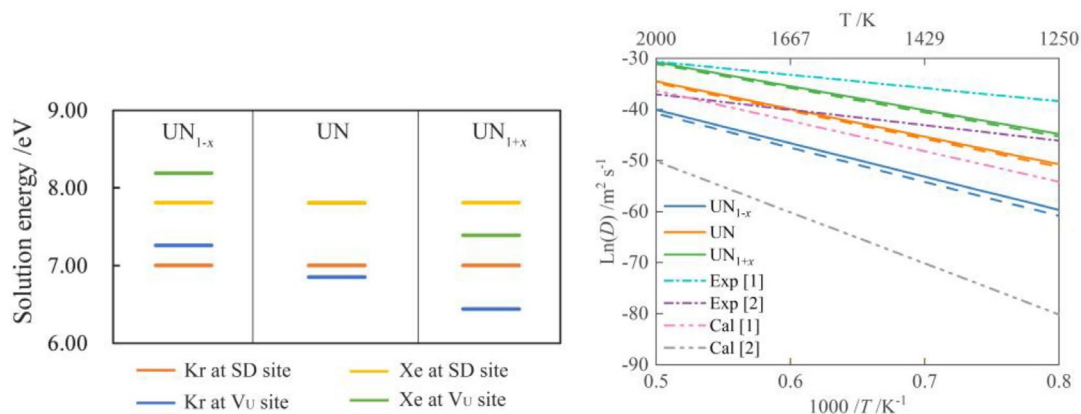


Figure 44 Left, the solution energy of Kr and Xe at U vacancy ( $V_U$ ) and Schottky defect (SD) site in UN under three stoichiometric conditions. Right, the calculated diffusion coefficient of Kr (solid line) and Xe (dashed line) in UN as a function of temperature under three stoichiometric conditions. The experimental and theoretical works used for comparison are from reference [2-5].

## References

1. J. Rest, M.W.D. Cooper, J. Spino, J.A. Turnbull, P. Van Uffelen, C.T. Walker. *J. Nucl. Mater.*, 2019, 513, 310-345.
2. N. Oi. *Z. Naturforschung A*, 1966, 21, 863-864.
3. J.B. Melchan, J.E. Gates. United States Report BMI-1701, 1964.
4. S. Starikov, A. Kuksin, D. Smirnova, A. Dolgodvorov, V. Ozrin. *Defect and Diffusion Forum*, 2017, 375, 101-113.
5. A. Claisse, T. Schuler, D.A. Lopes, P. Olsson. *Phys. Rev. B*, 2016, 94, 174302.

\* Corresponding author. Tel.: +44 (0)7529934017.  
E-mail address: lin.yang-10@postgrad.manchester.ac.uk

# An innovative approach of studying uranium dioxide corrosion at the microscale

Jennifer Yao<sup>a</sup>, Nabajit Lahiri<sup>b</sup>, Shalini Tripathi<sup>a</sup>, Shawn L. Riechers<sup>a</sup>, Eugene S. Ilton<sup>b</sup>, Sayandev Chatterjee<sup>c</sup>, Edgar C Buck<sup>a,\*</sup>

<sup>a</sup>Energy and Environment Directorate, Pacific Northwest National Laboratory, 902 Battelle Blvd., Richland, WA 99354, USA

<sup>b</sup>Physical and Chemical Sciences Directorate, Pacific Northwest National Laboratory, 902 Battelle Blvd. Richland, WA 99354, USA

<sup>c</sup>TerraPower LLC, Bellevue, WA, 98008, USA

## Abstract

Study of  $\text{UO}_2$  corrosion is important in understanding the spent nuclear fuel (SNF) disposal. Research<sup>1-2</sup> has shown the value of measuring the electrochemical corrosion potential of  $^{238}\text{UO}_2$ . However, experiments with bulk amounts of SNF are expensive owing to the need for shielded hot cell facilities to protect researchers from the intense  $\beta/\gamma$  radiation field. To address the challenges in investigating large amount of SNF materials, we incorporated  $\text{UO}_2$  in a microfluidic electrochemical cell to facilitate  $\text{UO}_2$  corrosion study at the microscale. Instead of using bulk spent fuel pieces as working electrode, less than 10 microgram of  $\text{UO}_2$  powder was mixed with polyvinylidene fluoride (PVDF) and carbon black to form the working electrode (1 mm in diameter). The  $\text{UO}_2$  electrode was fabricated into a three-electrode particle-attached microfluidic electrochemical cell (PAMEC) (Figure 1). The  $\text{UO}_2$  particle electrode went through electrochemical corrosion in 0.1 M  $\text{NaClO}_4$  (pH=9.5) aqueous electrolyte using the electrochemical station. Multimodal imaging analysis, including in situ scanning electron microscope (SEM) (Figure 1C) coupled with Energy-dispersive X-ray spectroscopy (EDS) as well as ex situ transmission electron microscopy (TEM) and atomic force microscopy (AFM), was applied to reveal the morphological change, oxidation layer distribution, and topographical information of  $\text{UO}_2$  before and after corrosion. In addition, X-ray photoelectron spectroscopy (XPS) was used to determine the oxidation state of the  $\text{UO}_2$  electrode surface disassembled from PAMEC after anodic oxidation. Our results demonstrate a promising approach to characterize  $\text{UO}_2$  corrosion at the microscale using multimodal characterization techniques. Particularly, in situ SEM imaging and EDS mapping allow direct observation of corrosion in liquid. This approach is useful in studying the interaction between geological repository environments (e.g., groundwater) and SNF to validate and improve the Fuel Matrix Dissolution Model.

## References

1. D. W. Shoesmith, *Journal of Nuclear Materials*, 2000, 282, 1-31.
2. S. Sunder, N. H. Miller and D. W. Shoesmith, *Corrosion Science*, 2004, 46, 1095-1111.

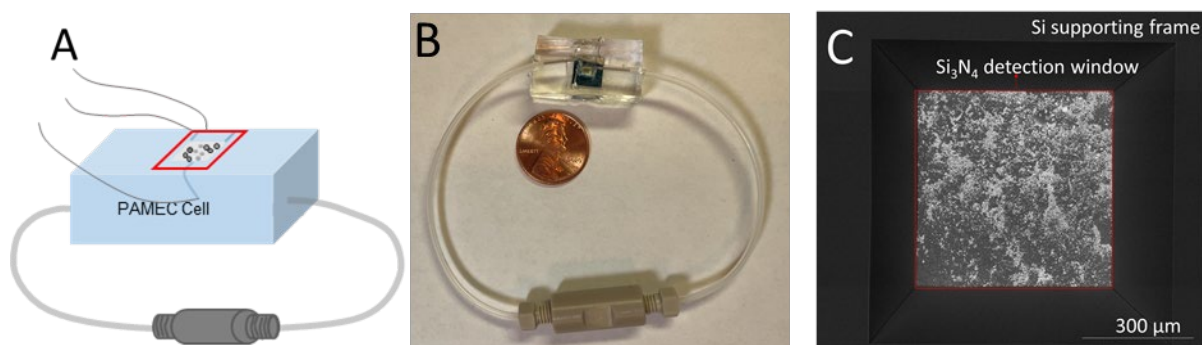


Figure 45 (A) Schematic of three-electrode PAMEC device, (B) its photograph, and (C) backscattered electron image of  $\text{UO}_2$  working electrode (bright features) attached underneath the detection window of PAMEC.

\* Corresponding author. Tel.: +1 (509) 375-5166.  
E-mail address: Jennifer.yao@pnl.gov

## Venue – Poster Prize Ceremony



The Poster Prize Ceremony will be held on Thursday from 7 pm at MARCOLINIS Welt, Bautzner Straße 96 in 01099 Dresden.

You can reach the location either by

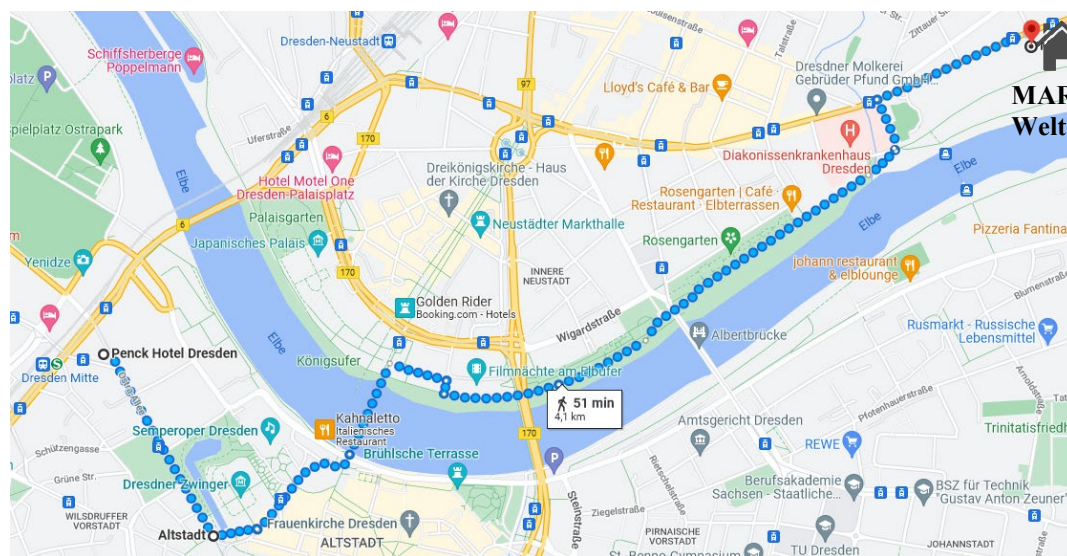
- public transport (take tram 11 from stop “Kongresszentrum” in direction “Bühlau” and exit at “Nordstrasse”, which is directly at the entrance of the venue. To reach the party walk past the building, down the stairs into the garden.



**Tram 11**



- take a walk along the river Elbe and enjoy the view of Dresden old town. The venue garden is accessible directly from the Elbe meadows.



**MARCOLINIS Welt**

- drive your car to the above address. A limited number of parking spots is available at the locations parking garage.

The ceremony will start at 7 pm, after which there will be a buffet and party with drinks.



# Actinides revisited 2022

Dresden, 21<sup>st</sup> to 23<sup>rd</sup> September 2022

The conference is partially funded by the German Ministry of Education and Research (BMBF) within the research project f-Char (02NUK059).

SPONSORED BY THE



Federal Ministry  
of Education  
and Research